MODELING OF UREA HYDROLYSIS WITH MICROENCAPSULATED UREASE

by

Keunbok Lee

Department of Chemical Engineering

McGill University, Montréal

February 1993

A thesis submitted to the Faculty of Graduate Studies and Research in partial fulfillment of the requirements for the degree of Doctor of Philosophy

ABSTRACT

The factors which influence the steady state performance of a continuous stirred tank reactor (CSTR) and a fixed bed reactor (FBR) operation with microencapsulated urease for the regeneration of dialysate solution have been studied at various enzyme activities. The theoretical model considered microcapsule size effects, pH kinetic effect, product inhibition and substrate depletion effects, in relation to urea conversion and the microcapsule effectiveness factor. The limiting effects of pH kinetics, product inhibition and substrate depletion were also studied individually and in combination under eight case studies. External mass transfer resistances were studied, by isolating the contributions by the external liquid film and the membrane wall resistances.

A simulation for the prediction of a patient's response to treatment using a microencapsulated urease artificial kidney system was made, taking into account the deactivation of the urease. The model has the ability to predict the performance of the artificial kidney and the patient's blood urea level simultaneously, at various operating conditions.

Résumé

Les facteurs qui influencent la performance d'état stable d'un réacteur à réservoir agité constamment et d'un réacteur à base fixe avec de l'urée microencapsulée pour la regénération de solution dialysate furent étudiés à diverses activités d'enzymes. Le modèle théorique considéra les effets de dimension microcapsulaire, l'effet kinétique pH, l'inhibition du produit et effets d'épuisement de sous couche en relation à la conversion d'urée et le facteur effectif microcapsule. Les effets limitants de kinétiques pH, l'inhibition de produit et épuisement de sous-couche furent aussi étudiés individuellement et en combiné sous huit études de cas. Les résistances de transfert externe de masse ont été étudiées en isolant les contributions par le film de liquide externe et les résistances du mur membrane.

On a fait une simulation pour la prédiction de réponse au traitement d'un patient employant un système de rein artificiel à l'urée microencapsulée prenant en compte la déactivation de l'urée. Le modèle a l'habilité de prédire la performance du rein artificiel et le niveau d'urée sanguine du patient simultanément à diverses conditions d'opération.

ACKNOWLEDGMENTS

I wish to express my sincere and deep appreciation to my supervisor, Professor R.J. Neufeld for his encouragement and guidance through this study. Much appreciation and special thanks for his good advice go to Dr. D.K. Boadi.

Appreciation for their encouragements are extended to P.L. Tang, C. Tong, A. Alecu, and K. Tsui. I would like to thank my father and mother for encouraging me throughout this work. My brothers, Keun Yong Lee and Keun Sok Lee and my sister, Mi Kyung Lee merit special thanks for encouraging me when I was in low spirits. Appreciation is extended to my grandparents for their emotional supports. Finally, I wish to express my sincere gratitude to my wife Mikyung Shin, my two sons June-Hee Lee and Chang-Hee Lee for their patience and moral support throughout the course of my study.

TABLE OF CONTENTS

LIST OF FIGURES

LIST OF TABLES

CHAPTER 1
INTRODUCTION

1.1 Motivation and Problem Definition

Nearly half a million people worldwide maintain their lives on hemodialyzers (artificial kidneys) which support malfunctioning kidneys (Nosé, 1990). The hemodialyzer functions on two basic principles: 1) dialysis to remove uraemic metabolic wastes (e.g., urea), and 2) ultrafiltration to remove water. The amount of dialysate required by the hemodialyzer is ca. 300 l (Krajewska et al., 1988). Although it has been in clinical use for the past 5 decades, the standard artificial kidney is bulky, complex and expensive. Thus, several improvements have been considered. The enzyme urease, which catalyzes the hydrolysis of urea, has been considered for use in artificial kidney devices as a dialysate regeneration tool. The only dialysate regeneration system currently available for clinical use is the Organon Teknika Co. Sorbsystem® (originally known as the REDY® system). It utilizes a combination of enzymatic degradation, ion exchange, and carbon adsorption in different compartments to provide the desired dialysate composition. In this system, urease is immobilized on an aluminum support; a potential toxic risk. The presence of aluminum in dialysate has been associated with dialysis dementia (Alfrey, 1978) and bone disease (Ward et al., 1978).

In an attempt to alleviate the problems associated with the conventional hemodialyzer system, Chang (1964) proposed the use of microencapsulated urease as an alternative. In this system, urease is immobilized within ultra-thin, semi-permeable, non-toxic polymeric membranes as microcapsules which could be used

for dialysate regeneration or direct blood urea clearance purposes. Secondly, the urease could be coencapsulated with ion exchange resins for pH control. This may lead to a more portable configuration than the conventional system. Although this microcapsule artificial kidney concept is a great potential alternative to the conventional hemodialyzer, it is still at the experimental stages. Also, the delay in the development of this new concept is partly due to the lack of appropriate theoretical models for the characterization of the microencapsulated system. Dialysate regeneration or blood urea clearance involves the hydrolysis of urea to ammonia and carbon dioxide. Thus, the kinetics are influenced by pH fluctuations and product inhibition effects. Although several theoretical models have been developed to describe the hydrolysis of urea in various immobilized systems, the existing models are too general and therefore quantitative information on the specific impact of limiting factors, individually and in combination, on reactor performance is lacking. Models for predicting the performance of an immobilized urease artificial kidney (Levine and LaCourse, 1967; Lin, 1979; Moynihan et al., 1989) have been confined either exclusively to the kinetic behavior of the immobilized enzyme for steady-state reactor performance, or effects such as axial dispersion and enzyme denaturation have been neglected.

1.2 Objectives and Plan

The specific aims of this research are as follows:

1) Develop a theoretical model for dialysate regeneration using nylon microencapsulated urease in both a continuous stirred tank reactor (CSTR) and a fixed bed reactor (FBR). The steady-state model will be used to study the specific impact of individual and combined effects of kinetic limiting factors such as pH

kinetic effects, product inhibition, and substrate depletion. Such effects will be studied at various enzyme activities. Also, the influence of microcapsule diameter and external mass transfer resistances due to liquid film and membrane wall, on reactor performance will be addressed.

2) Develop a transient-state model for the simulation of a patient's blood urea clearance using a microencapsulated FBR artificial kidney system. In this simulation, the reactor design and the kinetic transients will be considered. The change in the patients blood urea level with time will be compared to the conditions in the connected artificial kidney (FBR).

CHAPTER 2. LITERATURE SURVEY

2.1 Introduction

Enzymes are responsible for catalytic activity within living cells and have been utilized by humans for thousands of years to catalyze various biochemical reactions. Berzelius (1835) developed the first general theory of catalysis and showed that diastase was better than sulfuric acid for catalyzing the hydrolysis of starch. Louis Pasteur (1869) speculated that fermentation of sugar to alcohol was catalyzed by enzymes. This led to the first extraction of the enzymes for alcoholic fermentation by Buchner (1897), who also showed that they were capable of functioning outside of the cells. Later, Sumner (1926) purified the enzyme urease and suggested that the enzyme was a protein devoid of organic coenzymes and metal ions.

Currently, several thousand enzymes are known with many having been isolated and studied. Enzymes are known for their highly reactive, highly specific nature. Although enzymes are active in free solution, retention of dissolved enzyme is economically not feasible upon completion of the reaction. Immobilization permits retention of enzyme within the reactor and facilitates recovery and reuse. General operational advantages of immobilized enzymes are reusability, possibility of continuous operational modes, and greater variety of engineering designs for continuous processes. Thus, immobilization has made the use of enzymes economically feasible.

In this chapter, many specific examples of immobilization techniques are reviewed. The properties and deactivation of the enzyme urease is briefly presented, followed by a discussion of its biomedical application as an artificial kidney. Various

studies presenting the kinetic modelling of urea conversion in the immobilized-urease reactor are also reviewed.

2.2. Enzyme Immobilization Techniques

The term "immobilization," may be defined as the physical confinement or localization of enzyme molecules during a continuous catalytic process. Methods for enzyme immobilization can be classified into three basic categories(see also Figure 2-1).

(1) Entrapment involves encapsulating the enzyme within semi-permeable membranes or incorporating enzymes into the lattice of a semi-permeable gel matrix.
(2) Carrier-binding involves attachment of the enzyme to water-insoluble supports. This method can be further divided into three categories according to the binding mode of the enzyme; that is, adsorption, ionic binding and covalent binding.
(3) Cross-linking involves intermolecular cross-linking of enzyme by means of bifunctional or multifunctional reagents.

The terms, "immobilization" and "insolubilization," are often erroneously used interchangeably in the literature. Zaborsky (1973) defines "insolubilization" as one of several methods that can be used for the immobilization of an enzyme. According to Zaborsky (1973), another common misconception is that enzymes entrapped within microcapsules or within the lattice structure of polymers are "insolubilized enzymes". These enzymes are only physically entrapped within a localized region and still have considerable diffusional freedom, retaining their inherent "solution" characteristics. They are simply restricted in their movements to the microenvironment of the matrix structure.

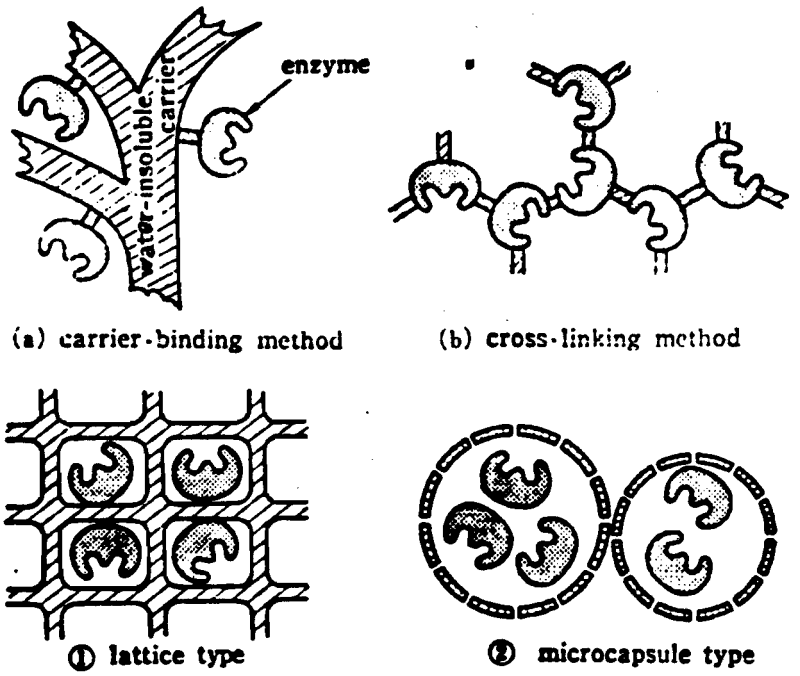

Figure 2-1

Schematic Diagrams of Immobilized Enzymes.

(Reproduced from Chibata (1978)).

This thesis is oriented toward techniques involving the microencapsulation of urease. Other approaches are surveyed briefly.

2.2.1 Entrapment Methods

As mentioned earlier, this method can be classified into microencapsulation and lattice entrapment.

2.2.1.1 Microencapsulation

During the past several decades, substantial activity has been directed toward the development of methodologies for the preparation of semipermeable membrane bound, aqueous core microcapsules for a wide variety of applications in the pharmaceutical and other industries. Applications include the encapsulation of drugs, cosmetics, foods, dyes, solvents, etc. (Chang, 1964, 1965, 1966, 1980; Gu, 1991; Neufeld et al., 1989; Poncelet et al., 1992). Several reviewers discuss a variety of processes and should be consulted for more details (Thies, 1975,1979; Bakan and Anderson, 1976; Watanabe and Hayashi, 1976; Kondo, 1979; Kydonieus, 1980). Chang (1965) demonstrated that microcapsules can be prepared with semi-permeable or perm-selective membranes to allow the selective interaction of the fluids inside and outside of the membrane. Prior to Chang (1965), non-permeable or slightly permeable membranes were used and release of the encapsulated material depended on the breakage of the membrane by pressure, heat or dissolution of the membrane itself (Zaborsky, 1973).

Encapsulation as a method for enzyme immobilization started with the "artificial cell" concept. Chang (1957), was the first to propose and demonstrate the feasibility of farming "artificial cells". Chang noted, "artificial cell is not a specific physical

entity. It is an idea involving the preparation of artificial structures of cellular dimensions for possible replacement or supplement of deficient cell functions" (Chang, 1972). Microencapsulation consists of enveloping microportions of enzyme solution within an ultrathin polymeric membrane. Membranes have been made of a variety of materials such as nylon, collodion, silastic, polystyrene, and cross-linked protein. The membrane is permeable to lower molecular weight solutes, but impermeable to larger molecular weight molecules such as proteins.

Although detailed procedures for microencapsulation have been described by Chang (1966, 1972, 1974b, 1976),the typical procedure for microencapsulation is as follows: the aqueous enzyme solution containing a water soluble polymerization monomer is emulsified in a water-immiscible organic solvent to form microdroplets. The size of the aqueous microdroplets depends on the speed of emulsification, the concentration of the emulsifying agent and the viscosity of the organic phase. The second reactive monomer (solvent soluble) is added to the stirred emulsion resulting in an interfacial polymerization reaction at the droplet surface. When membrane formation is complete, the microcapsules are filtered and the organic solvent washed away aided by an emulsifying agent, and stored in saline.

2.2.1.1.1 Properties of Microcapsules

Microcapsules are normally spherical as shown in Figure 2-2; however, cup-shaped, multiple microcapsules can also be produced. The mean diameter may range from a few microns to a few millimeters, depending on the speed of mechanical emulsification, surfactant concentration, and the viscosity of the organic liquid (Chang, 1965).

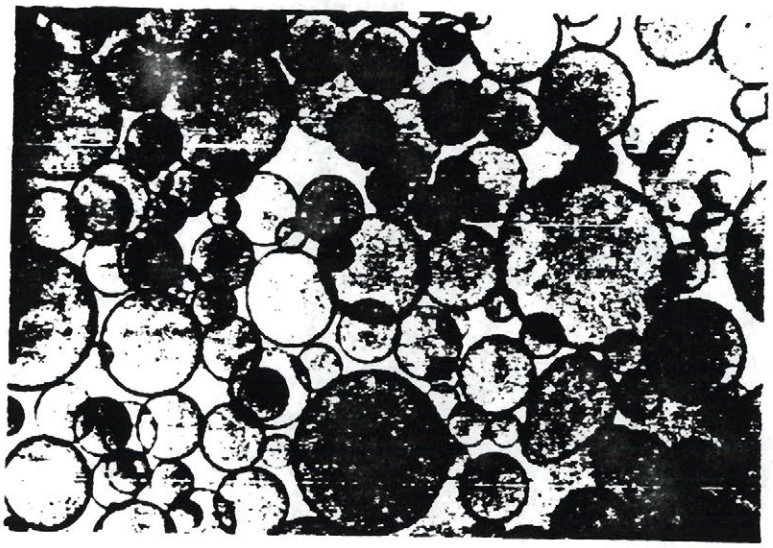

Figure 2-2

Photograph of Nylon Microcapsules.

(Reproduced from Chang (1972))

Typically the thickness of the membrane is about 0.02 μm (Chang, 1974a), which is influenced by a number of factors such as the time of capsule formation, organic solvent composition, and the concentrations and the chemical nature of the components used to make the membrane (Zaborsky, 1973). The equivalent pore radius of nylon microcapsules (270 μm in diameter and 0.02 μm thick) was found to be about 0.0018 μm.

Regarding net surface charge of nylon microcapsules, Chang et al. (1966) reported nylon microcapsules suspended in saline had no surface charge measurable by electrophoresis. On the other hand, negative charged nylon membranes were produced by the polymerization of 1,6-diaminohexane, 4,4'-diamino-2-2'-diphenyldisulfonic acid and sebacoyl chloride (Chang, 1964; 1965; Chang et al., 1966).

Many authors investigated the microencapsulation of urease (Chang, 1965, 1980; Chang and Malouf, 1978, 1979; Gu and Chang, 1988a, 1988b, 1990a, 1990b; Gu, 1991; Levine and LaCourse, 1967; Mogensen and Vieth, 1973; Sundaram, 1973; Lin, 1979, Miyawaki et al., 1979; Neufeld et al., 1984; Ortmanis et al., 1984; Dueck et al., 1986; Monshipouri and Neufeld, 1991, 1992). In the next section, some properties of microencapsulated urease are briefly reviewed.

2.2.1.1.2 Properties of Microcapsulated Urease

Microencapsulated enzyme molecules are free in solution; however, apparent changes in enzyme activity, Michaelis constant, etc. may occur because of diffusional effects in and/or within the membrane or enzymatically generated microenvironments (Zaborsky, 1973).

2.2.1.1.2.1 Activity

Zaborsky (1973) noted that the activity of a microencapsulated enzyme compared to the free enzyme has been reported to range from 10 to nearly 100%. The apparent activity of urease, enclosed within collodion microcapsules (mean diameter 100 μm) was found to be 20% as active as the urease in free solution (Chang et al., 1967). However, it is not clear whether this low urease activity was caused by inactivation, diffusion limitations or low encapsulation efficiency. According to Sundaram (1973), the activity of encapsulated urease within nylon membranes in the presence and absence of hemoglobin was 90% and 35% the activity of urease in free solution, respectively. No explanation was provided. Miyawaki et al. (1979) reported that urease enclosed within nylon membranes resulted in an activity of 78% compared to that of free urease.

Recently, Monshipouri (1991) noted that the lower apparent activity of encapsulated urease was probably caused by the inhibitory effect of both buffers and product, and difficulties in calculating the true mass yield of encapsulation. It was observed that the apparent activity of urease coencapsulated with hemoglobin was similar to that of free urease.

2.2.1.1.2.2 Michaelis Constant

Sundaram (1973) reported that the Michaelis constant of the enzyme increased upon encapsulation, the effect being more significant with large diameter microcapsules. Monshipouri (1991) noted that for free enzymes, K_m may be affected by enzyme conformational changes. On the other hand, for encapsulated enzyme, K_m may be influenced by substrate diffusion rate through the membrane besides enzyme

conformational changes. The K_m values reported for free and encapsulated urease in the literature are shown in Table 2-1.

Table 2-1.

Michaelis Constant of Urease

Free Urease K_m (mM)	Encapsulated Urease K_m (mM)	References
2.76	9.09	Sundaram (1973)
10.20	10.60	Miyawaki et al. (1979)
7.60	8.40	Monshipouri (1991)

The microencapsulation of enzymes offers a number of advantages compared to other forms of immobilization; the more important are as follows: (1) large surface area due to small diameters for contact of enzyme and substrate (Chang, 1974); (2) simultaneous immobilization of many enzymes in a single step (Zaborsky, 1974); (3) combinations of enzyme and/or buffers may be microencapsulated (Chang, 1977). However, if an interfacial polymerization reaction is employed for encapsulation, relatively severe conditions are encountered resulting in the loss of enzyme activity in some cases. Therefore, it is necessary to select the most suitable conditions for the encapsulation of various enzymes (Chibata, 1978).

2.2.1.2 Lattice entrapment

All lattice-type entrapment methods are based on mechanical, usually irreversible entrapment of enzyme molecules within the interstitial spaces of a network of a

water-insoluble constraining structure, such as a gel matrix. Entrapment of the enzyme is generally done by polymerizing an aqueous solution containing the polymerization monomer with the enzyme, in the presence of a crosslinking agent. Polyacrylamide and starch gels have been widely used in this manner (Pennington et al., 1968; Guilbault and Das, 1970; Mosbach and Larsson, 1970). This technique was first used by Bernfeld and Wan (1963), who entrapped trypsin, papain, amylase, ribonuclease, etc., in a gel lattice of polyacrylamide. This entrapment offers the advantage of mild reaction conditions minimizing enzyme alteration or inactivation. Two major drawbacks of the method are: 1)continuous loss of activity, because the distribution of pore sizes invariably leads to some that are large enough to permit loss of enzyme, and 2) large diffusional barriers to the transport of substrate and product lead to reaction retardation (Vieth and Venkatasubramanian, 1973). Urease has been immobilized by entrapment within gelatin (Bollmeier and Middleman, 1974), and acrylamide copolymers (Atkinson and Rousseau, 1977; Atkinson et al., 1977).

2.2.2 Carrier-binding method

This method can be subdivided into three categories, that is, adsorption, covalent binding and ionic binding.

2.2.2.1 Adsorption

Probably the earliest method of enzyme immobilization - adsorption - is also one of the easier and fastest methods (for review of early work, see Zaborsky, 1973, 1977; Mosbach, 1987). This method is based on the physical adsorption of enzyme protein on the surface of water-insoluble carriers, and causes little or no conformational

change of the enzyme protein, or destruction of its active center (Chibata, 1978). It consists of mixing the enzyme and the adsorbents, incubating for a time, and later filtering and washing off any unadsorbed enzyme (Scouten, 1987). The attachment may be due to one of several types of bonds, such as ion-ion, hydrophobic, coordinate-covalent or hydrogen or due to a combination of factors. The final bond strength will depend on maintaining a delicate balance of ionic strength, pH, and protein concentration. In addition, one must carefully control the temperature of the bonding reaction (Messing, 1976; Zaborsky, 1977). This method has the disadvantage that the adsorbed enzyme may leak from the carrier during usage, because the binding force between the enzyme protein and the carrier is weak.

Adsorption of urease has been achieved with kalinite clay (Sundaram and Crook, 1971), and with porous titanium (Messing, 1974a).

2.2.2.2 Covalent Binding

The covalent binding approach has been the most widely investigated. This method involves covalent coupling of enzymes to water-insoluble or water-soluble supports of various chemical and physical characteristics. The supports can be either organic or inorganic polymers. Terms used to describe the covalent formation between the enzyme and support include "fixation, attachment, binding, bonding, linkage, and coupling" (Zaborsky, 1973). The functional groups that take part in the covalent binding of enzyme to carrier are as follows; (1) α- or ϵ-amino; (2) α-, β-, or γ-carboxyl; (3) sulfhydryl ; (4) hydroxyl; (5)imidazole; and (6) phenolic groups.

Compared to adsorption methods, this technique results in greater difficulty in the selection of conditions for immobilization. Since the reaction conditions required for covalent attachment are not particularly mild, covalent linkage may alter the

conformational structure of the enzyme, resulting in loss of enzyme activity to a certain extent. Nevertheless, this method has the advantage that the binding force between carrier and enzyme is strong and enzyme leakage is not encountered even in the presence of substrate or salt solutions of high ionic strength (Chibata, 1978).

Various supports and binding schemes have been used for urease immobilization: binding to the diazo salts of various copolymers (Reisel and Katchalski, 1969), aminofunctional silane coupling onto glass (Weetall and Hersch, 1969), diazo coupling onto glass (Weetall,1971; Ramachandran and Perlmutter, 1976), binding onto controlled-pore titanium using a stannous bridge (Messing, 1974b), and reaction with aminoaryl-polyacrylamide modified nylon (Shemer et al., 1979).

2.2.2.3 Ionic Binding

This method is based on the ionic binding of enzyme protein to water-insoluble supports containing ion-exchange residues. As supports for ionic binding, polysaccharides and synthetic polymers having ion-exchange residues are used. The immobilization conditions are mild in comparison to those necessary for the covalent binding technique, reducing changes in conformation and the active site of the enzyme protein, resulting in immobilized enzymes having high activity. However, as the binding forces between supports and enzyme protein are weaker than in covalent binding, leakage of enzyme from the support may occur in substrate solutions of high ionic strength or upon variation of pH. More details are available in the literature (Chibata, 1978). Immobilization of urease by this method was first reported by Hofstee (1973). Urease with isoelectric points in the acid region was virtually irreversibly immobilized by mere adsorption to agarose (Sepharose 4B) substituted with either n-butyl-amine or n-octylamine.

2.2.3 Cross-linking

To eliminate the problem of enzyme loss due to leaching, a membrane/enzyme complex may be crosslinked using bifunctional reagents. Such reagents that induce intermolecular crosslinking can bind enzymes to solid supports. Examples of these reagents are: glutaraldehyde, bisdiazobenzidene 2,2'-disulfonic acid, toluene-2-isocyanate, 4-isothio-cyanate, and trichloro-s-triazine (Ogata et al., 1968; Barker et al., 1970; Bollmeier and Middleman, 1974). Cross-linking consists in formation of transverse covalent bonds between enzyme molecules, which thus form large insoluble enzymatic cross-linked particles. Enzymes may also be cross-linked with other inactive materials e.g. polymer membranes. Immobilization of enzymes via this technique eliminates some of the difficulties associated with other modes of immobilization; however, the problem with this technique is that it can be harsh, employing reagents that damage the three dimensional structure of the enzyme or the active site. In either case, there will be some loss of enzyme activity.

Gluteraldehyde, by far the most commonly used cross-linking reagent, has been employed for the immobilization of urease onto nylon (Sundaram and Hornby, 1970), glass (Ramachandran and Perlmutter, 1976), chitin (Iyengar and Rao, 1979), and molecular sieves (Iyengar et al., 1982).

2.3 Urease

2.3.1 Properties of urease

Urease is a hydrolytic enzyme which transforms urea into ammonia and carbon dioxide. Urease was first purified in a crystalline form by Sumner (1926) and the molecular weight determined to be 480,000 (Vasudevan et al., 1990), although

commercial varieties typically have a molecular weight of several million (Fishbean, 1969). The reaction catalyzed by urease is usually expressed as follows:

$$(NH_2)_2CO + H_2O \rightharpoonup 2NH_3 + CO_2$$

However, the literature outlines several other commonly used descriptions of urea hydrolysis such as:

$$(NH_2)_2CO + 2\,H_2O \rightharpoonup H_2CO_3 + 2\,NH_3 \quad \text{(Kissel, 1974)}$$

$$NH_3 + HCO_3^- \rightharpoonup NH_2COO^- + H_2O \quad \text{(Christensson et al., 1978)}$$

$$(NH_2)_2CO + H_2O \rightharpoonup HCO_3^- + 2\,NH_4^+ + OH^- \quad \text{(Moynihan, 1987)}$$

These disparate expressions are equivalent to each other in the sense that the products of urea hydrolysis exist in several ionic states in solution. Sumner et al. (1931) first demonstrated that ammonium carbamate is formed as one of the products of urea hydrolysis. Thus, the reaction proceeds through the steps of ammonium carbamate formation, followed by further breakdown to ammonia and carbon dioxide which then reacts with water to form bicarbonate and hydroxyl ions. Further details are available in the original literature.

2.3.2 Deactivation of Urease

Similar to traditional heterogeneous catalysts, enzymes also suffer from the common failing of being deactivated (or poisoned), often by reactants (substrates) and reaction products. Understanding mechanisms of enzyme deactivation is very important in biotechnology. Knowledge of deactivation mechanisms might not only be essential for optimal applications of enzymes in biotechnology (Mosbach, 1976),

but also lead to solution of problems of enzyme stabilization (Klibanov, 1983) and reactivation (Martinek et al., 1980). A comprehensive review of the molecular mechanisms of enzyme protein deactivation has been given by Mozhaev and Martinek (1982). In this section, deactivation studies on the enzyme urease only is reviewed. According to Chang (1965), urease is unstable in solution, but is more stable in the presence of 2 % gum arabic or 5 % egg albumin and very stable in the immobilized form. He investigated the stability of urease encapsulated within artificial cells. Urease encapsulated alone without the presence of hemolysate rapidly lost activity with half-life of three hours when stored at 37° C, whereas for the case of hemolysate-stabilized microencapsulated urease, the activity lasted about one week when held at 37° C and two weeks at 4°C.

Ramachandran and Perlmutter (1976), working with both diazo-coupled and glutaraldehyde-coupled urease immobilized on nonporous glass beads in a packed column reactor, reported that over a period of 7 days, the urease in both cases lost 17% of its original activity. These authors concluded that the loss in activity was due to denaturation rather than washing away of the enzyme.

Lencki (1987) offered a more detailed discussion of urease denaturation. He developed the quasi-native model of urease denaturation to clarify the confusion regarding the mechanisms of enzyme denaturation. He concluded that in general, the rate of enzyme denaturation is a function of solute concentration.

Vasudevan et al. (1990) conducted deactivation studies on the enzyme urease, and reported the results of experiments in a fixed-bed reactor and a CSTR containing urease immobilized on a nonporous support. They concluded that the effect of poisoning of urease by ammonia alone, which is a product in the decomposition of

urea, points to a poisoning mechanism where the product attacks the free form of the enzyme.

2.4 Kinetic Modelling of Immobilized-Urease System

Several studies have appeared in the literature on modelling the immobilized urease enzyme reactor (Levine and LaCourse, 1967; Mogensen, 1972; Sundaram, 1973; Lin, 1979, Neufeld et al., 1984; Ortmanis et al., 1984; Dueck et al., 1986; Moynihan et al., 1989; Monshipouri, 1991). In fact, such kinetic models contribute to the understanding of the phenomena occurring inside the reactor, besides providing a basis for rational reactor design strategies. Also, mathematical models allow one to identify rate-limiting steps and hence focus efforts at process improvement in the proper areas. In this section various mathematical models describing the kinetics of urea hydrolysis by immobilized-urease will be briefly presented.

Levine and LaCourse (1967) developed a design theory for a compact artificial kidney utilizing microcapsules containing urease, ion exchange resin, and adsorbents for uric acid and creatinine. The study which was confined to the steady state case, concluded that it should be possible to construct a compact artificial kidney with dimensions of 2 cm in diameter and 10 cm in length, using the multicomponent microcapsules.

Mogensen and Vieth (1973) analyzed the steady-state operation of a column packed with urease microcapsules. Using transport models for mass transfer, analytical solutions for the cases of diffusion alone or with first-order irreversible reaction were developed. The collodion membrane permeability (mass transfer coefficient) for urea was determined to be 10^{-5} m/sec.

In the study reported by Sundaram (1973), urease was encapsulated both in the presence and absence of the protein hemoglobin. The K_m values were seen to increase upon encapsulation, with larger capsules showing a greater increase. The encapsulated urease was reported to follow Michaelis-Menten kinetics with optimum activity occurring at lower pH values than for the native urease in free solution. A theory was proposed to investigate the effects of diffusion and mass transfer on the Michaelis-Menten kinetics of the encapsulated urease. The model predicted that membrane resistance would control relative to internal and external mass transfer for capsules with diameters in the microcapsule range (< 200 μm).

The model, which was based on initial rate experiments, did not account for the inhibitory effect of product (ammonium ions), thus the model may not predict inhibition kinetics over the full course of reaction. In fact, the focus of the present study is on the long-term behavior of a reactor containing immobilized urease. Initial rate measurements were also made by Laidler and Hoare (1949), who found that as the reaction proceeded, the rate gradually decreased even without significant substrate depletion.

Ramachandran and Perlmutter (1976) immobilized urease from Jack bean on nonporous glass beads by covalent bonding and the kinetics were studied in a packed-column differential reactor. To facilitate comparison, the urease was immobilized by both diazo and glutaraldehyde coupling. The kinetic properties of immobilized urease were similar to those of the soluble enzyme and different immobilization methods did not appreciably alter the kinetic properties.

Atkinson et al. (1977a,b) investigated the influence of pH on rate of reaction and overall rates of reaction of unbuffered gel-immobilized urease particles. An apparatus was devised which allowed a rapid determination of the hydrogen ion

concentration in the center of a particle for any given size, urease and urea concentration, and external pH. The pH at the center of the particle was seen to approach the self-buffering pH of 8.83 with an increase in particle size and enzyme concentration.

Bollmeier and Middleman (1979) presented experimental results and appropriate mathematical models to elucidate and separate the effects of mass transfer and immobilization on the apparent kinetics of the hydrolysis of urea by urease immobilized within a crosslinked gelatin film. Diffusion of urea through the gelatin matrix appeared to exert the major influence on the observed kinetics. Because of diffusion resistance, the reaction products led to an increase pH level which remained high within the gelatin matrix. For pH levels in the 6.7 to 9.0 range, the activity of urease was a strongly decreasing function of pH.

Lin (1979) proposed a model for predicting the performance of an artificial kidney. A plug flow equation, incorporating the internal and external urea diffusion resistances in the microencapsulated urease particle, was employed to describe the urea transport in the blood flow. Results of numerical simulation indicated that the urea diffusion resistances played a dominating role in the determination of urea removal from the artificial kidney. Effects of other physical parameters, such as the urea concentration in the microcapsules, the membrane thickness and the partition coefficient between the membrane and the urease solution, on the performance of the artificial kidney were found to be of less significance.

Ortmanis and Neufeld (1984) constructed theoretical curves relating substrate conversion, substrate feed concentration and enzyme content based on a mathematical model for a continuous feed stirred tank reactor (CSTR) and experimentally verified them for the microencapsulated urease. The proposed model

was derived from the Michaelis-Menten relationship. It was concluded that microencapsulated urease in a CSTR reactor may be described by a model based on Michaelis-Menten kinetic principles.

With a fluidized bed reactor containing microencapsulated urease, Neufeld et al. (1984) studied the hydrolysis rates of urea under various operating conditions. The percentage degradation of urea was observed to be inversely proportional to the mean diameter and proportional to the volume of capsules. It was suggested that this may be due to mass transfer limitations affecting reaction rate, and that the phenomena of the degradation enhancement observed may be due to the pH effect. The optimum pH of the free urease was noted to be 6, the collodion membrane that enclosed the urease was negatively charged and that protons, being positively charged, were trapped inside the capsules. Hence the pH inside the capsule could be less than the measured pH in the bulk phase. In the case of a nylon membrane, Sundaram (1973) reported that a pH gradient usually develops as a result of the presence of charges on the solid phase. However, except at extremes of pH, the net effective charge on the nylon is zero so that no pH gradient should develop for this reason.

Dueck et al. (1986) encapsulated urease in ultra-thin semi-permeable cellulose nitrate membranes and studied hydrodynamics and urea hydrolysis in a fluidized bed reactor. A liquid-fluidized bed was studied as the reactor type because of the low shear environment suitable for the fragile microcapsules. Problems such as breakage of the microcapsules as observed in a CSTR (Ortmanis et al., 1984), or deformation or plugging as experienced in a packed bed (Chang, 1966) were avoided. It was concluded that there was evidence for both internal mass transfer limitations at high

superficial velocities and large microcapsule diameter, and external mass transfer limitations at lower superficial velocities.

Arbeloa et al. (1986) measured hydrolysis of urea under conditions simulating that of an artificial kidney device as a function of reactor residence time, microcapsule diameter, volume of microcapsules, urea concentration in the feed, and urease activity. Empirical correlations were developed based on dimensional analysis in order to predict urea conversion within the range of experimental operating conditions. It was concluded that the design of a microencapsulated-urease reactor must take into account the mass transfer limitations imposed by the membrane-bound microcapsules.

Moynihan et al. (1987) studied urea hydrolysis by urease immobilized onto ion exchange resins in a fixed-bed reactor. A modified Michaelis-Menten rate expression was used to describe the pH-dependent, substrate- and product-inhibited kinetics. Ionic equilibria of product and buffer species were also included to account for pH changes generated by reaction. An effectiveness factor was used to describe the reaction-diffusion process within the particle phase. This immobilized urease system exhibited quite different kinetic behavior from soluble urease because the pH near the enzyme active sites is different from that of the pore fluid. This effect resulted in a shift of the optimal pH value of V_{max}(pH) curve from 6.6 (soluble urease) to ca. 7.6 in dialysate solution, and ca. pH 8.0 in 20 mM phosphate buffer.

Recently, Monshipouri (1991) reported experimental results relating to two main objectives: 1) determining whether the low activity yield is an inherent property of enzyme microencapsulation; 2) to examine the impact of diffusional restriction caused by the membrane on the kinetics of microencapsulated urease. Some of conclusions drawn by this author were as follows: 1) Activity yields reported in the

literature seemed to underestimate the true activity yield of microencapsulated urease; 2) The apparent activity of urease co-encapsulated with hemoglobin was similar to that observed for pure urease microcapsules; 3) The apparent activity of urease microcapsules was closely similar to that of released urease from microcapsules, which suggested minimal effects of diffusion and mass transfer limitation on the activity of microencapsulated urease; 4) Ionic interactions between the charged product (e.g. NH_4^+) and the nylon membrane were not present.

2.5 Artificial Kidney Devices

2.5.1 The kidneys

The kidneys are two organs located in the back center of the abdominal cavity. The function of the two kidneys is to clear the blood of body wastes, processing up to 1500 cc of blood each minute (Cooney, 1976). The daily excretion of body wastes is listed in Table 2-2.

The amount of water and urea excreted varies with body mass, diet, and intake of water. Normal renal function includes the following processes: removal of the end products of metabolism such as urea, uric acid, creatinine, ammonium, sulfates, and phenol; regulation of the body chemistry; regulation of the amount of water in the body, to prevent edema and hypertension; and removal of the substances that are not utilized or metabolized in the body, such as drugs and
toxins, thus preventing renal poisoning.

When the normal functioning of the kidney stops or deteriorates due to disease, the patient becomes progressively ill; metabolic waste products, excess electrolytes

Table 2-2

Daily Waste Production in Normal and Uremic Persons (from Cooney, 1976)

Component	Normal man (g/day)	Uremic patient (g/day)[a]
Water	1500	300[b]
Urea	30	12
Creatinine	0.6	0.2
Uric acid	0.9	0.4
Na^+	5	0.4
Cl^-	10	1.2
K^+	2.2	0.5
Ca^{+2}	0.2	0.1
PO_4^{-3}	3.7	1.8
HSO_4^-	8.2	—
Phenols	Trace	—

Note a: Based on strict dietary control of protein, sodium, water, etc.

b: May vary considerably.

When the normal functioning of the kidney stops or deteriorates due to disease, the patient becomes progressively ill; metabolic waste products, excess electrolytes and water accumulate in his body, and the chemical balance is upset and death may occur within days. Intermittent treatment with a mechanical device like the artificial kidney will reduce the accumulation of waste products and water, and thus the blood concentrations of these substances are returned to near normal levels (see Figure 2-3).

2.5.2 Current Approaches for Urea Removal

In this section, current apprpoaches for the removal of urea and other waste metabolites in chronic renal failure will be introduced.

2.5.2.1 Conventional Artificial kidney

To aid malfunctioning human kidneys, well-elaborated medical devices, the hemodialyzer, or conventional artificial kidney as it is called, have been in clinical use since 1943 when a prototype was developed by Kolff in Holland (Kolff and Berk, 1944). The artificial kidney can remove waste metabolites and water and maintain chemical equilibrium sufficiently to return the patient to a nearly normal condition for several days. Currently there are approximately 400,000 patients worldwide being kept alive by hemodialysis (Nosé, 1990), and among them about 100,000 people in the United States (Kolff, 1990).

Hemodialysis is the procedure to clear the body of metabolic wastes and excess species. Blood from a major vessel is fed to a device containing a membrane which separates the blood from a dialysate solution, and the partially cleansed blood is circulated back to the body (see Figure 2-4). The membrane is normally of a porosity such that all species except proteins and blood cells can potentially transfer. The rate

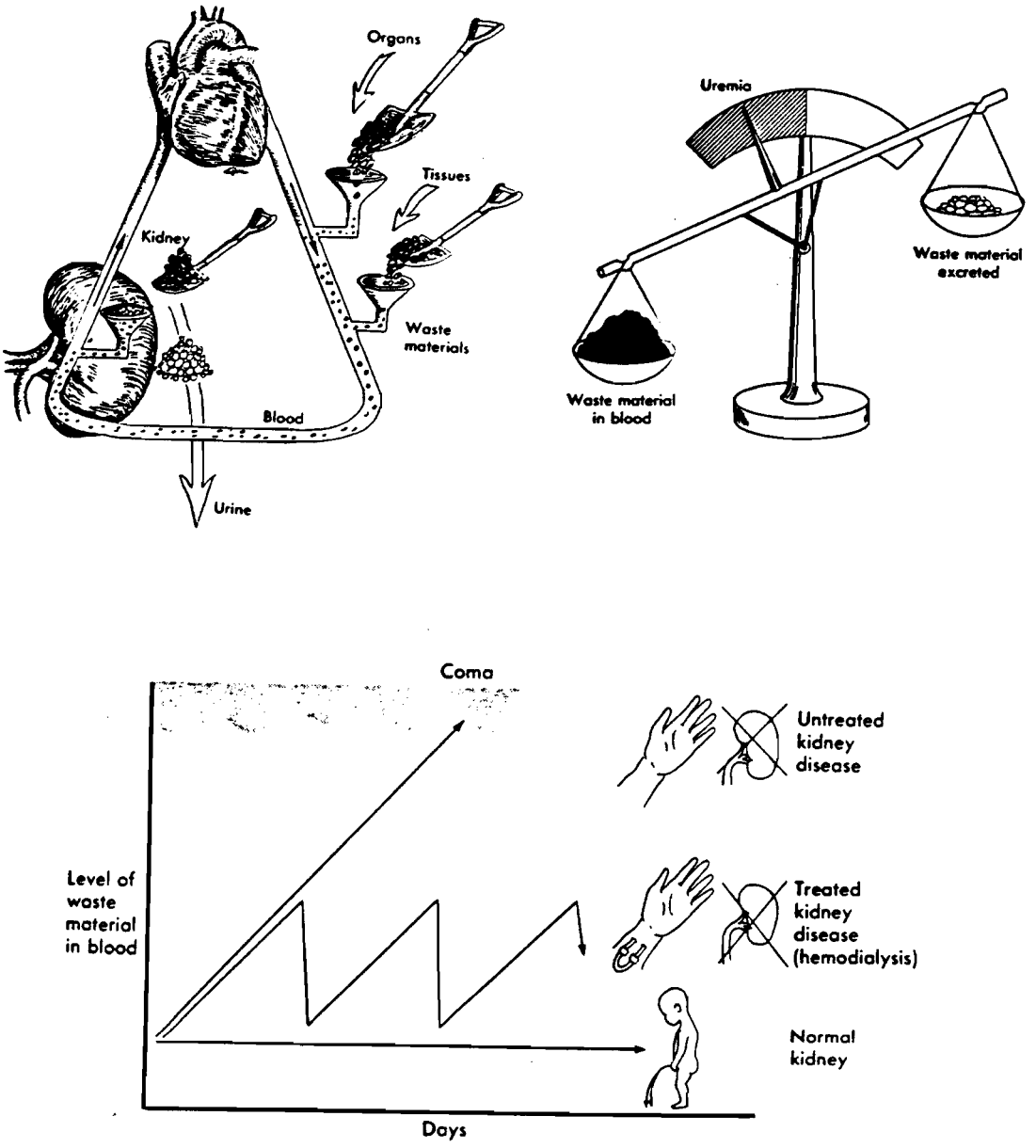

Figure 2-3

Dysfunction of the Kidneys — Correction by Hemodialysis. (Reproduced from Nosé (1969))

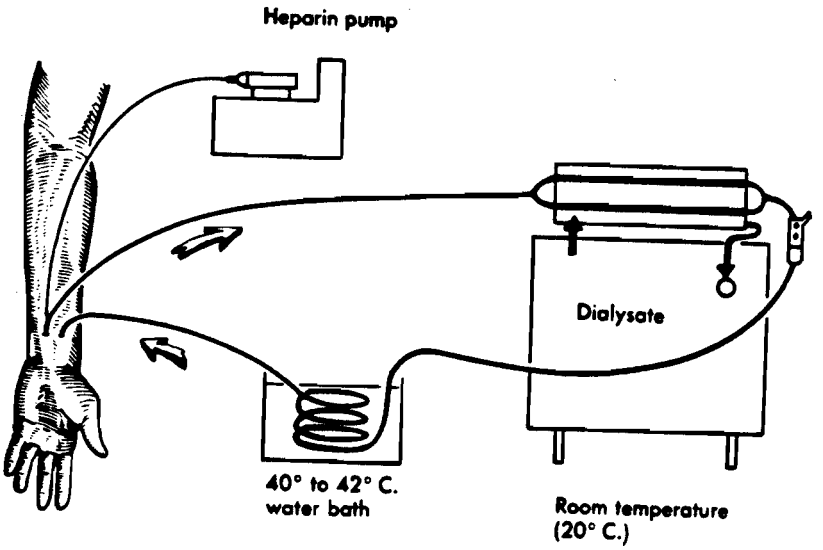

Figure 2-4

Tubing system for the blood circuit.

(Reproduced from Nosé (1969))

of waste metabolites depends on a number of factors, such as membrane thickness and total membrane area available for diffusion. By effectively removing waste metabolites from blood, the hemodialyzer replaces the function of the natural kidneys and is able to maintain the patient close to a normal condition.

Although hemodialysis has been effective for the treatment of kidney failure, there are a number of problems related to its use. The conventional artificial kidney is a bulky, heavy, complex and expensive machine, difficult to handle limiting mobility of the patient (Chang, 1978). Furthermore, in addition to the time required for treatment (6-12 hours three times a week), the cost involved for this treatment is prohibitive. The amount of dialysate required by a standard artificial kidney for each hemodialysis is ca 300 l (Krajewska et al., 1988). Thus 900 liters per week are required for 3 treatments (Drukker et al., 1983). The dialysate (a typical composition is given in Table 2-3) is an aqueous solution similar in composition to the normal body fluids except that it contains no wastes. Therefore, the body fluid contacted with the dialysate will lose urea, creatinine, uric acid, sulfates, phenols, etc., to the dialysate by diffusion across the membrane. The dialysate is expensive and requires a complex preparation procedure.

Therefore, a large amount of research has been carried out to simplify the machine and to reduce its size (Walker et al., 1977; Denti and Biagini, 1977; Kolff, 1978; Shettigar and Reul, 1982). Dialysate regeneration has reduced the amount of dialysate recirculated in the machine. In a regeneration system, dialysate undergoes physico-chemical processes which remove uraemic metabolites.

Table 2-3

Typical dialysate composition (from Cooney, 1976)

Component	g/L	Component	meq/L
NaCl	5.8	Na^+	132
$NaHCO_3$	4.5	K^+	2.0
KCl	0.15	Cl^-	105
$CaCl_2$	0.18	HCO_3^-	33
$MgCl_2$	0.15	Ca^{2+}	2.5
Glucose	2.0	Mg^{+2}	1.5

2.5.2.2 Dialysate Regeneration

The basic process applied in dialysate regeneration is adsorption. Of all adsorbents for uraemic metabolites tested, activated charcoal appears to be the best (Winchester, 1977; Gordon, 1978). The only problem connected with its use is a low affinity for urea (Davis, 1975; Denti and Biagini, 1977; Gordon et al., 1978). To solve this problem a two-step system for urea removal from dialysate was proposed (Krajewska et al., 1988) constituting of urea hydrolysis catalyzed by the enzyme urease and subsequent adsorption of resulting products, NH_4^+ and CO_3^{-2} on ion exchangers. This is the principle of the "Redy® dialysis system" developed by Gordon's group in Los Angeles in 1971 and 1972. (Gordon et al., 1969, 1978; Scott et al., 1975; Maxwell et al., 1975). This system has been extensively tested (Gordon et al., 1969; Shapiro et al., 1978; Shaldon et al., 1978), and until now has proven to be the only complete, comparatively small dialysate regeneration system of practical use.

Figure 2-5 illustrates the principles of the circulation systems of the machine. The dialysate reservoir (A) may hold a coil dialyzer, or the short circuit (C) may be opened to let the dialysate pass through other types of dialyzers. The negative pressure valve (B) and a temperature control device (J) are placed before the dialyzer. After the dialyzer, a dialysate pressure manometer (D), a blood leak detector (E), and a dialysate pump are placed before the adsorption cartridge (F).

On use of a coil dialyzer in the dialysate reservoir, the circulation pump (1) serves to pump the dialysate through the dialyzer, while mixing the dialysate when a dialyzer outside the machine is being used. Ultrafiltered fluid may flow into a special reservoir (H) or may collect in the reservoir for dialysate (A). The infusate system (3) provides the dialysate with a continuous supply of calcium, magnesium and, if wanted,

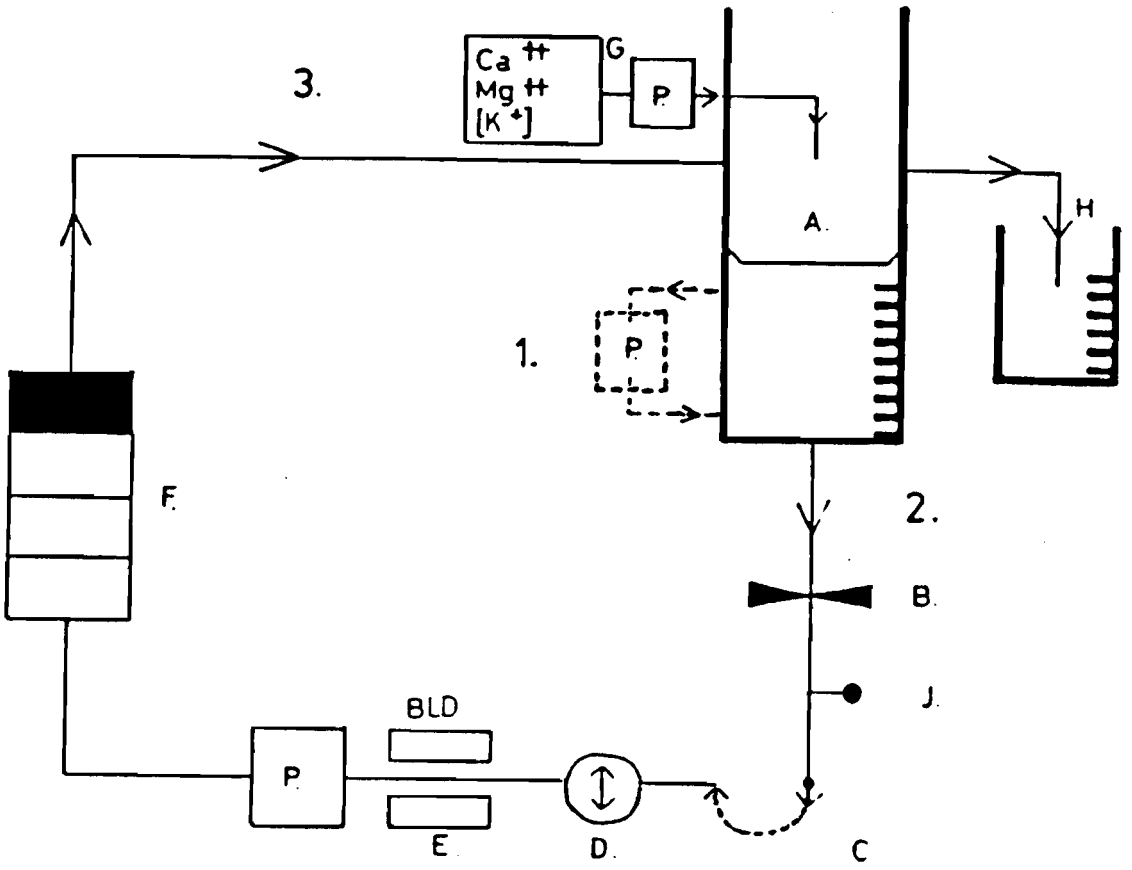

Figure 2-5

Schematic Illustration of the Composition of the Circulation Systems in the REDY® Machine; for Explanation see Text. (Reproduced from Nielsen (1976))

potassium from an infusate reservoir (G), pumped slowly into the dialysate reservoir by a roller pump (P). The adsorption cartridge (F) consists of four layers, through which dialysate is perfused, as shown on the drawing in Figure 2-6. The bottom layer contains alumina particles (aluminum oxide) on which there is partially immobilized urease which splits the urea into ammonia and carbon dioxide. The second is a layer of zirconium phosphate which serves as a cation exchanger to remove NH_4^+. It also removes Ca^{+2}, Mg^{+2} and K^+ in exchange for Na^+ and H^+. The third is a layer of hydrated zirconium oxide which serves as an anion exchanger to remove CO_3^{-2}, HCO_3^-, as well as PO_4^{-3} and SO_4^{-2} in exchange for Cl^- or CH_3COO^- depending on the preparation of the exchanger. The last layer contains activated charcoal which adsorbs the rest of such nitrogenous uraemic metabolites as creatinine, uric acid, organic acids, and phenols. The weight of the system is 3.5 kg; the system normally requires 5 l of dialysate but will function with as little as 1.5 l of dialysate (Gordon et al., 1978; Maxwell et al., 1975; Klein and Holland, 1980).

A series of questions has been raised on the capacity of the regenerating cartridge, on possible bacteriological problems in the use of the system, on the possible leakage of potentially toxic substances from the system, and on the efficiency of the system to correct the metabolic acidosis of uraemic patients. Whether all these questions can be resolved is a question that shall have to be answered with time. Despite many disadvantages, the Redy® system remains the only dialysate regeneration in practical use (Klein and Holland, 1980). Attempts have been made to modify the original design of the Redy system; however, most of them concern the layers of urease and ion exchangers.

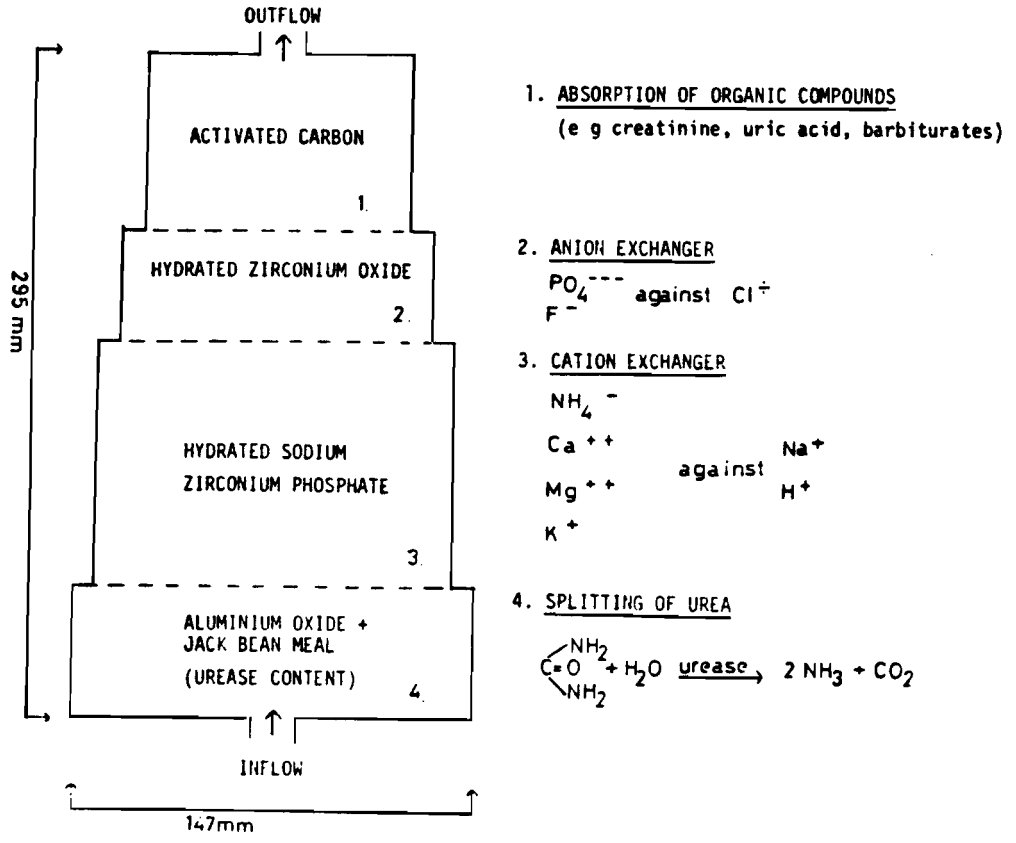

Figure 2-6

Schematic Illustration of the Absorption Cartridge with Indication of the Effect of the Four Layers.
(Reproduced from Nielsen(1976))

2.5.2.3 Microcapsule Artificial Kidney

With the thought that different approaches may also contribute to the further development of an improved artificial kidney, Chang (1964) initiated investigations into the possible uses of artificial cells as the basis for the construction of an artificial kidney (see Fig. 2-7). Each of the artificial cells consist of a spherical ultrathin polymer membrane enveloping a microdroplet of hemoglobin and enzymes from hemolysate. The membranes of artificial cells were initially made of ultrathin (0.05 μm) cellulose nitrate (Chang, 1957). Later, many other types of synthetic polymers such as Silastic rubber (Chang, 1966) and those prepared from interfacial polymerization (Chang, 1966; Chang et al., 1966) were used.

The basic principle in the use of artificial cells for the construction of compact artificial kidneys was first proposed in 1966 (Chang, 1966). According to Chang (1972), the concept in the construction of a compact artificial kidney from semipermeable artificial cells is as follows: With 10 ml of 20 μm diameter artificial cells packed in a column, the total membrane area (about 2 m^2) available for diffusion should be greater than that of a conventional artificial kidney. In the case of the standard dialyzers used as artificial kidneys, the total membrane area used is 1 m^2. Any extensive increase in the total surface area will result in an undesirable increase of the priming volume of the dialyzers. In dialyzers, the membrane thickness is usually about 20 μm, since with thinner membranes there would be problems of membrane leakage or breakage. Moreover, since the membrane thickness (less than 0.05 μm) is at least two order of magnitude less than that in the conventional artificial kidney (20 μm), metabolites from blood flowing past these artificial cells can cross the membrane into the artificial cells at least 100 times faster than in standard artificial kidneys. Chang (1974) noted, "If one were to use a volume of microcapsules

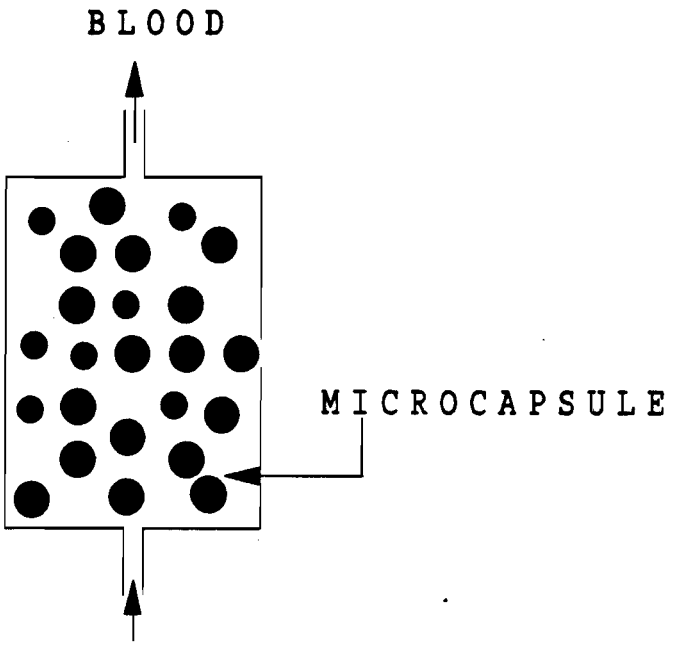

Figure 2-7

Schematic Illustration of 'Microcapsule Artificial Kidney'. (Modified from Chang (1977))

compared to the total priming volume of the standard 1 m^2 dialysis system (approximately 300 ml), the theoretical initial transport rate would be at least 6000 times higher in the case of 10 μm microcapsule and 50 times higher in the case of the very large 200 μm microcapsule." Chang (1972) reported that the theoretical basis for a small, compact artificial kidney can be established if something can be placed inside the artificial cells to trap or act on the metabolites which cross the membrane.

At this point it should be pointed out that alternatives to hemodialysis for urea removal are still at the experimental stage. In the main, these methods can be divided into three categories: 1) adsorbents that bind urea directly; 2) co-immobilized urease and an adsorbent which adsorbs the ammonium ions liberated from urea; 3) microencapsulated multi-enzyme systems for the conversion of urea and ammonia into essential amino acids (Gu, 1991). In the first case, oxystarch, one of adsorbents for urea, has been extensively studied (Friedman et al., 1976; Giordano, 1980; Sparks et al., 1971). However, the problem with this adsorbent is that the ingestion of a large amount of oxystarch produces side effects, such as diarrhoea, nausea, etc.

Next, the conversion of urea into ammonia, which is then removed by adsorbents (e.g., activated charcoal), constitutes another method of removing urea. Chang (1966) reported that microencapsulated urease effectively reduced urea levels in animals, with the resulting ammonia removed by coencapsulated ion exchange resins (Chang, 1966; Sparks et al., 1969).

Thirdly, regarding microencapsulated multi-enzyme systems for urea removal, T.M.S. Chang's Group at the Artificial Cells and Organs Research Center of McGill University in Montreal has been at the forefront of the research to find improvements of artificial organs including the artificial kidney. Using a special nylon polymer, a multi-enzyme system was encapsulated, that converts ammonia and

urea into three essential amino acids-valine, leucine and isoleucine. Since Cousineau and Chang (1977) published their observations of a multienzyme system consisting of urease, L-glutamic dehydrogenase, and glucose-6-phosphate dehydrogenase, many ingenious approaches have been used to study microencapsulated mutienzyme systems (Chang and Malouf, 1978; Chang and Malouf; 1979; Gu and Chang, 1988a, 1988b, 1990a, 1990b, Gu, 1991, Alsugair and Chang, 1991).

CHAPTER 3

THEORY AND NUMERICAL SOLUTION

3.1 General Theory

Urease catalyzes the hydrolysis of urea to ammonia and carbon dioxide as follows:

$$(NH_2)_2CO + H_2O \rightleftharpoons 2\,NH_3 + CO_2 \tag{3-1}$$

In aqueous medium, the product species produced by urea hydrolysis can exist in several ionic states. The inter-conversion of ionic species is coupled with the process of hydrolysis since both events occur simultaneously. An acetate/bicarbonate buffer (unless otherwises stated) will be considered for the development of the theory. Assuming that the ionization processes are rapid compared to the formation and breakdown of the enzyme-substrate complex, then each component reaction in the system will be in equilibrium. Therefore, the appropriate ionization reactions can be summarized as follows:

$$NH_4^+ \rightleftharpoons H^+ + NH_{3(aq)}; \quad K_1 = 5.60 \times 10^{-10}\ [M] \tag{3-2}$$

$$H_2CO_3 \rightleftharpoons H^+ + HCO_3^-; \quad K_2 = 5.61 \times 10^{-11}\ [M] \tag{3-3}$$

$$HCO_3^- \rightleftharpoons H^+ + CO_3^{2-}; \quad K_3 = 4.30 \times 10^{-7}\ [M] \tag{3-4}$$

$$H_2O \rightleftharpoons H^+ + OH^-; \quad K_4 = 1.0 \times 10^{-14}\ [M] \tag{3-5}$$

$$CH_3COOH \rightleftharpoons H^+ + CH_3COO^-; \quad K_5 = 1.86 \times 10^{-5}\ [M] \tag{3-6}$$

where, K_j's (j=1,,,5) denote the ionization equilibrium constants for the respective reactions. The rate of substrate reaction, R_s, is described by a modified Michaelis-Menten equation, taking into account the inhibition by urea and ammonium ions, and pH-dependent kinetic constants (Moynihan et al., 1989), as follows:

$$R_s = \frac{V_m E S}{(S + K_m + S^2/K_s)(1 + P/K_i)} \tag{3-7}$$

where, E, $S$and Pdenote the concentration of urease (enzyme), urea (substrate) and ammonium ion (product) respectively, and $K_s$and $K_i$are the substrate and product inhibition constants. V_m and K_m are the pH dependent maximum reaction velocity and Michaelis constant respectively which may be expressed as follows (Dixon and Webb, 1964):

$$V_m = V_{m,o} \frac{1}{1 + K_{es1}/H^+ + H^+/K_{es2}} \tag{3-8}$$

$$K_m = K_{m,o} \frac{1 + K_{e1}/H^+ + H^+/K_{e2}}{1 + K_{es1}/H^+ + H^+/K_{es2}} \tag{3-9}$$

where, $V_{m,o}$ and $K_{m,o}$ are the pH independent maximum reaction velocity and Michaelis constant, respectively. The parameters K_{e1} and K_{e2} are the ionization equilibrium constants of the enzyme, whereas K_{es1} and K_{es2} are the equilibrium constants of the enzyme-substrate complex.

3.1.1 The General Conceptual System

The conceptual system consists of urease microencapsulated within nylon membranes by the method of interfacial polymerization (Chang et al., 1966; Ortmanis and Neufeld, 1984). The capsules are sieved to obtain a uniform particle size distribution. The enzyme (urease) is enclosed within a thin semipermeable nylon membrane as shown in Fig. 3-1. The microcapsules are loaded into a CSTR or a FBR at a given void volume for the purpose of dialysate regeneration or blood cleansing. The conceptualized CSTR and FBR configurations operating on a once-through basis are shown in Figs. 3-2 and 3-3, respectively.

3.1.2 Major Assumptions

The following assumptions were made in formulating the mass balance equations for simulation of urea hydrolysis in a CSTR or FBR with microencapsulated urease:

Figure 3-1.

Cross section of membrane-bound microcapsule containing urease in solution

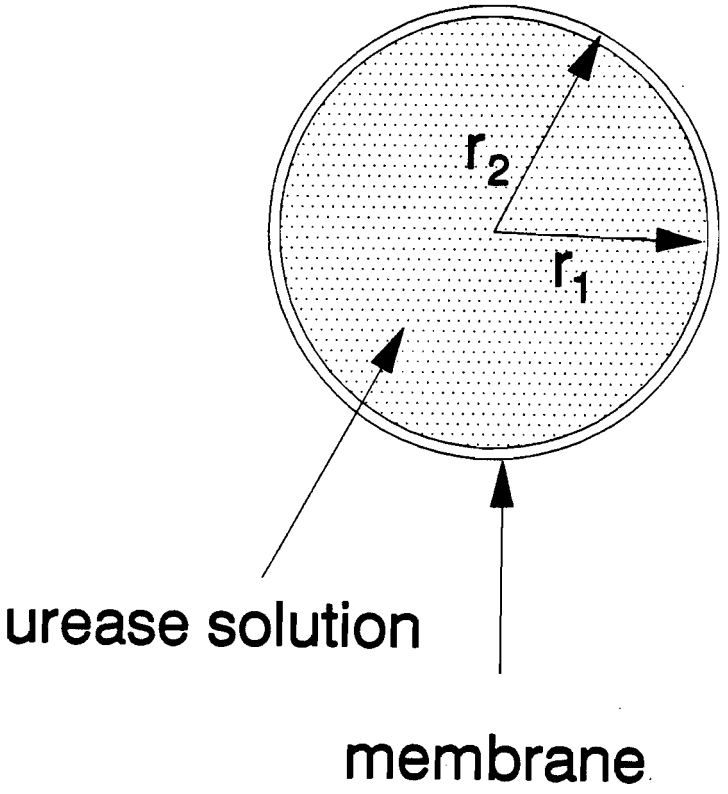

Figure 3-2.

Illustration of CSTR containing microencapsulated urease

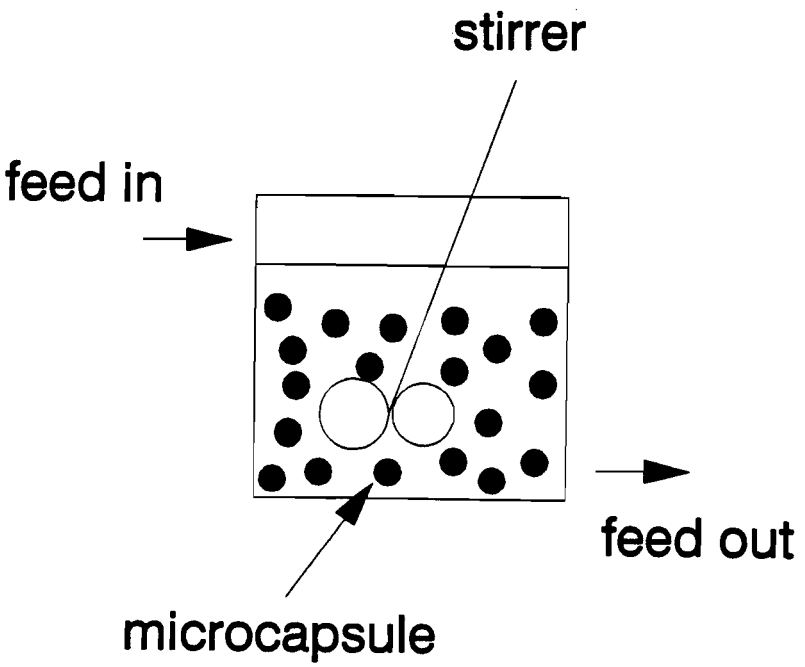

Figire 3-3.

Schematic Diagram of Fixed-Bed Reactor Containing Microcapsules

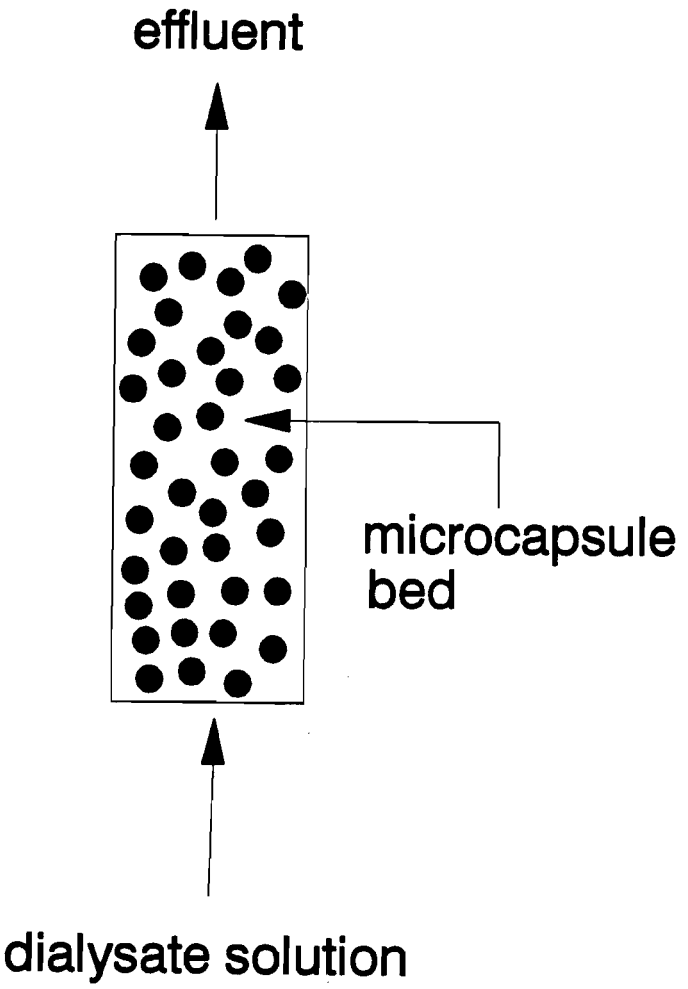

(a) mass transport through and within the semipermeable membrane takes place by passive molecular diffusion.

(b) external transport takes place by passive molecular diffusion and convection.

(c) the enzyme reaction rate is described by a modified Michaelis-Menten form, which accounts for the substrate and product inhibition, and pH-dependent kinetic constants.

(d) no interactions exist among the enzyme, the diffusing solutes, and the encapsulating membrane.

(e) enzyme is uniformly distributed in the enzyme phase of the microcapsule.

3.2 Model: Regeneration of Dialysate Solution

In this section the concepts underlying a model for dialysate regeneration using microencapsulated urease will be described. This will be followed by a discussion of the necessary equations and the method of solution.

3.2.1 Material Balance Equations

The determination of the conditions within a microencapsulated urease reactor requires the solution of the governing differential equations describing the mass balance inside the microcapsule as well as that in the bulk phase.

3.2.2 Intraparticle Mass Balance

The medium in the reactor may consist primarily of twelve species (urea, NH_4^+, NH_3, H_2CO_3, HCO_3^-, CO_3^{2-}, CH_3COOH, CH_3COO^-, H^+, OH^-, Na^+, Cl^-). The required twelve equations can be reduced to four by combining the equations for the product

species (i.e., Eqs. 3-2 to 3-5). Therefore, specific balance equations within the microcapsule can be expressed as follows:

$$\frac{dC_{s,1}}{dt} = -\nabla \cdot N_{s,1} - R_s \tag{3-10}$$

$$\frac{dC_{NH_4^+,1}}{dt} = f_{NH_4^+} \{ -\nabla \cdot (N_{NH_4^+,1} + N_{NH_3,1}) + 2R_s \} \tag{3-11}$$

$$\frac{dC_{HCO_3^-,1}}{dt} = f_{HCO_3^-} \{ -\nabla \cdot (N_{H_2CO_3,1} + N_{HCO_3^-,1} + N_{CO_3^{2-},1}) + R_s \} \tag{3-12}$$

$$\frac{dC_{CH_3COO^-,1}}{dt} = f_{CH_3COO^-} \{ -\nabla \cdot (N_{CH_3COOH,1} + N_{CH_3COO^-,1}) \} \tag{3-13}$$

where

$$f_{NH_4^+} = \frac{H^+}{H^+ + K_1} \tag{3-14}$$

$$f_{HCO_3^-} = \frac{1}{1 + \frac{H^+}{K_2} + \frac{K_3}{H^+}} \qquad (3\text{-}15)$$

$$f_{CH_3COO^-} = \frac{K_5}{H^+ + K_5} \qquad (3\text{-}16)$$

In these equation, N is the molar flux and R_s is the rate of urea removal. The subscript 1 denotes the enzyme phase. The concentration of Na^+, Cl^- species would be constant throughout the reactor since it is not involved in any of the reactions. At any given time, a balance of charges in the enzyme solution require that

$$\{-\nabla(N_{H^+,1} + N_{NH_4^+,1})\} - \{-\nabla(N_{OH^-,1} + N_{HCO_3^-,1} + 2N_{CO_3^{2-},1} + N_{CH_3COO^-,1})\} = 0 \qquad (3\text{-}17)$$

Fickian diffusion is often used to describe the transport of species within the microcapsule. However, the molecular dynamics of diffusing ions may affect the molar flux of other species. Therefore, the Nernst-Planck equation (Bard and Faulkner, 1980) will be adopted as follows :

$$-N_{i,1} = D_{i,1}\left(\nabla C_{i,1} + C_{i,1}Z_i\frac{F\nabla\psi}{R_gT}\right);$$

$$-\nabla\cdot N_i = D_i\nabla^2 C_i - \left[\frac{-Z_iD_iC_i\left(\sum_i Z_iD_i\nabla C_i\right)\sum_i Z_i^2D_i\nabla C_i}{\left(\sum_i Z_i^2D_iC_i\right)^2} + \right. \tag{3-18}$$

$$\left.\frac{\left(\sum_i Z_iD_i\nabla C_i\right)(Z_iD_i\nabla C_i)}{\sum_i Z_i^2D_iC_i} + \frac{Z_iD_iC_i\left(\sum_i Z_iD_i\nabla^2 C_i\right)}{\sum_i Z_i^2D_iC_i}\right]$$

where, D, F, R_g and T are the coefficient of diffusion, Faraday constant, molar gas constant, and temperature respectively. ψ is the potential of a streaming charge Z_i and C_i is the concentration of species i in the solution. The detailed derivation of Eq. 3-18 is provided in Appendix A. The boundary conditions are:

$$@\ r = 0,\quad \frac{dC_{i,1}}{dr} = 0 \tag{3-19}$$

$$@\ r = r_1,\quad C_{i,1} = C_{i,2}$$
$$-N_{i,1} = k_{i,O}(C_{i,b} - C_{i,r=r_1}) \tag{3-20}$$

where, r_1 is the inner radius of curvature of the membrane and $k_{i,O}$ is the combined transfer coefficient of species i for the liquid-phase mass transfer and diffusion through the membrane, which is defined by

$$\frac{1}{k_{i,O}} = \frac{1}{k_{i,L}} + \frac{1}{k_{i,M}} \tag{3-21}$$

where, $k_{i,L}$ and $k_{i,M}$ are the liquid phase mass transfer coefficient and mass transfer coefficient through the membrane of species i, respectively. The effectiveness factor η, which represents the influence of mass transfer on the overall reaction process, is defined for the present system by

$$\eta = \frac{\frac{3}{r_1} D_{s,1} \left(\frac{\partial S_1}{\partial r}\right)\Big|_{r=r_1}}{\frac{V_m E S_b}{(S_b + K_m + \frac{S_b^2}{K_s})(1 + \frac{P_b}{K_i})}} \tag{3-22}$$

3.2.3 Liquid Film Mass Transfer Coefficient

A rigorous treatment of the effect of external diffusion resistance on urease kinetics would require a precise knowledge of the hydrodynamic conditions in the liquid and the integration of the differential equation, which expresses the conservation of the substrate and product, with the appropriate boundary conditions. In many practical cases, however, the treatment can be greatly simplified by the use of an external mass transfer coefficient.

The rate of transport of the species i under consideration from the bulk solution to microcapsule surface can be simply expressed by the product of a mass transfer

coefficient and the corresponding driving force, which is the concentration difference between the surface and the bulk liquid. Thus,

$$J_i = k_{i,L}(C_{i,b} - C_{i,s}) \qquad (3\text{-}23)$$

where J_i = the flux of species i(moles/sec.m^2)

$k_{L,i}$ = mass transfer coefficient of species i(m/sec)

$C_{i,b}$ = concentration of species $i$at bulk phase (M)

$C_{i,s}$ = concentration of species $i$at microcapsule surface (M).

In the absence of external diffusion resistance, $J_i = 0$, which means that the concentration of species $i$at the surface of the microcapsules is equal to that of the bulk liquid, or visa versa.

The mass transfer coefficient, $k_{i,L}$, is sometimes replaced by an effective boundary layer thickness, δ_l, which satisfies the following relation:

$$k_{i,L} = \frac{D_i}{\delta_l} \qquad (3\text{-}24)$$

where, D_i is the diffusion coefficient of the species i. It is important to note that δ_l is only a fictitious distance, and its use by no means implies that mass transfer takes place only by molecular diffusion through a stagnant liquid layer of thickness δ_l adjacent to the surface (Levich, 1962). Indeed, experimental measurements showed that liquid motion may occur at distances from the surface much smaller than δ_l (Engasser and Horvath, 1976). The assumption of an unstirred layer and molecular diffusion as the sole transport mechanism can be highly misleading when the simultaneous transport of several species is investigated. Since δ_l depends not only on the hydrodynamic

conditions, but also on the diffusivity, so that in general each species has a particular value of δ_f.

3.2.3.1 Continuous Stirred Tank Reactor (CSTR)

The external film resistance in a CSTR decreases when the stirring of the suspension is vigorous. However, the reactor should be gently agitated at speeds sufficient to maintain the microcapsules in suspension while avoiding particle breakage since urease microcapsules have been reported to burst due to vigorous agitation in a stirred-tank reactor (Mogensen, 1972; Poncelet and Neufeld, 1989). Under limited agitation conditions, the formation of a near-stagnant film around the exterior of the capsule may be inevitable so that external transport resistance may have a noticeable influence on the observed over-all reaction rate. According to Satterfield (1976), the mass transfer coefficient for suspended microcapsules is not too different from that in free fall. Since the density of microcapsules is only slightly higher than that of dialysate solution, in a CSTR the suspended microcapsules may be expected to closely follow the liquid stirring pattern with little motion relative to the liquid. Satterfield predicted that

$$\frac{k_{i,L}}{k^{*}_{i,L}} \; - \; 1 \; to \; 4 \qquad (3\text{-}25)$$

where, $k^{*}_{i,L}$ denotes the liquid phase mass transfer coefficient in free fall. For design purposes, a ratio of 2 was suggested (Satterfield, 1976). Here, $k^{*}_{i,L}$ can be estimated by combining Stokes' Law for the velocity of free fall with analytical expressions for the velocity field around the microcapsules (Brian and Hales, 1969) expressed by

$$(N^*_{Sh,i} - 4)^{\frac{1}{2}} - 1.1\, N^*_{Pe,i}{}^{\frac{1}{3}} \qquad (3\text{-}26)$$

where the Sherwood number for free fall, $N^*_{Sh,i}$ is

$$N^*_{Sh,i} - \frac{k^*_{i,L}\, d_p}{D_i} \qquad (3\text{-}27)$$

and the Peclet number for free fall, $N^*_{Pe,i}$ is

$$N^*_{Pe,i} - \frac{U_t\, d_p}{D_i} \qquad (3\text{-}28)$$

The terminal velocity of microcapsules, U_t is given by

$$U_t - \frac{g\, d_p^2\, \Delta\rho}{18\, \mu} \qquad (3\text{-}29)$$

where, **g** is the acceleration due to gravity, $\Delta\rho$ is the difference in density between microcapsule and bulk fluid, and μ is the fluid viscosity. Combining Eqs. (3-26) to (3-29),

$$k_{i,L}^{*} = \frac{D_i}{d_p}\left[4 + 1.1\left(\frac{U_t\, d_p}{D_i}\right)^{\frac{2}{3}}\right]^{\frac{1}{2}} \qquad (3\text{-}30)$$

3.2.3.2 Fixed Bed Reactor (FBR)

In a FBR, a fluid flowing through a bed of microcapsules develops a boundary layer very near the microcapsule surface where the fluid velocity is very low. Therefore, the external film resistance from bulk liquid to packed microcapsules may influence the overall reaction rate to some extent. In such a situation, $k_{i,L}$ may be estimated from the following correlation proposed by Wilson and Geankoplis (1966): For $0.0016 < N_{Re} < 55$,

$$\varepsilon j_D = \frac{k_{i,L}\rho}{G} N_{Sc}^{2/3} = \frac{1.09}{N_{Re}^{2/3}} \qquad (3\text{-}31)$$

where ε is the void fraction of the bed, G is the mass velocity of the fluid in g/sec.cm^2 of superficial bed cross section normal to mean flow. From Eq. (3-32),

$$k_{i,L} = 1.09\,\frac{U_s^{1/3}\, D_i^{2/3}}{\varepsilon\, d_p^{2/3}} \qquad (3\text{-}32)$$

which was reported to correlate data for values of N_{Sc} in the range of 165-70,600.

3.2.4 Overall Reactor Balance

The overall material balance in a CSTR and a FBR will be presented to account for each species involved in the reaction system.

3.2.4.1 Continuous Stirred Tank Reactor (CSTR)

The conceptualized model for the CSTR is shown in Fig. 3-2. In this figure, dialysate solution containing species i, at a concentration $C_{i,f}$, is continuously fed at a volumetric rate Q_D into the reactor which contains urease microencapsulate of volume V_c. Product containing unreacted feed is simultaneously removed from the reactor such that a total reaction volume, V_T, is maintained for the entire operational period. The system is constantly stirred to maintain a homogeneous bulk fluid fractional void space ε. Suppose that the concentrations at the exit and at the inner surface of the membrane are $C_{i,b}$ (bulk concentration) and $C_{i,r=r_1}$, respectively. A balance of charges in the bulk solution require that

$$\left(C_{H^+,b} + C_{NH_4^+,b} + C_{Na^+,b} \right) - \left(C_{OH^-,b} + C_{HCO_3^-,b} + 2\,C_{CO_3^{2-},b} + C_{CH_3COO^-,b} + C_{Cl^-,b} \right) = 0$$

The balance of a species for the CSTR is as follows:

$$\frac{\partial C_{s,b}}{\partial t} = \frac{Q_D}{\varepsilon V_T}(C_{s,f} - C_{s,b}) - \frac{3\alpha k_{s,O}}{\varepsilon\, r_2}(C_{s,b} - C_{s,r=r_1}) \qquad (3\text{-}33)$$

$$\frac{\partial C_{NH_4^+,b}}{\partial t} = f_{NH_4^+}\{\frac{Q_D}{\varepsilon V_T}\{(C_{NH_4^+,f} + C_{NH_3,f}) - (C_{NH_4^+,b} + C_{NH_3,b})\} - \frac{3\alpha}{\varepsilon r_2}\{k_{NH_4^+,O}(C_{NH_4^+,b} - C_{NH_4^+,r-r_1}) + k_{NH_3,O}(C_{NH_3,b} - C_{NH_3,r-r_1})\}\}$$

$$\frac{\partial C_{HCO_3^-,b}}{\partial t} = f_{HCO_3^-}\{\frac{Q_D}{\varepsilon V_T}\{(C_{H_2CO_3,f} + C_{HCO_3^-,f} + C_{CO_3^{2-},f}) - (C_{H_2CO_3^*,b} + C_{HCO_3^-,b} + C_{CO_3^{2-},b})\} - \frac{3\alpha}{\varepsilon r_2}\{k_{H_2CO_3,O}(C_{H_2CO_3,b} - C_{H_2CO_3,r-r_1}) + k_{HCO_3^-,O}(C_{HCO_3^-,b} - C_{HCO_3^-,r-r_1}) + k_{CO_3^{2-},O}(C_{CO_3^{2-},b} - C_{CO_3^{2-},r-r_1})\}\} \quad (3\text{-}35)$$

$$\frac{\partial C_{CH_3COO^-,b}}{\partial t} = f_{CH_3COO^-}\{\frac{Q_D}{\varepsilon V_T}\{(C_{CH_3COOH,f} + C_{CH_3COO^-,f}) - (C_{CH_3COOH,b} + C_{CH_3COO^-,b})\}\} \quad (3\text{-}36)$$

where, α is the fraction of reactor volume occupied by the microcapsules and t is the physical time for reaction.

3.2.4.2 Fixed Bed Reactor (FBR)

Fig. 3-3 shows the model fixed bed reactor of length L which is packed with microcapsules. The system is fed with dialysate at a superficial velocity U_s and undergoes removal of urea by passage through the encapsulated packing in a reactor of total volume V_T. Utilizing the concept of dispersion coefficient D_z to account for axial

mixing, a mass balance on urea, NH_4^+, HCO_3^-, CH_3COO^- in the bulk liquid within the column yields:

$$\frac{\partial C_{s,b}}{\partial t} = \frac{1}{\tau_r Bo_s}\frac{\partial^2 C_{s,b}}{\partial Z^2} - \frac{1}{\tau_r}\frac{\partial C_{s,b}}{\partial Z} - \frac{3\alpha k_{s,O}}{\varepsilon r_2}(C_{s,b} - C_{s,r_1}) \tag{3-37}$$

$$\begin{aligned}\frac{\partial C_{NH_4^+,b}}{\partial t} = f_{NH_4^+}\{&\frac{1}{\tau_r\, Bo_{NH_4^+}}\frac{\partial^2 C_{NH_4^+,b}}{\partial Z^2} - \frac{1}{\tau_r}\frac{\partial C_{NH_4^+,b}}{\partial Z} - \\ &\frac{3\alpha\, k_{NH_4^+,O}}{\varepsilon r_2}(C_{NH_4^+,\,b} - C_{NH_4^+,\,r_1}) + \frac{1}{\tau_r\, Bo_{NH_3}}\frac{\partial^2 C_{NH_3,b}}{\partial Z^2} - \\ &\frac{1}{\tau_r}\frac{\partial C_{NH_3,b}}{\partial Z} - \frac{3\alpha\, k_{NH_3,O}}{\varepsilon r_2}(C_{NH_3,\,b} - C_{NH_3,\,r_1})\}\end{aligned} \tag{3-38}$$

$$\begin{aligned}\frac{\partial C_{HCO_3^-,b}}{\partial t} = f_{HCO_3^-}\{&\frac{1}{\tau_r\, Bo_{HCO_3^-}}\frac{\partial^2 C_{HCO_3^-,b}}{\partial Z^2} - \frac{1}{\tau_r}\frac{\partial C_{HCO_3^-,b}}{\partial Z} - \\ &\frac{3\alpha k_{HCO_3^-,O}}{\varepsilon r_2}(C_{HCO_3^-,b} - C_{HCO_3^-,r_1}) + \frac{1}{\tau_r Bo_{H_2CO_3}}\frac{\partial^2 C_{H_2CO_3,b}}{\partial Z^2} - \\ &\frac{1}{\tau_r}\frac{\partial C_{H_2CO_3,b}}{\partial Z} - \frac{3\alpha\, k_{H_2CO_3,O}}{\varepsilon r_2}(C_{H_2CO_3,b} - C_{H_2CO_3,r_1}) + \\ &\frac{1}{\tau_r\, Bo_{CO_3^{2-}}}\frac{\partial^2 C_{CO_3^{2-},b}}{\partial Z^2} - \frac{1}{\tau_r}\frac{\partial C_{CO_3^{2-},b}}{\partial Z} - \\ &\frac{3\alpha\, k_{CO_3^{2-},O}}{\varepsilon r_2}(C_{CO_3^{2-},\,b} - C_{CO_3^{2-},\,r_1})\}\end{aligned} \tag{3-39}$$

$$\frac{\partial C_{CH_3COO^-,b}}{\partial t} = f_{CH_3COO^-}\left\{\frac{1}{\tau_r\, Bo_{CH_3COOH}}\frac{\partial^2 C_{CH_3COOH,b}}{\partial Z^2} - \frac{1}{\tau_r}\frac{\partial C_{CH_3COOH,b}}{\partial Z}\right.$$
$$\left. + \frac{1}{\tau_r\, Bo_{CH_3COO^-}}\frac{\partial^2 C_{CH_3COO^-,b}}{\partial Z^2} - \frac{1}{\tau_r}\frac{\partial C_{CH_3COO^-,b}}{\partial Z}\right\} \qquad (3\text{-}40)$$

where, τ_r is the residence time, Z is the vertical coordinate direction in the axial length of the bed, and Bo is the Bodenstein number, and

$$Bo_i = \frac{U_s L}{D_{z,i}} \qquad (3\text{-}41)$$

$$\alpha = \frac{V_c}{V_T} \qquad (3\text{-}42)$$

$$\tau_r = \frac{L\varepsilon}{U_s} \qquad (3\text{-}43)$$

The boundary conditions for solving Eqs. (3-37) to (3-40) is given by

$$@\ Z = 0, \qquad \frac{1}{Bo_i}\frac{\partial C_i}{\partial Z} = C_{i,o^+} - C_{i,f} \qquad (3\text{-}44)$$

$$@\ Z = 1, \qquad \frac{\partial C_i}{\partial Z} = 0 \qquad (3\text{-}45)$$

where the position Z=0 is chosen to be the bottom inlet port of the bed. The dispersion coefficient D_z is given by the following correlation (Chung and Wen (1968)):

$$D_z = \frac{N_{Re}}{0.20 + 0.011\ N_{Re}^{0.48}}\frac{\varepsilon\mu}{\rho_f} \qquad (3\text{-}46)$$

where N_{Re} = particle Reynolds number ($d_p U_s \nu$) [-]

d_p = mean microcapsule diameter [m]

U_s = superficial velocity [m/s]

μ = dialysate viscosity [g/cm.s]

ε = bed void fraction [-]

ρ_f = dialysate density [g/mL]

ν = kinematic viscosity [m^2/s]

Eq. 3-44 implies that the rate at which the species i is fed to the FBR is equal to the rate at which it crosses the plane $Z=0^+$ by combined convection and diffusion. Eq. 3-45 is based on intuition rather than quantitative considerations (Dankwerts, 1953).

Its implication is that the concentration change of species i becomes negligible at the exit of the FBR. A balance of charges in the bulk solution require that

$$D_z \nabla^2 (C_{H^+,b} + C_{NH_4^+,b} - C_{OH^-,b} - C_{HCO_3^-,b} - 2 C_{CO_3^{2-},b} - C_{CH_3COO^-,b}) - U_z \nabla (C_{H^+,b} + C_{NH_4^+,b} - C_{OH^-,b} - C_{HCO_3^-,b} - 2 C_{CO_3^{2-},b} - C_{CH_3COO^-,b}) = 0 \quad (3\text{-}47)$$

3.3 Simulation of Blood-urea Clearance

In this section, a model will be developed to demonstrate the applicability of a microencapsulated urease FBR as an artificial kidney system with time-varying blood urea composition. Figure 3-4 shows the model scheme in which the FBR is directly connected to the patient in a closed-loop artificial kidney system. As shown, blood is pumped from the patient to feed a FBR which is packed with microencapsulated urease. It is assumed that the urease is coencapsulated (Levine and LaCourse, 1967; Sparks et al., 1969) with ion exchange resins for ammonia and pH control. The partially cleansed blood is continuously recycled to the patient by blood pumps or by the natural arterial to venous pressure difference.

Although the human body can be broken down into a number of compartments (e.g., the blood system, the extra vascular pool, the liver), the usage of a single-pool model provides sufficient clinical accuracy (Bell et al., 1965; Popovich et al., 1975).

3.3.1 Theory

The blood pH (7.4) is considered to be homeostatically regulated in the body. The three chemical buffer systems in blood are: (1) bicarbonate/carbonic acid buffer, $HCO_3^- + H_2CO_3$ especially in plasma; (2) dihydrogen phosphate/dibasic phosphate

Figure 3-4.

A schematic representation of a patient-FBR system.

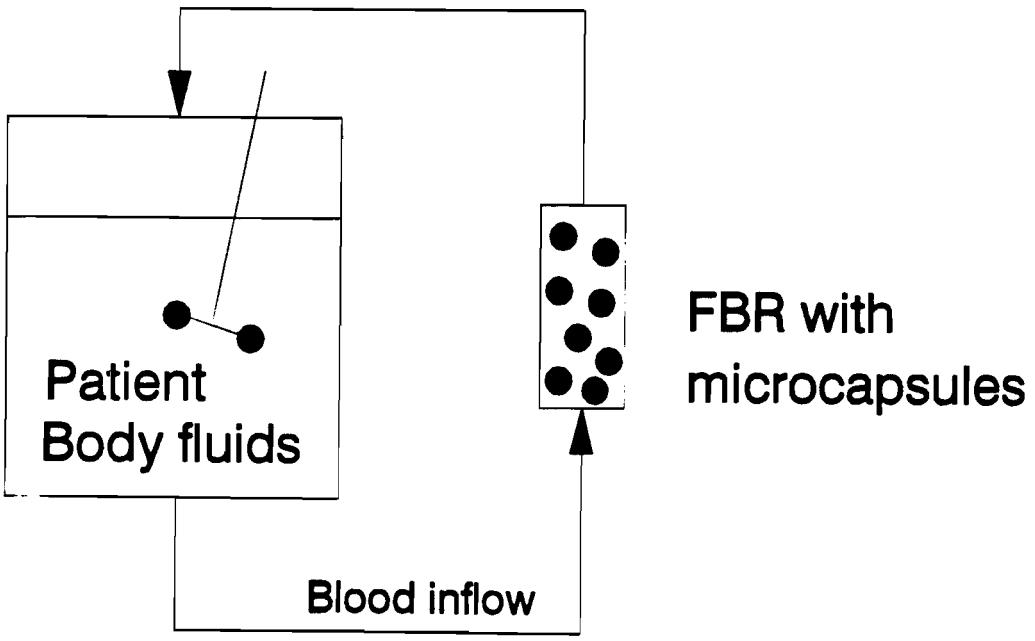

buffer, $H_2PO_4^- + HPO_4^{2-}$, which is of minor importance in blood and; (3) protein buffer to some extent in plasma (Ferguson, 1965). Among these, the bicabonate buffer system is most important for controlling blood pH. Thus the appropriate ionization reactions for this model can be summarized as follows:

$$NH_4^+ = H^+ + NH_{3(aq)} \; ; \qquad K_1 = 5.60 \times 10^{-10} \; [M] \tag{3-48}$$

$$H_2CO_3 = H^+ + HCO_3^- \; ; \qquad K_2 = 7.94 \times 10^{-7} \; [M] \tag{3-49}$$

$$HCO_3^- = H^+ + CO_3^{2-} \; ; \qquad K_3 = 6.31 \times 10^{-12} \; [M] \tag{3-50}$$

$$H_2O = H^+ + OH^- \; ; \qquad K_4 = 1.0 \times 10^{-14} \; [M] \tag{3-51}$$

$$NaHCO_3 \rightarrow Na^+ + HCO_3^- \tag{3-52}$$

Microencapsulated urease was reported (Chang, 1965) to lose some activity with half-time of one week at a body temperature of 37 °C. This experimental data was introduced into the following empirical equation for enzyme deactivation using the Marquardt-Levenberg algorithm in SigmaPlot® 4.1 software package (Jandel Scientific, C.A., USA).

$$\xi = 1 + c_1 t + c_2 t^2 + c_3 t^3 + c_4 t^4 + c_5 t^5 \qquad (3\text{-}53)$$

where, ξ is the activity coefficient which is the ratio of the reaction rate between deactivating urease and the fresh urease, t is the time in seconds and c_1 to c_5 the empirical constants -2.97×10^{-6}, 1.84×10^{-11}, -7.15×10^{-17}, 1.33×10^{-22}, and -9.25×10^{-29} respectively.

The rate of substrate reaction, R_s (Eq. 3-7), is therefore modified to account for urease deactivation as follows:

$$R_s = \frac{V_m E S}{(S + K_m + S^2/K_s)(1 + P/K_i)} \xi \qquad (3\text{-}54)$$

For simplicity, the human body will be considered as a 50 liter well-stirred tank of fluid of uniform concentration (Cooney, 1976).

3.3.2 Material Balance Equations

The major assumptions involved in the development of mass conservation equations are as described in section 3.1.2.

3.3.2.1 Body Fluid Balance

Since a single compartment model for the patient (Fig. 3-4) is considered here, a differential mass balance for the body fluid pool, which is assumed to be perfectly mixed, takes the form

$$\frac{\partial C_{s,in}}{\partial t} = \frac{Q_B}{V_B}(C_{B,out} - C_{B,in}) + G_s \qquad (3\text{-}55)$$

where V_B represents the volume of body fluids, Q_B is the volumetric flow rate of blood, $C_{B,out}$ is the urea concentration of blood returning to the patient body, $C_{B,in}$ is the urea concentration of blood leaving the body, and G_s is the urea production rate by the body metabolism. Note that the subscripts here refer to the FBR inlet (body outlet) and outlet (body inlet) concentrations as shown in Figure 3-4.

3.3.2.2 Intraparticle Balance

The intraparticle balance for this system is given by Eqs. (3-10) to (3-12). At any given time, the balance of charges in the enzyme solution becomes

$$(C_{H^+,1} + C_{NH_4^+,1} + C_{Na^+,1}) - (C_{OH^-,1} + C_{HCO_3^-,1} + 2\, C_{CO_3^{2-},1}) = 0 \qquad (3\text{-}56)$$

3.3.2.3 Overall reactor balance

The overall reactor balance equations are given by Eqs. (3-37) to (3-39). At any given time, the balance of charges in the bulk solution becomes

$$(C_{H^+,b} + C_{NH_4^+,b} + C_{Na^+,b}) - (C_{OH^-,b} + C_{HCO_3^-,b} + 2\, C_{CO_3^{2-},b}) = 0 \qquad (3\text{-}57)$$

Note that Eqs. (3-56) and (3-57) are different from Eqs. (3-17) and (3-47) respectively, since simulation of blood urea clearance was made by transient computations, whereas that of dialysate solution regeneration was done by steady-state computations (see the details in Lee et al., 1993).

3.4 Computational Method

The method of orthogonal collocation (Villadsen and Stewart, 1967), was used for solving the sets of differential equations which were developed for the models described above. At steady-state, the set of intraparticle equations (Eqs. (3-10) to (3-13)) become a symmetrical second-order boundary-value problem in one independent variable, R (the dimensionless radial position inside the microcapsule). In the region $R^2<1$, the solution is a symmetric function of R, involving only even powers of R. Therefore, the concentration, $C_{i,r}$ was approximated by orthogonal polynomials which are functions of R^2 as follows:

$$C_{i,1}(R^2) - C_{i,1}\big|_{R-1} + (1 - R^2)\sum_{k-1}^{N} a_k P_{k-1}(R^2) \; . \qquad (3\text{-}58)$$

where a_k are undetermined constants and N is the number of interior collocation points and $P_k(R^2)$ is an orthogonal polynomial of degree k in R^2 which is defined by

$$\int_0^1 w(R^2)P_j(R^2)P_i(R^2)R^2dR = 0;\; j \le i-1, \qquad (3\text{-}59)$$

where $w(R^2)$ is a weighting function. The first coefficient of each polynomial is taken as one. In order to simplify the computations, an equivalent of equations were formulated in terms of the concentrations by rewriting Eq. (3-58) as

$$C_{i,1}(R^2)=\sum_{k=1}^{N+1} d_k R^{2k-2} \tag{3-60}$$

The gradient and the Laplacian Eq. (3-60) at the collocation points were evaluated as follws:

$$\left.\frac{dC_{i,1}}{dR}\right|_{R_j} = \sum_{k=1}^{N+1} \frac{dR^{2k-2}}{dR} d_k, \tag{3-61}$$

$$\nabla^2 C_{i,1}\big|_{R_j} = \sum_{k=1}^{N+1} \nabla^2 (R^{2k-2})\Big|_{R_j} d_k \tag{3-62}$$

for $j = 1, \ldots, N+1$. The $N+1$ collocation point is $R = 1$.

Equations (3-61) and (3-62) were converted into the following matrix notation form

$$\left.\frac{dC_{i,1}}{dR}\right|_{R_j} = \sum_{k=1}^{N+1} A_{jk} C_{i,1}(R_k) \tag{3-63}$$

$$\nabla^2 C_{i,1}\big|_{R_j} = \sum_{k=1}^{N+1} B_{jk} C_{i,1}(R_k) \tag{3-64}$$

where A_{jk} and B_{jk} are collocation matrices. Using this notation, the intraparticle differential equations (Eqs. (3-10)-(3-13)) at the collocation point $R = R_j$ become

$$\frac{\partial C_{s,1}(R_j)}{\partial \tau} = \frac{D_s}{r_O^2} \cdot \frac{L \cdot \varepsilon}{U_s} \cdot \sum_{k-1}^{N+1} B_{jk} C_{s,1}(R_k)$$

$$- \frac{L \cdot \varepsilon}{U_s} \cdot \frac{C_{s,1}(R_j)}{(C_{s,1}(R_j) + K_m + \frac{C_{s,1}(R_j)}{K_s})(1 + \frac{C_{NH_4^+,1}(R_j)}{K_i})} \qquad (3\text{-}65)$$

$$\frac{\partial C_{NH_4^+,1}(R_j)}{\partial \tau} = f_{NH_4^+} \{ \frac{D_{NH_4^+}}{r_o^2} \cdot \frac{L \cdot \varepsilon}{U_s} \sum_{k-1}^{N+1} B_{jk} C_{NH_4^+,1}(R_k)$$

$$+ \frac{D_{NH_3}}{r_o^2} \cdot \frac{L \cdot \varepsilon}{U_s} \sum_{k-1}^{N+1} B_{jk} C_{NH_3,1}(R_k) \qquad (3\text{-}66)$$

$$+ 2\frac{L\varepsilon}{U_s} \frac{C_{s,1}(R_k)}{(C_{s,1}(R_k) + K_m + \frac{C_{s,1}(R_j)}{K_s})(1 + \frac{C_{NH_4^+,1}(R_j)}{K_i})} \}$$

$$\frac{\partial C_{HCO_3^-,1}(R_j)}{\partial \tau} = f_{HCO_3^-}\{ \frac{D_{H_2CO_3}}{r_o^2}\frac{L\varepsilon}{U_s}\sum_{k-1}^{N+1} B_{jk}C_{H_2CO_3,1}(R_k) + \frac{D_{HCO_3^-}}{r_o^2}\frac{L\varepsilon}{U_s}\sum_{k-1}^{N+1} B_{jk}C_{HCO_3^-,1}(R_k) + \frac{D_{CO_3^{2-}}}{r_o^2}\frac{L\varepsilon}{U_s}\sum_{k-1}^{N+1} B_{jk}C_{CO_3^{2-},1}(R_k) + \frac{L\varepsilon}{U_S}\frac{C_{s,1}(R_k)}{(C_{s,1}(R_k) + K_m + \frac{C_{s,1}(R_k)}{K_s})(1 + \frac{C_{NH_4^+,1}(R_k)}{K_i})} \quad (3\text{-}67)$$

$$\frac{\partial C_{CH_3COO^-,1}(R_j)}{\partial \tau} = f_{CH_3COO^-}\{\frac{D_{CH_3COOH}}{r_o^2}\frac{L\varepsilon}{U_s}\sum_{k-1}^{N+1} B_{jk}C_{CH_3COOH,1}(R_k) + \frac{D_{CH_3COO^-}}{r_o^2}\cdot\frac{L\cdot\varepsilon}{U_s}\sum_{k-1}^{N+1} B_{jk}C_{CH_3COO^-,1}(R_k)\ \} \quad (3\text{-}68)$$

with the boundary condition (Eq. 3-17),

$$\sum_{k-1}^{N+1} A_{N+1,k}C_{i,1}(R_k) = Sh_i[C_{i,b} - C_{i,1}(R_{N+1})] \quad (3\text{-}69)$$

where $C_{i,b}$ refers to the bulk liquid concentration. Equation (3-69) enables the value of $C_{i,1}(R_{N+1})$ to be expressed in terms of $C_{i,1}(R_k)$.

The FBR concentration profiles for the bulk liquid were expanded in terms of a non-symmetric polynomial of order M using the trial function

$$C_{i,b}(Z) = b + cZ + Z(1-Z)\sum_{k=1}^{M} a_k P_{k-1}(Z) \tag{3-70}$$

where $P_{k-1}(Z)$ are shifted orthogonal polynomials defined by

$$\int_0^1 w(Z)P_j(Z)P_i(Z)dZ = 0 \qquad j = 0,1,\ldots i-1 \tag{3-71}$$

and Z is the dimensionless axial position along the column Z. In the region $Z<1$, the equations have no special symmetric properties, so that odd and even powers of Z had to be included in the trial function. Rewriting Eq. (3-70):

$$C_{i,b}(Z) = \sum_{k=1}^{M+2} d_k Z^{k-1} \tag{3-72}$$

The gradient and the Laplacian of Eq. (3-72) evaluated at the collocation points are to become:

$$\left.\frac{dC_{i,b}}{dZ}\right|_{Z_j} = \sum_{k=1}^{M+2} (k-1)\, Z_j^{k-2} d_k \tag{3-73}$$

$$\nabla^2 C_{i,b}\big|_{Z_j} = \sum_{k=1}^{M+2} (k-1)(k-2)\, Z_j^{k-3} d_k \qquad (3\text{-}74)$$

for $j = 1,\ldots,M+2$.

Equations (3-73) and (3-74) were converted into the following matrix notation form

$$\left.\frac{dC_{i,b}}{dZ}\right|_{Z_j} = \sum_{k=1}^{M+1} A'_{jk} C_{i,b}(Z_k) \qquad (3\text{-}75)$$

$$\nabla^2 C_{i,b}\big|_{Z_j} = \sum_{k=1}^{M+1} B'_{jk} C_{i,b}(Z_k) \qquad (3\text{-}76)$$

where A'_{jk} and B'_{jk} are collocation matrices.

The differential equations, Eqs. (3-37) to (3-40), at the collocation point $Z = Z_j$ then become:

$$\frac{\partial C_{s,b}(Z_j)}{\partial \tau} - \frac{1}{Bo_s} \sum_{k=1}^{M+2} B'_{jk} C_{s,b}(Z_k) - \sum_{k=1}^{M+2} A'_{jk} C_{s,b}(Z_k) - \frac{3\alpha}{r_2} \cdot \frac{L}{U_s} \cdot k_{s,o} \{C_{s,b}(Z_j) - C_{s,r-1}\} = 0 \qquad (3\text{-}77)$$

$$\frac{\partial C_{NH_4^+,b}(Z_j)}{\partial \tau} = f_{NH_4^+}\left[\frac{1}{Bo_{NH_4^+}}\sum_{k-1}^{M+2} B'_{jk}C_{NH_4^+,b}(Z_k) - \sum_{k-1}^{M+2} A'_{jk}C_{NH_4^+,b}(Z_k)\right.$$

$$- \frac{3\alpha}{r_2}\frac{L}{U_s}k_{NH_4^+,o}\{C_{NH_4^+,b}(Z_j) - C_{NH_4^+,R-1}\} + \frac{1}{Bo_{NH_3}}\sum_{k-1}^{M+2} B'_{jk}C_{NH_3,b}(Z_k) \qquad (3\text{-}78)$$

$$\left. - \sum_{k-1}^{M+2} A'_{jk}C_{NH_3,b}(Z_k) - \frac{3\alpha}{r_2}\frac{L}{U_s}k_{NH_3}\{C_{NH_3,b}(Z_j) - C_{NH_3,R-1}\}\right]$$

$$\frac{\partial C_{HCO_3^-,b}(Z_j)}{\partial \tau} = f_{HCO_3^-}\left[\frac{1}{Bo_{H_2CO_3}}\sum_{k-1}^{M+2} B'_{jk}C_{H_2CO_3,b}(Z_k) - \right.$$

$$\sum_{k-1}^{M+2} A'_{jk}C_{H_2CO_3,b}(Z_k) - \frac{3\alpha}{r_2}\frac{L}{U_s}k_{H_2CO_3,o}\{C_{H_2CO_3,b}(Z_j) - C_{H_2CO_3,R-1}\}$$

$$+ \frac{1}{Bo_{HCO_3^-}}\cdot\sum_{k-1}^{M+2} B'_{jk}C_{HCO_3^-,b}(Z_k) - \sum_{k-1}^{M+2} A'_{jk}C_{HCO_3^-,b}(Z_k) \qquad (3\text{-}79)$$

$$- \frac{3\alpha}{r_2}\cdot\frac{L}{U_s}\cdot k_{HCO_3^-,0}\{C_{HCO_3^-,b}(Z_j) - C_{HCO_3^-,R-1}\}$$

$$+ \frac{1}{Bo_{CO_3^{2-}}}\sum_{k-1}^{M+2} B'_{jk}C_{CO_3^{2-}}(Z_k) - A'_{jk}C_{CO_3^{2-},b}(Z_k)$$

$$\left. - \frac{3\alpha}{r_2}\cdot\frac{L}{U_s}\cdot k_{CO_3^{2-},o}\{C_{CO_3^{2-},b}(Z_j) - C_{CO_3^{2-}R-1}\}\right]$$

$$\frac{\partial C_{CH_3COO^-,b}(Z_j)}{\partial \tau} = f_{CH_3COO^-}\left[\frac{1}{Bo_{CH_3COO^-}}\sum_{k=1}^{M+2} B'_{jk} C_{CH_3COO^-,b}(Z_k) - \sum_{k=1}^{M+2} A'_{jk} C_{CH_3COO^-,b}(Z_k) - \frac{3\alpha L}{U_s r_2} k_{CH_3COO^-,O}\{C_{CH_3COO^-,b}(Z_j) - C_{CH_3COO^-,R-1}\}\right.$$

$$\left. + \frac{1}{Bo_{CH_3COOH}}\cdot\sum_{k=1}^{M+2} B'_{jk} C_{CH_3COOH,b}(Z_k) - \sum_{k=1}^{M+2} A'_{jk} C_{CH_3COOH,b}(Z_k) \right. \qquad (3\text{-}80)$$

$$\left. - \frac{3\alpha}{r_2}\cdot\frac{L}{U_s}\cdot k_{CH_3COOH,O}\{C_{CH_3COOH,b}(Z_j) - C_{CH_3COOH,R-1}\}\right]$$

where

$$C_{i,b}(Z_{M+2}) = -\frac{A'_{M+2,1}}{A'_{M+2,M+2}}\cdot C_{i,b}(Z_1) - \sum_{k=2}^{M+1}\frac{A'_{M+2,k}}{A'_{M+2,M+2}} C_{i,b}(Z_k) \qquad (3\text{-}81)$$

Here the point Z_1 corresponds to the inlet of the column reactor ($Z = 0$); the point Z_{M+2} refers to the exit of the reactor ($Z = 1$). The boundary conditions given by Eqs. (3-44) and (3-45) respectively become

$$\sum_{k=1}^{M+2} A'_{M+2,k} C_{i,b}(Z_k) = 0 \qquad (3\text{-}82)$$

$$\sum_{k=1}^{M+2} A'_{1k} C_{i,b}(Z_k) - Bo_i\{ C_{i,b}(Z_1) - C_{i,f} \} \tag{3-83}$$

Eqs. (3-76) to (3-78) were then combined to obtain

$$C_{i,b}(Z_1) = \frac{-Bo_i C_{i,f} - \{ \sum_{k=2}^{M+2} A'_{ik} C_{i,b}(Z_k) + A'_{1,M+2} C_{i,b}(Z_{M+2}) \}}{A'_{1,1} - Bo_i} \tag{3-84}$$

The effectiveness factor equation Eq. (3-23) was written for both the CSTR and FBR as

$$\eta = \frac{\frac{3}{r_1} \sum_{k=1}^{N+1} W_k \frac{V_m E C_{s,1}(R_k)}{\{ C_{s,1}(R_k) + K_m + \frac{C^2_{s,1}(R_k)}{K_s} \} \{ 1 + \frac{C_{NH_4^+,1}(R_k)}{K_i} \}}}{\frac{V_m E C_{s,b}}{\{ C_{s,b} + K_m + \frac{C^2_{s,b}}{K_s} \} \{ 1 + \frac{C_{NH_4^+,b}}{K_i} \}}} \tag{3-85}$$

and

$$\eta(Z_k) = \frac{\dfrac{3}{r_1}\sum_{k=1}^{N+1} W_k \dfrac{V_m EC_{s,1}(R_k,Z_k)}{\{C_{s,1}(R_k,Z_k) + K_m + \dfrac{C^2_{s,1}(R_k,Z_k)}{K_s}\}\{1 + \dfrac{C_{NH_4^+,1}(R_k,Z_k)}{K_i}\}}}{\dfrac{V_m EC_{s,b}(Z_k)}{\{C_{s,b}(Z_k) + K_m + \dfrac{C^2_{s,b}(Z_k)}{K_s}\}\{1 + \dfrac{C_{NH_4^+,b}(Z_k)}{K_i}\}}} \quad (3\text{-}86)$$

respectively.

The equations were solved using subroutines from the International Mathematical and Statistical Library (IMSL). For steady-state cases, the DNEQNF (double precision nonlinear equations by finite differences) subroutine was used. This routine applies the Levenberg-Marquardt algorithm and a finite difference approximation to the Jacobian. Transient computations were also made using the Gear method from the DIVPAG (double precision initial value problem by Adam-Moulton and Gear) subroutine. The details of the computer program are reported elsewhere (Lee et al. (1993).

CHAPTER 4

STEADY-STATE ANALYSIS OF MICROENCAPSULATED UREASE REACTORS FOR DIALYSATE REGENERATION

The ability of urease to catalyze the hydrolysis of urea has resulted in numerous studies into the application of the microencapsulated form of the enzyme in artificial kidney devices (Chang, 1964, 1965, 1966; Saleme et al., 1971, and Sparks et al., 1971). Numerous investigators have studied the kinetics of microencapsulated urease (Chang, 1965, 1980; Levine and LaCourse, 1967; Mongensen and Vieth, 1973; Sundaram, 1973; Chang and Malouf, 1978, 1979; Lin, 1979; Miyawaki et al., 1979; Neufeld et al., 1984; Ortmanis et al., 1984; Dueck et al., 1986; Gu and Chang, 1988a, 1988b, 1990a, 1990b; Gu, 1991; and Monshipouri and Neufeld, 1991, 1992). Several theoretical models (Mongensen, 1973, Bolmeier, 1979, and Moynihan, 1989), have been developed to describe the hydrolysis of urea in various immobilized systems. These studies demonstrated that urea hydrolysis obeys a modified Michalis-Menten reaction mechanism, which incorporates pH dependent kinetics, substrate inhibition, and noncompetitive product inhibition. Although, these effects have been well studied, the existing models are too general and therefore quantitative information on the impact of the limiting factors on the kinetic rates is lacking.

A steady-state theoretical model for urea hydrolysis using microencapsulated urease in a continuous stirred reactor (CSTR), and a fixed bed reactor (FBR) will be presented in this chapter. Four main factors; pH kinetic effect, product inhibition,

substrate depletion and external diffusional effects, are generally known to limit the rate of reaction of urea by urease. The impact of these factors (individually and in combination) on reactor performance was elucidated by considering conceptual models for the two reactor configurations. Information on intraparticle diffusional resistances was obtained from studying the effect of capsule diameter on urea conversion, ammonia production, and the effectiveness factor for various enzyme activities. The studies on the effectiveness factor were limited to the CSTR. A phase diagram was developed for the estimation of the contribution by each of the inhibitory parameters on the reaction.

4.1 Reactor Performance Factors

The effect of particle diameter on urea conversion, ammonium ion concentration, pH, and the effectiveness factor was computed for the two reactor configurations (CSTR and FBR). Also, the effects of pH, product inhibition, urea depletion, and external diffusion (i.e., transport from the fluid to the membrane, transport through the membrane) on the conversion and effectiveness factor were calculated. Eqs. (3-10)-(3-13) were solved simultaneously with the reactor balance equations (3-33)-(3-36) for the CSTR and Eqs. (3-37)-(3-40) for the FBR, at steady-state conditions (i.e. $\partial C_i/\partial t = \partial C_{ib}/\partial t = 0$). Since these equations are coupled, the equilibrium relations given by Eqs. (3-2)-(3-6) were used to obtain decoupled solutions. In the calculations for the simulation, the following conditions were assumed for both reactor configurations: 1) the initial concentration of urea in the dialysate solution is 10 mM at pH = 7.4; 2) a uniform membrane thickness (δ) of 0.02 μm was assumed for all microcapsule diameters considered; 3) uniform reactor temperature, T=25°C, residence time, τ_r=46 s, and reactor void volume, α=0.5, 4) the values for $k_{i,M}$ were obtained from

Mogensen (1972), unless otherwise specified. The values of the kinetic constants used in the calculations are listed in Table 4-1.

4.1.1 Microcapsule Diameter effects.

Microcapsule diameter effects were studied using the following assumptions:

a) Assume that urea depletion, ammonium ion inhibition, and pH kinetic effects are occurring within the reactor.
b) Fix microcapsule diameter, d_t
c) Choose the initial enzyme activity, $A_e = V_{m,o}E$.
d) Compute the conversion, ammonium ion concentration, pH and the effectiveness factor.
e) Repeat the calculation for various enzyme activities.
f) Compare conversion, ammonium ion concentration, pH, and effectiveness factor to initial enzyme activity for various microcapsule diameters (fixed).

4.1.2 Product Inhibition, pH Dependent Kinetics and Substrate Depletion Effects

The effects of product inhibition, pH and substrate depletion were studied individually and in combination by making the necessary adjustment to the reaction kinetic equation (3-7), using the eight conditions shown in Table 4-2. In this table, the conditions are categorized into case studies and the active conditions for each case are noted. For each of these combinations, the calculations were performed as follows:

a) Fix particle size.

Table 4-1. Kinetic constants used for computing urea hydrolysis by urease.

Species	Diffusion Coefficient, D_i ($\times 10^{-9}$ m^2/s)	Reference
Urea	1.38	Cussler (1984)
NH_4^+	1.954	Newman (1973)
NH_3	1.715	Reid et al. (1977)
HCO_3^-	1.105	Newman (1973)
CO_3^{-2}	0.9	Moynihan (1987)
H_2CO_3	1.92	Moynihan (1987)
CH_3COO^-	1.089	Newman (1973)
CH_3COOH	1.19	Reid et al. (1977)
H^+	9.312	Newman (1973)
OH^-	5.26	Newman (1973)
Na^+	1.334	Newman (1973)
Cl^-	2.032	Newman (1973)
Species	**Equilibrium Constant**	**Reference**
K_1	5.60×10^{-10}	Moynihan (1987)
K_2	5.61×10^{-11}	Moynihan (1987)
K_3	4.30×10^{-7}	Moynihan (1987)
K_4	1.0×10^{-14}	Moynihan (1987)
K_5	1.86×10^{-5}	Moynihan (1987)
Species	**Ionization Constant (M)**	**Reference**
K_{e1}	3.1×10^{-8}	Moynihan (1987)
K_{e2}	1.4×10^{-6}	Moynihan (1987)
K_{es1}	7.1×10^{-9}	Moynihan (1987)
K_{es2}	3.6×10^{-5}	Moynihan (1987)

Table 4-2.

Kinetic conditions in the CSTR considered in the present study. Active conditions are designated.

	Product Inhibition	pH-dependent Kinetics	Substrate Depletion
CASE 1	X	X	X
CASE 2		X	X
CASE 3	X	X	
CASE 4		X	
CASE 5	X		X
CASE 6			X
CASE 7	X		
CASE 8			

b) Choose an initial enzyme activity.

c) Impose the combined effect.

d) Compute the conversion and the effectiveness factor.

e) Repeat the calculations for various enzyme activities.

f) Plot conversion and effectiveness factor vs. activity, for each combined effect for a fixed microcapsule diameter.

4.2 Results and Discussion

In this discussion, enzyme activity (A_e) and the Thiele modulus squared (ϕ^2_o) will be defined as

$$A_e = V_{m,o} E , \tag{4-1}$$

and

$$\phi_o^2 = \frac{A_e d_i^2}{D_{i,m} K_{m,o}}, \tag{4-2}$$

respectively. $V_{m,o}$ and $K_{m,o}$ are the pH-independent maximum specific reaction rate and substrate depletion constant, respectively, and d_i is the inner diameter of the microcapsule. It was considered inappropriate to use the pH-dependent values since any pH effect is implicitly reflected in the values of the urea conversion, and the effectiveness factor.

4.2.1 Microcapsule diameter effects.

The influence of microcapsule diameter on the performance characteristics of a CSTR and a FBR was studied under steady-state conditions. The pH kinetic effect, ammonium ion (product) inhibition and substrate depletion were taken into account.

The results for the effect of microcapsule diameter on these parameters as well as the effectiveness factor will be discussed in the following.

The effect of the size of nylon-microencapsulated urease on the conversion of urea to products is shown for a CSTR (Fig. 4-1a) and a FBR (Fig. 4-1b). These results show that there is an increase in conversion at small diameter for all enzyme activities. The increase is enhanced at higher enzyme activities. The increased surface area for mass transfer by small particles, combined with the reduced characteristic time for intraparticle diffusion results in enhanced rates of reaction. The increased conversion is accompanied by an increase in the ammonium ion production as shown in Fig. 4-2, for both reactor configurations. The calculated results for the reactor exit pH variation with particle diameter are presented in Fig. 4-3. There is a small but consistent increase in the pH, for a CSTR (Fig. 4-3a), when the capsule size decreases. This conforms to the results for the conversion and ammonium ion production. A similar result is obtained for the FBR (Fig. 4-3b), which shows a complex mix of profiles. At very low activities, there is an increase in pH for a decreasing size. This trend changes at activities greater than 1.7 mM/s. In this range, the exit pH for the smallest particle, 5 μm, is consistently lower than that for 300, and 500 μm. Beyond 3 mM/s, the pH profiles are similar and reach a plateau at a pH of about 8.8. Although the highest pH values for activities greater than 5 mM/s were predicted for 300 μm microcapsules, the largest difference in pH between the various profiles is about 0.3. Thus, there is no direct influence of the capsule diameter on pH.

The effectiveness factor is often used to express the efficiency of immobilized enzymes. There is a drop in the effectiveness factor with increasing microcapsule size, as seen in Fig. 4-4, for a CSTR. This is attributed to the longer characteristic time for diffusion which is associated with large particles. Hence, the reaction rate is low. Also,

Figure 4.1

The overall conversion of urea by microencapsulated urease in a CSTR (a) and a FBR (b) under steady-state conditions as a function of the enzyme activity within the reactor. Simulations are presented for microcapsule diameters ranging from 5 to 2000 μm.

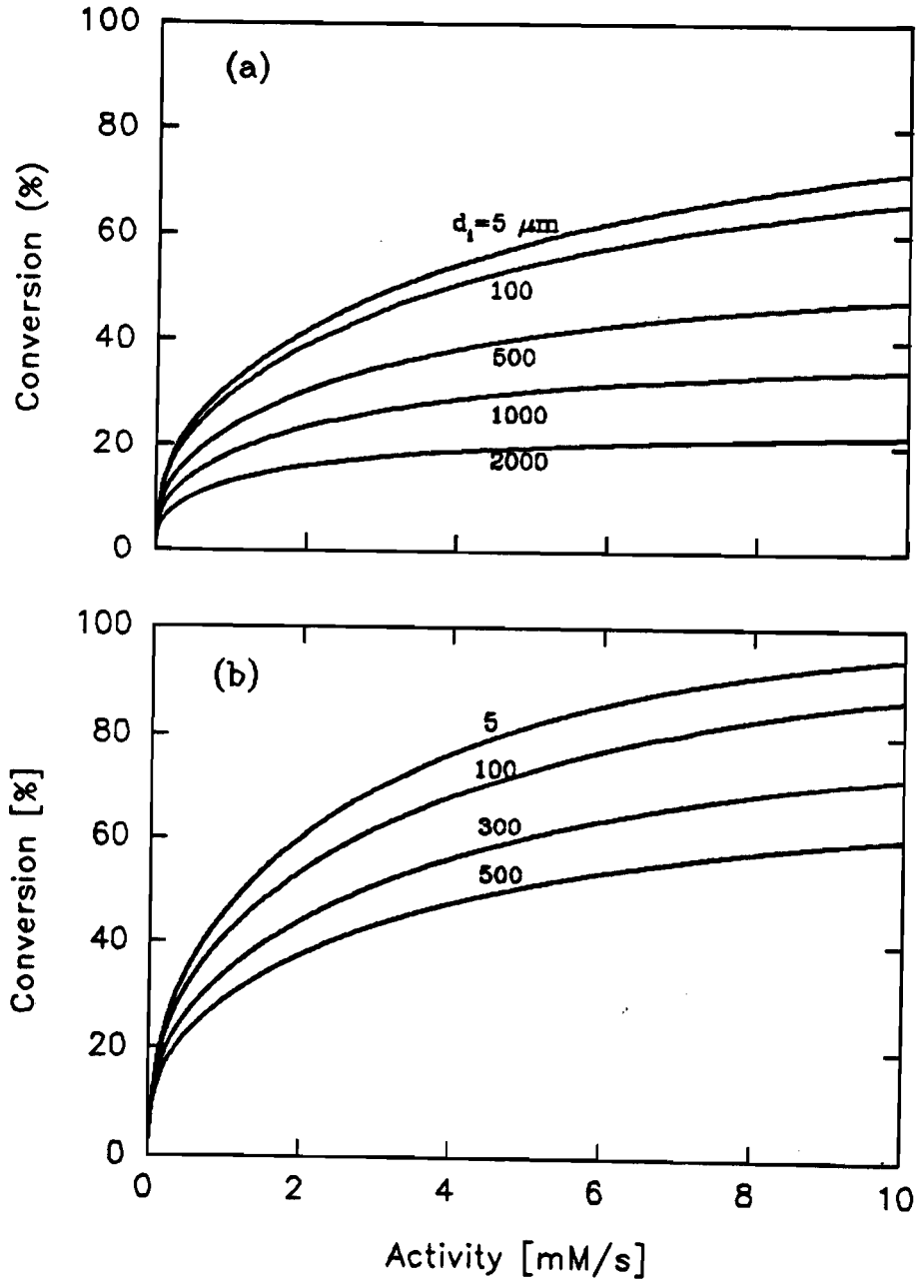

Figure 4-2.

Ammonium ion concentration within a CSTR (a) and FBR (b) as a function of enzyme activity. Simulations are presented for microcapsule diameters ranging from 5 to 2000 μm.

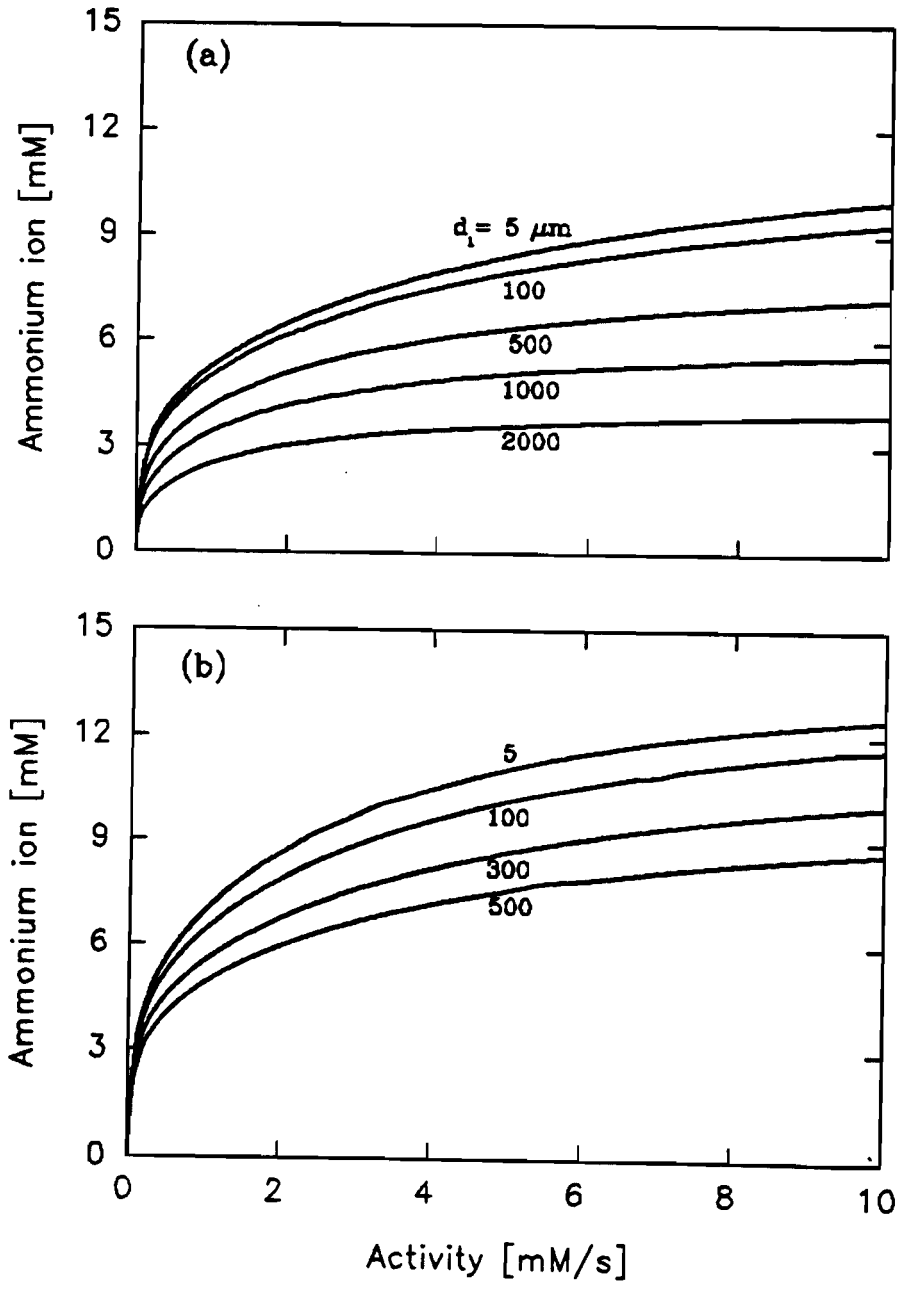

Figure 4–4.

Effect of microcapsule diameter (d_i) on effectiveness factor in a CSTR over a range of enzyme activities.

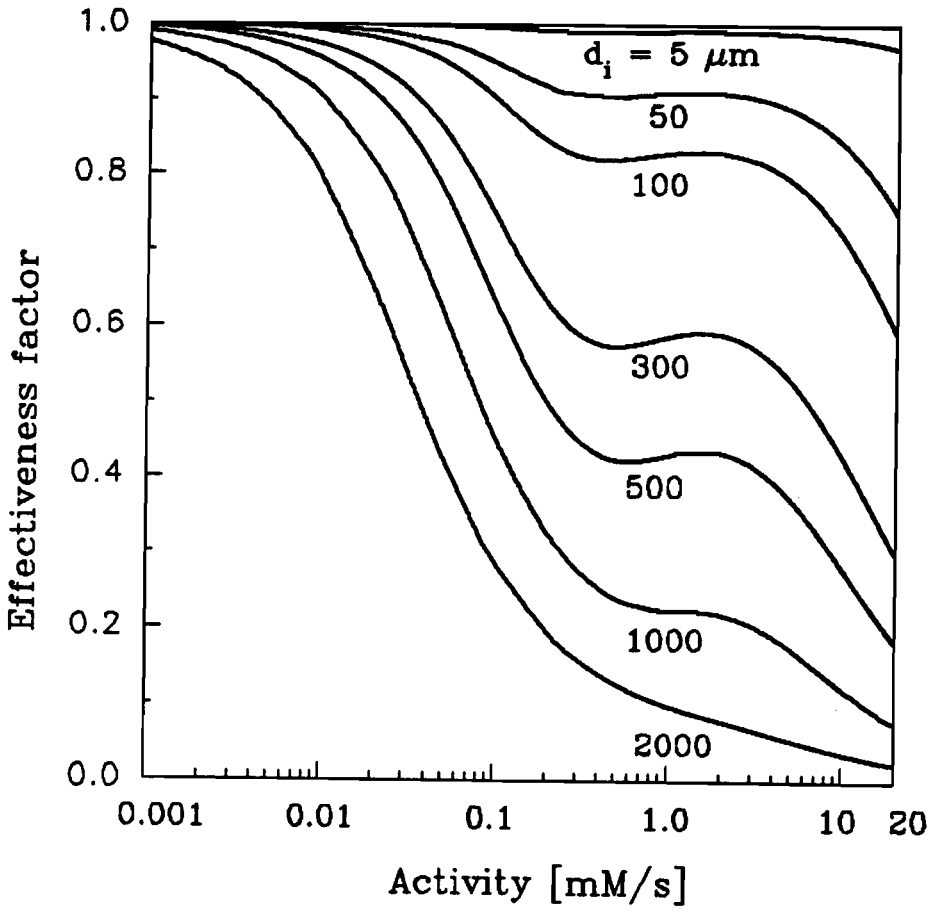

the range of enzyme activities for operating at a high effectiveness factor is more limited for a large as compared to a small diameter microcapsule. For example (Fig. 4-4), the activity range required to obtain 0.9-1 effectiveness factor for a 500 μm capsule is about 0-0.04 mM/s in comparison to 0-90 mM/s for a 5 μm capsule. The profiles in Fig. 4-4 follow an s-shape when the microcapsule diameter increases. At large diameters, the shape becomes pronounced. This may be due to a combined contribution of the large mass transfer resistance and the three limiting effects; pH kinetic effect, product inhibition, and substrate depletion. These effects will be further studied in the next section.

4.2.2 Product Inhibition, pH Kinetics, and Substrate Depletion Effects.

In this section, the results for the ammonium ion noncompetitive inhibition, pH kinetic and substrate depletion effects will be discussed. The individual and combined effects caused by these limiting parameters on the overall conversion of urea and the effectiveness factor were studied using the case studies shown in Table 4-2. Thus, Case 1 is a situation which involves all the three limiting factors whereas Case 6 considers only substrate depletion effects (Michelis-Menten kinetics).

4.2.2.1 The CSTR

The results for urea conversion in a CSTR are presented for the 5 μm (Fig. 4-5) and 500 μm (Fig. 4-6) diameter capsules. The profiles were labeled 1-8 corresponding to the eight cases respectively. Generally, Case 1 yields the lowest conversion values; an implication that the combined substrate depletion, pH kinetic effects, and ammonium ion inhibition, imposes a maximum limiting effect on the reaction rate. In their absence, as is evident with Case 8, the maximum conversion value of 100% was achieved at a very

Figure 4–5.

Reactor performance under various kinetic conditions using 5 μm diameter microcapsules. Conversion is plotted as a function of enzyme activity or ϕ_o^2. The various simulations are identified by the case study designation as summarized in Table 4–2.

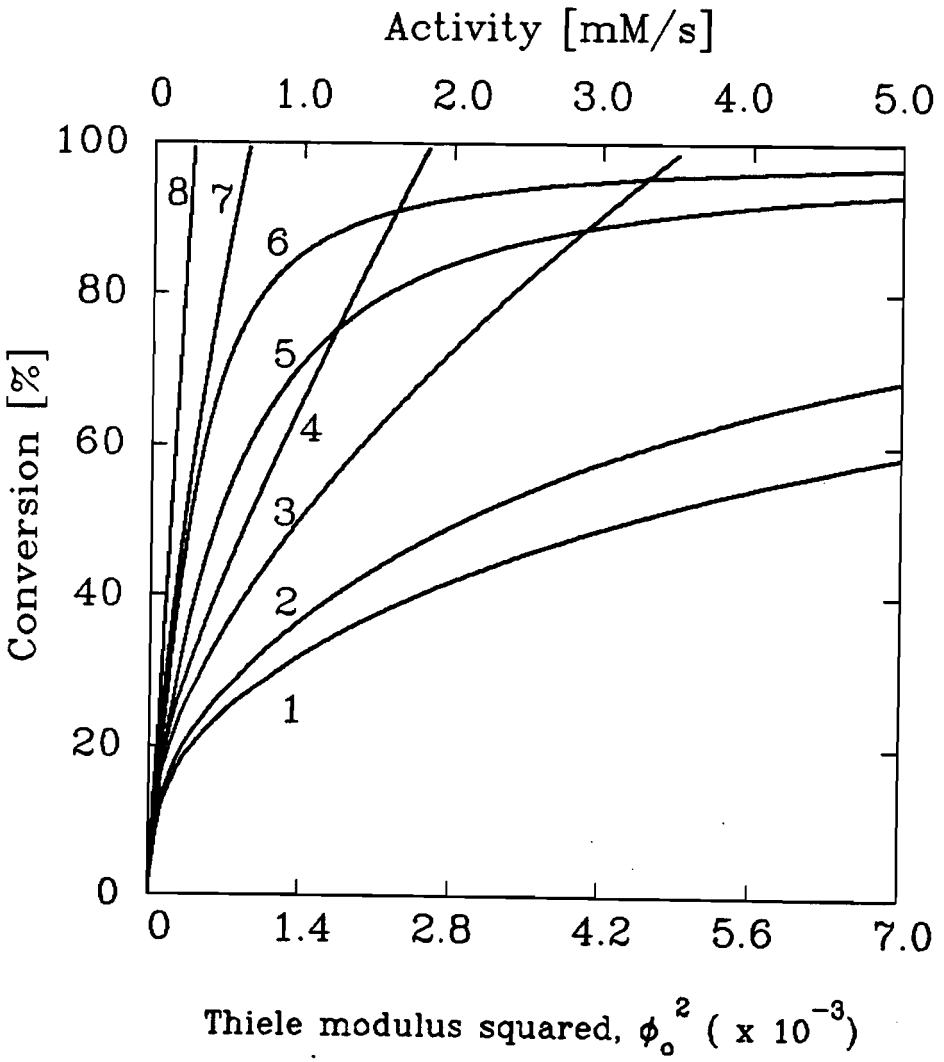

Figure 4–6.

Reactor performance under various kinetic conditions using 500 μm diameter microcapsules. Other simulation conditions are the same as Figure 4–5.

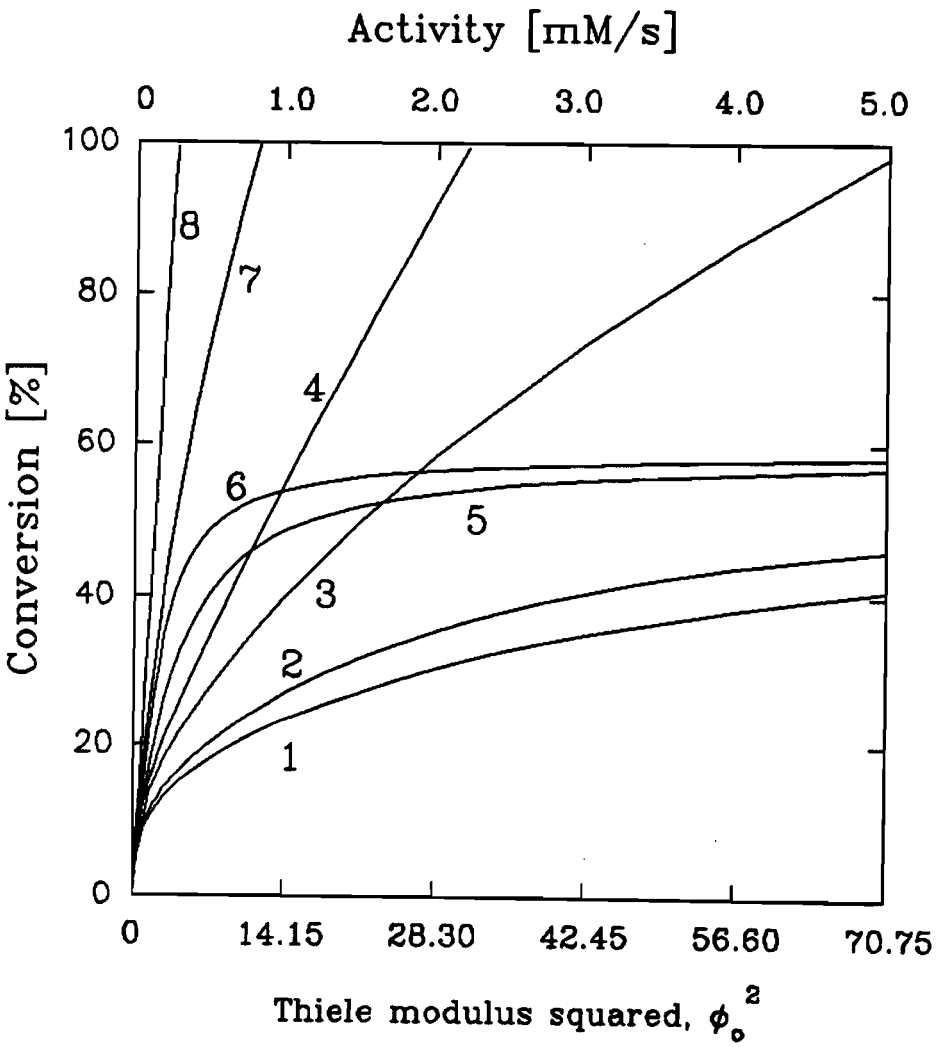

low activity. It was also observed that the conversion increased with an increase in enzyme activity. A 100% conversion was readily achieved by cases 3, 4, 7, and 8. These cases had a common condition of no substrate depletion. When such a condition was coupled with the absence of ammonium ion inhibition (Case 4), or absence of pH kinetic effects (Case 7) or absence of both (Case 8), then there was a dramatic enhancement of the conversion at lower enzyme activities. Hence, a better reactor performance could be achieved by reducing ammonium ion inhibition and pH kinetic effects and maintaining continuous supply of substrate. In practice, ammonium ions could be removed via an ion exchange resin. For a Michelis-Menten kinetic system, Case 6 (curve 6 in Figs. 4-5 and 4-6), for which substrate depletion was the only limitation, a better performance over Case 4 was possible at certain enzyme activities. The conversion values for Case 6, when using a 5 μm microcapsule (Fig. 4-5), were higher than those for Case 4 below an activity of 1.7mM/s, whereas at higher activities, Case 4 is favored. Such trends also exist for other inter-case comparisons. Therefore, Figs. 4-5 and 4-6 could be used as tools for enzyme activity selection as well as for the estimation of expected reactor performance under given operating conditions.

The effects of the limiting factors on the effectiveness factor were calculated for the 5 μm (Fig. 4-7) and 500 μm (Fig. 4-8) diameter microcapsules. In Fig. 4-7, the profiles for cases 1, 3, 4, 5, and 6 were presented, since the results for the other cases were invariant from that of Case 3. For a better understanding of the contributions by the limiting factors, two quantitative numbers f_c and f_η were calculated using Case 1 as a basis, to represent the percentage change in the conversion and effectiveness factor respectively. These numbers are presented in Tables 4-3 to 4-6 for two enzyme activities, 0.25, and 1 mM/s. Table 4-3 shows a consistent increase in f_η, for a 5 μm diameter capsule at 0.25mM/s enzyme activity, from Case 1 (0%) to Case 8 (1%). This is

Figure 4–7.

Effect of kinetic conditions on the effectiveness factor using 5 μm diameter microcapsules. Effectiveness factor is plotted as a function of enzyme activity or ϕ_o^2. The various simulations are identified by the case study designation as summarized in Table 4–2.

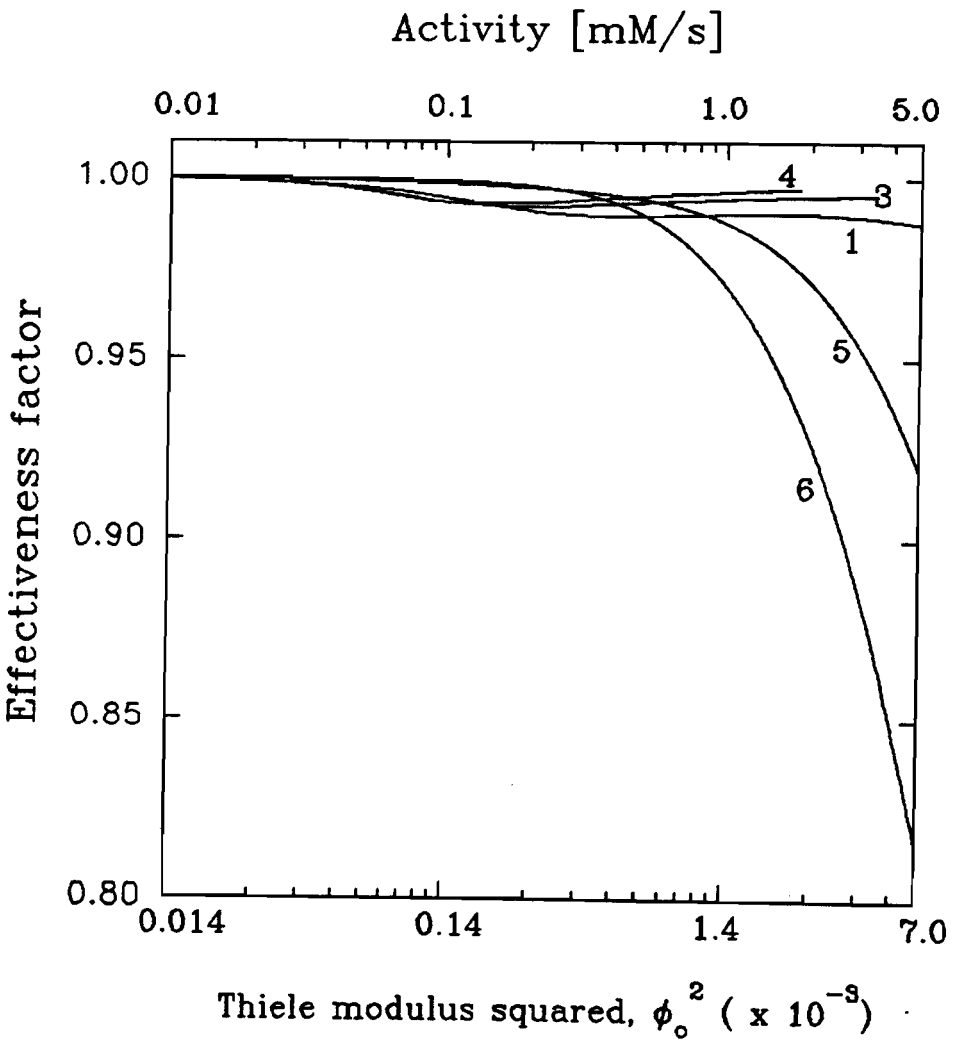

Figure 4–8.

Effect of kinetic conditions on the effectiveness factor using 500 μm diameter microcapsules. Other simulation conditions are the same as Figire 4–7.

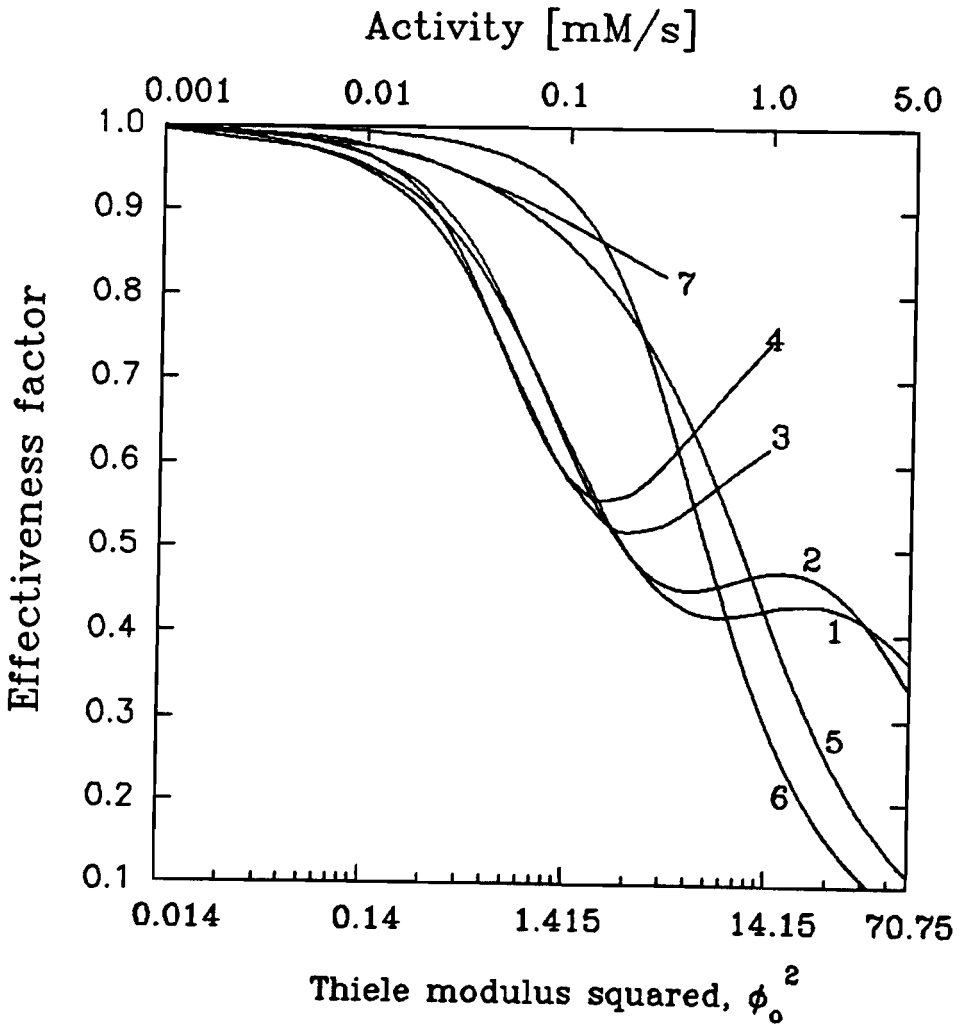

Table 4-3.

Steady state CSTR operating conditions for the various case studies examined, with a microcapsule diameter of 5 μm.

($V_{m,o}E = 0.25$ mM/s)

	CASE 1	CASE 2	CASE 3	CASE 4	CASE 5	CASE 6	CASE 7	CASE 8
S_f(ex.)	8.09	7.91	7.39	7.016	6.42	5.14	4.63	0.526
η	0.990	0.991	0.992	0.994	0.997	0.997	0.998	1.00
Conv.(%)	19.12	20.87	26.07	29.84	35.75	48.57	53.74	94.74
f_η(%)	0	0.1	0.2	0.4	0.7	0.7	0.8	1.0
f_c(%)	0	9.2	36.3	56.0	86.7	154.0	181.0	395.6

Table 4-4.

Steady state CSTR operating conditions for the various case studies examined, with a microcapsule diameter of 5 μm.

($V_{m,o}E = 1.0$ mM/s)

	CASE 1	CASE 2	CASE 3	CASE 4	CASE 5	CASE 6	CASE 7	CASE 8
S_r(ex.)	6.80	6.34	4.97	3.43	2.93	1.47		
η	0.990	0.991	0.994	0.996	0.988	0.971		
Conv.(%)	31.98	36.62	50.25	65.66	70.67	85.34	100.0	100.0
f_q(%)	0	0.1	0.4	0.6	- 0.2	- 1.9		
f_c(%)	0	14.5	57.1	105.3	121.0	166.8	212.7	212.7

Table 4-5.

Steady state CSTR operating conditions for the various case studies examined, with a microcapsule diameter of 500 μm.

($V_{m,o}E = 0.25$ mM/s)

	CASE 1	CASE 2	CASE 3	CASE 4	CASE 5	CASE 6	CASE 7	CASE 8
S_r(ex.)	8.585	8.455	8.01	7.68	7.04	6.11	5.24	0.526
η	0.467	0.472	0.521	0.580	0.742	0.7318	0.833	1.0
Conv.(%)	14.15	15.45	19.87	23.21	29.59	38.91	47.55	94.75
f_q(%)	0	1.07	11.56	24.20	58.89	56.75	78.37	114.0
f_c(%)	0	9.18	40.42	63.91	109.12	175.0	236.0	570.0

Table 4-6.

Steady state CSTR operating conditions for the various case studies examined, with a microcapsule diameter of 500 μm.

($V_{m,o}E = 1.0$ mM/s)

	CASE 1	CASE 2	CASE 3	CASE 4	CASE 5	CASE 6	CASE 7	CASE 8
S_r(ex.)	7.654	7.30	6.015	4.505	5.14	4.60		
η	0.429	0.472	0.6196	0.7446	0.417	0.290	0.79	1.0
Conv.(%)	23.456	26.99	39.85	54.95	48.63	53.97	100	100
f_η(%)	0	10	44.4	73.6	- 2.8	- 32.4	84.1	133.0
f_c(%)	0	15	69.9	134	107	130	326	326

accompanied by increasing f_c values from 0 - 396%. Although, the two cases, 5 (no pH effect), and 6 (no pH and ammonium ion effects) yielded the same f_η value of 0.7%, the corresponding f_c values were 86.7% and 154% respectively. This may be due to the limiting effects of ammonium ions (Case 5) on the rate of intraparticle substrate depletion. The absence of this effect in Case 6, permits better conversion of the urea by the microencapsulated urease. At an enzyme activity of 1 mM/s (Fig. 4-4), f_η values of -0.2% (Case 5) and -1.9% (Case 6) were recorded. These negative values depict a reduction in the effectiveness factor to below that of the base Case 1 (see Fig. 4-3). Despite the suppression of the effectiveness factor, improvements of 121% (Case 5) and 167% (Case 6) in the conversion were recorded. Again, Case 1 which yielded the lowest conversion at all activities (Fig. 4-3), rather predicted a higher effectiveness factor than Cases 5, and 6, at activities beyond 1 mM/s and 0.8 mM/s (Fig. 4-7) respectively. The phenomenon was pronounced at higher activities, and may be due to the fast depletion of substrate at such activities. This was substantiated by the values of the residual substrate concentration, S_r, at 1 mM/s activity (Table 4-4), which were 6.80 mM (Case 1), 2.93 mM (Case 5), and 1.47 mM (Case 6). In fact, the S_r value for Cases 5 and 6 were below the Michelis constant, $K_{m,o}$ = 3.2mM, for urease; an implication of a dramatic drop in the intraparticle reaction rate. Thus, effectiveness factor variations with conversion values are dependent on the conditions operating within the reactor. Similar results were obtained for a 500 μm diameter microcapsule (Figs. 4-6 and 4-8 and Tables 4-5 and 4-6). In the absence of pH kinetic effects (Cases 5, 6, and 7) there was a continuous decrease in the effectiveness factor (Fig. 4-8). Otherwise, the profiles for Cases 1, 2, 3, and 4 were s-shaped, with a minimum point. This minimum changes into a saddle point when the pH kinetic effect (Case 4) is coupled with product inhibition and substrate depletion effects (Cases 1).

From the foregoing discussions, the conditions under which a CSTR could be operated for best reactor performance are as follows: a) continuous operation to maintain substrate, b) reduction of ammonium ion inhibition by continuous removal, c) reduction of pH kinetic effects, and d) the use of small diameter microcapsules.

4.2.2.2 The FBR

The variation of the urea concentration, pH, ammonium ion concentration, and effectiveness factor along the FBR was studied from steady-state calculations for urea hydrolysis at different kinetic conditions (Table 4-2) using an assumed enzyme activity of 1 mM/s. The substrate and the product concentration profiles along the column are presented for the 5 μm (Fig. 4-9) and 500 μm (Fig. 4-10) diameters, respectively. It is evident (Figs. 4-9 and 4-10) that the urea concentration (continuous lines) decreases along the bed for all the Cases considered. There is a reduction in the slope of the profiles from Case 6 down to Case 1; an implication of the fact that limiting factors retard the hydrolysis of urea into products. The corresponding ammonium ion concentration (broken lines) show increasing trends as expected. These profiles could only be calculated for Cases 1, 3, and 5 which accounted for ammonium ion inhibition. The variation of pH along the reactor is presented in Figs. 4-11 (5 μm diameter) and 4-12 (500 μm diameter). In these figures, Cases 5, 6, 7, and 8 are independent of pH as implied in their definitions in Table 4-2, and therefore, only Cases 1 to 4 resulted in pH variations along the reactor length. The results for the 5 μm diameter microcapsule (Fig. 4-11) shows a steep rise in the pH at the bottom 30% (entrance) section of the reactor. The top 70% section of the reactor operated at fairly constant (buffering) pH's. The rise in the pH profiles for the 500 μm diameter (Fig. 4-12) was gradual across the entire bed

Figure 4-9.

Profiles of residual urea (solid line) and ammonium ion (dashed line) along the height of the FBR at $V_{m,o}E$=1mM/s for d_i=5 μm. The various simulations are identified by the case study designation as summarized in Table 4-2.

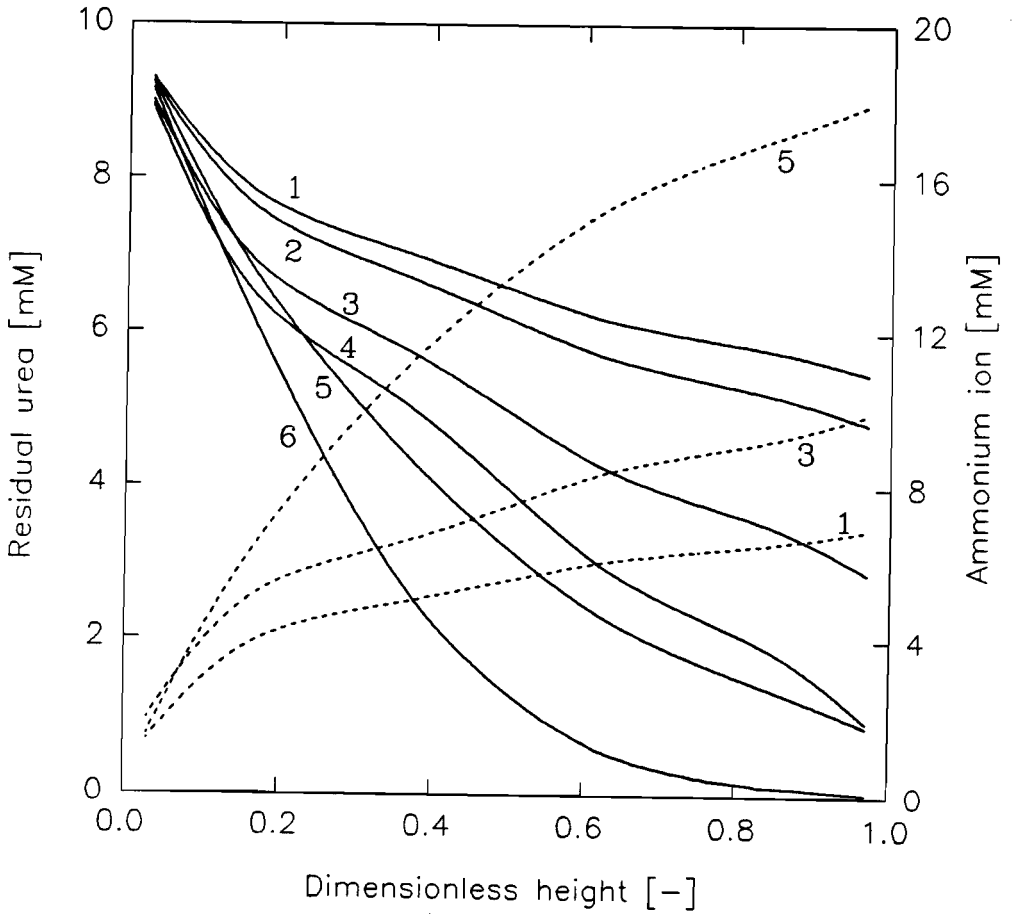

Figure 4–10.

Profiles of residual urea (solid line) and ammonium ion (dashed line) along the height of the FBR at $V_{m,o}E$=1 mM/s for d_i=500 μm. Other simulation conditions are the same as Figure 4–9.

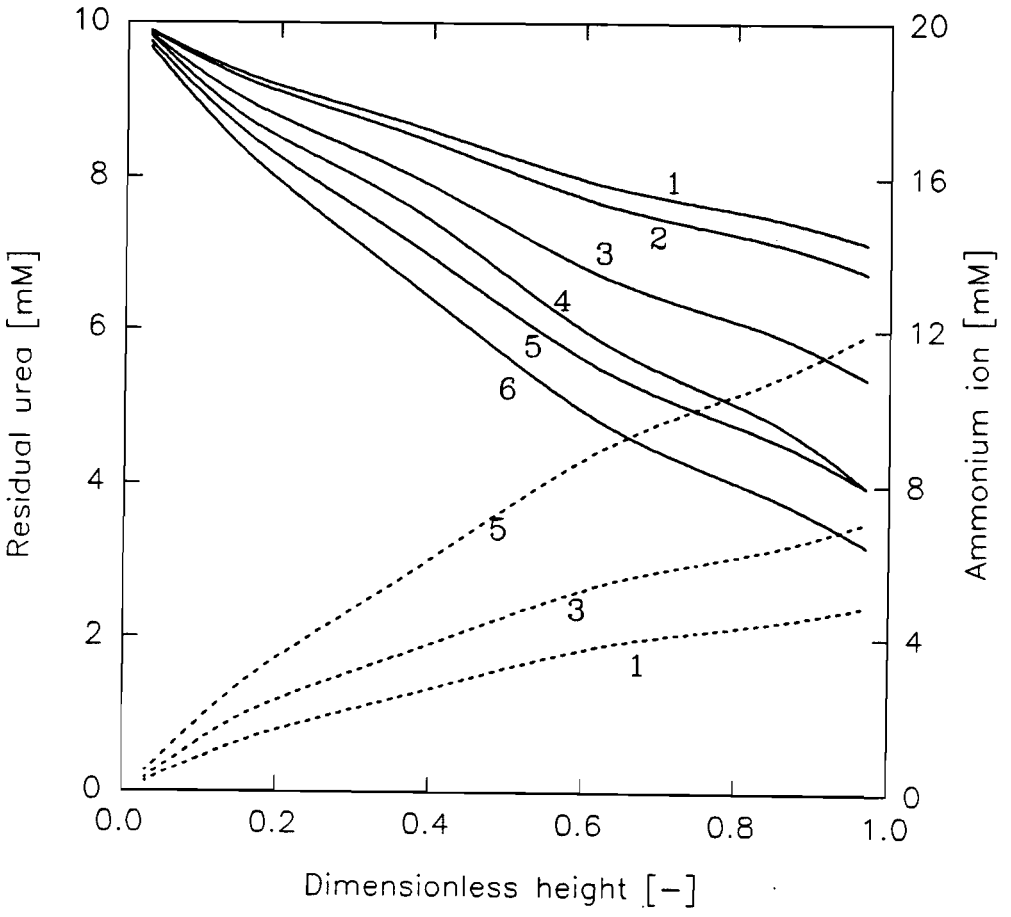

Figure 4-11.

Effect of kinetic conditions on pH profile along the reactor using 5 μm diameter microcapsules at $V_{m,o}$ E = 1 mM/s. The various simulations are identified by the case study designation as summarized in Table 4-2.

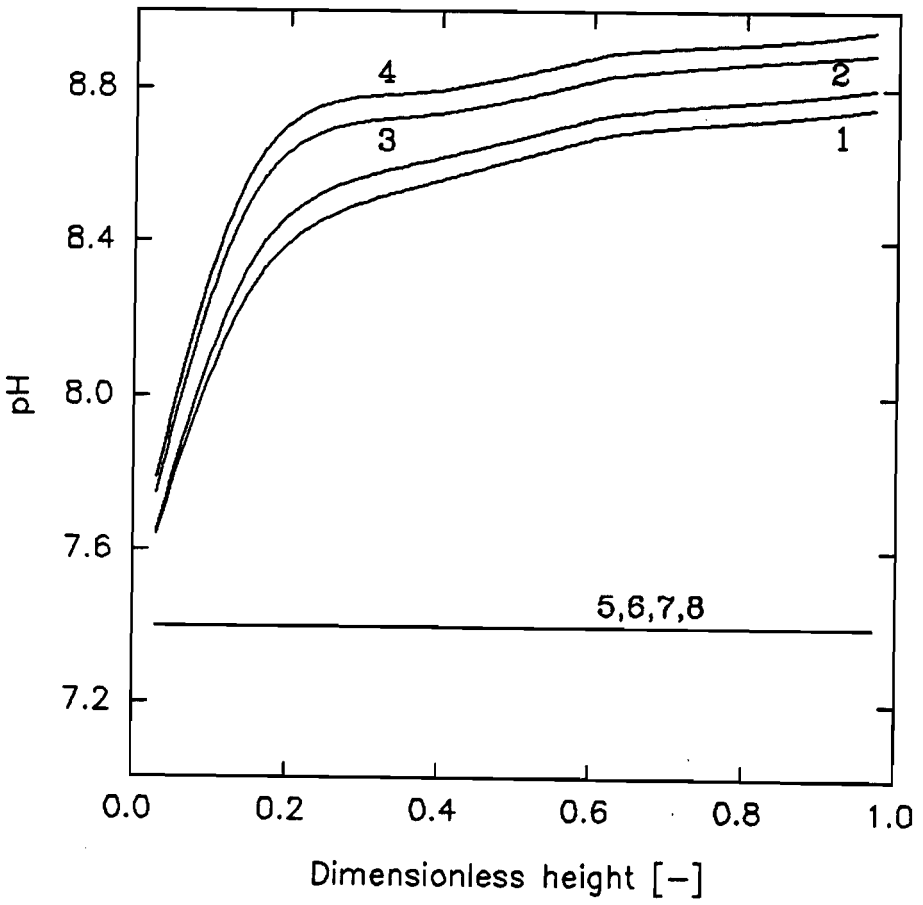

Figure 4–12.

Effect of kinetic conditions on pH profile along the reactor using 500 μm diameter microcapsules at $V_{m,o}$ E = 1 mM/s. Other simulation conditions are the same as Figure 4–11.

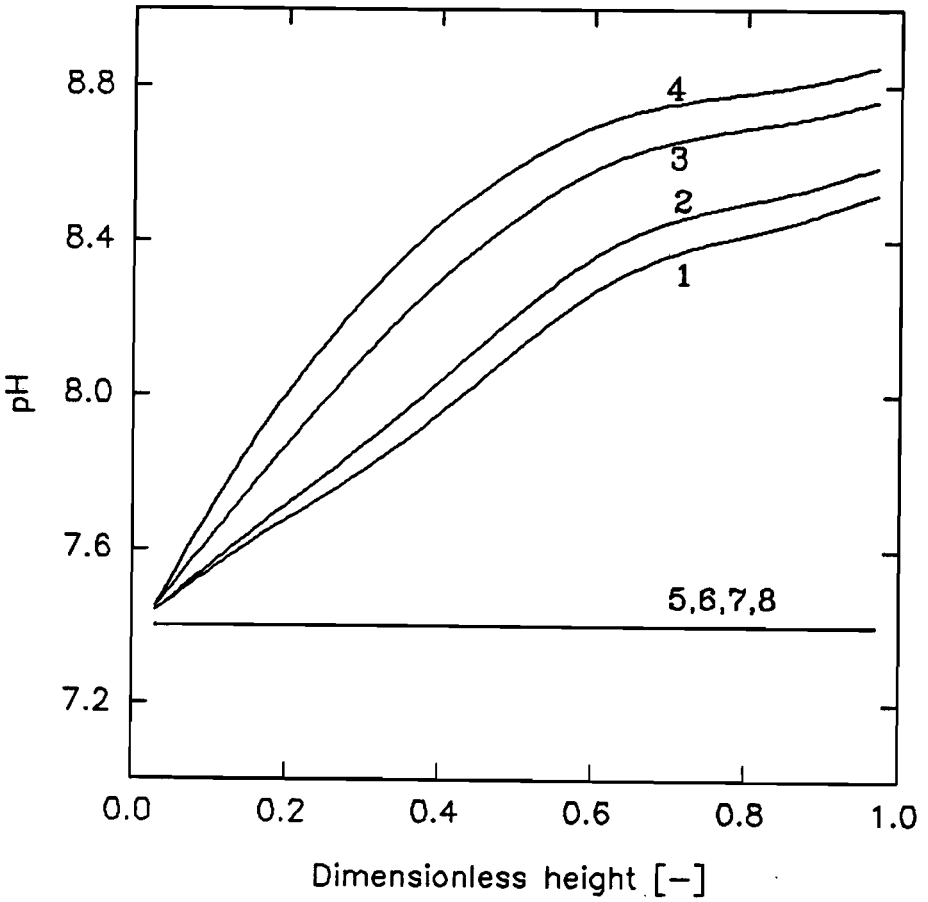

length. The diffusional resistance caused by the large diameter microcapsule may be responsible for this gradual rise in the pH.

Figs. 4-13 and 4-14 show the variation of the effectiveness factor along the bed for the 5 μm diameter and the 500 μm diameter microcapsules respectively. Effectiveness factors, along the reactor, tend to rise for Cases 1-4 whereas for Cases 5 and 6 a decreasing trend was obtained due to the rapid substrate depletion. At the bottom 30% of the reactor, Case 5 yields an increase in the effectiveness factor followed by a gentle reduction for the top 70% of the bed. Case 6 yields a gradual decrease in the effectiveness factor from the bottom to the top of the bed. It may be concluded from the results that, for Case 6, the bottom of the FBR is more efficient than the top and vice-versa for Cases 1-5.

In order to study the overall performance of the FBR, urea conversion was calculated at the exit of the reactor for various enzyme activities and the results presented in Figs. 4-15 (5 μm) and 4-16 (500 μm). Similar to the CSTR, Case 1 yielded the lowest conversion due to the combined operation of the three limiting factors. The enhancement factors, f_η and f_c are recorded in Tables 4-7 and 4-8 (5 μm) and 4-9 and 4-10 (500 μm). Urea conversion was enhanced with the elimination of the limiting factors; the extent of enhancement was dependent on the type of limitation which was removed. A mean microcapsule effectiveness factor was determined by averaging the values obtained for different axial sections of the reactor. This is presented in Fig. 4-17 (5 μm) for Cases 1, 5 and 6, and in Fig. 4-18 (500 μm) for Cases 1, 4, 5 and 6. All cases showed a general decrease in the effectiveness factor with increasing activity. Case 1 predicted a lower average effectiveness factor than Cases 5 and 6 at activities below 1mM/s. However, the trend was reversed at higher activities. This phenomenon has been explained by the conditions prevailing in the reactor. At low enzyme activities, the three

Figure 4–13.

Effect of kinetic conditions on the effectiveness factor using 5 μm diameter microcapsules at $V_{m,opt}E$ = 1 mM/s. The various simulations are identified by the case study designation as summarized in Table 4–2.

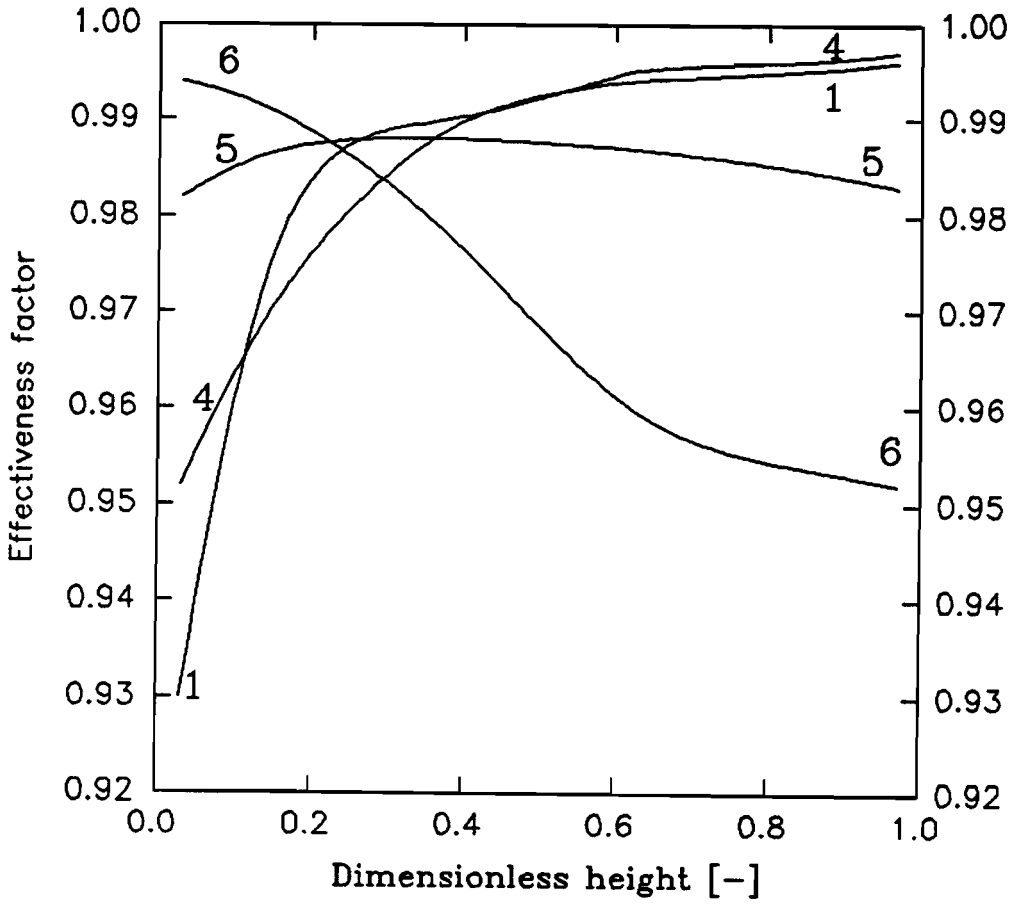

Figure 4–14.

Effect of kinetic conditions on the effectiveness factor using 500 μm diameter microcapsules at $V_{m,o}$ E = 1 mM/s. Other simulation conditions are the same as Figure 4–13.

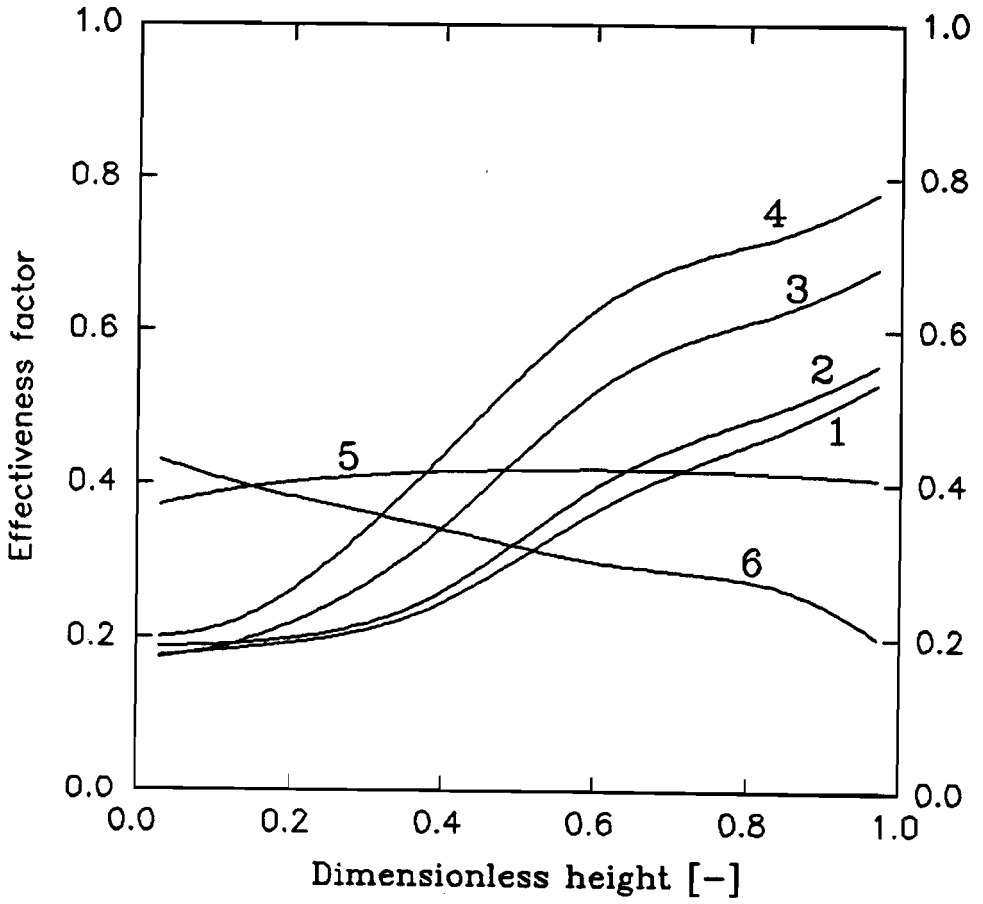

Figure 4–15.

FBR performance under various kinetic conditions using 5 μm diameter microcapsules. Conversion is plotted as a function of enzyme activity or ϕ_o^2. The various simulations are identified by the case study designation as summarized in Table 4–2.

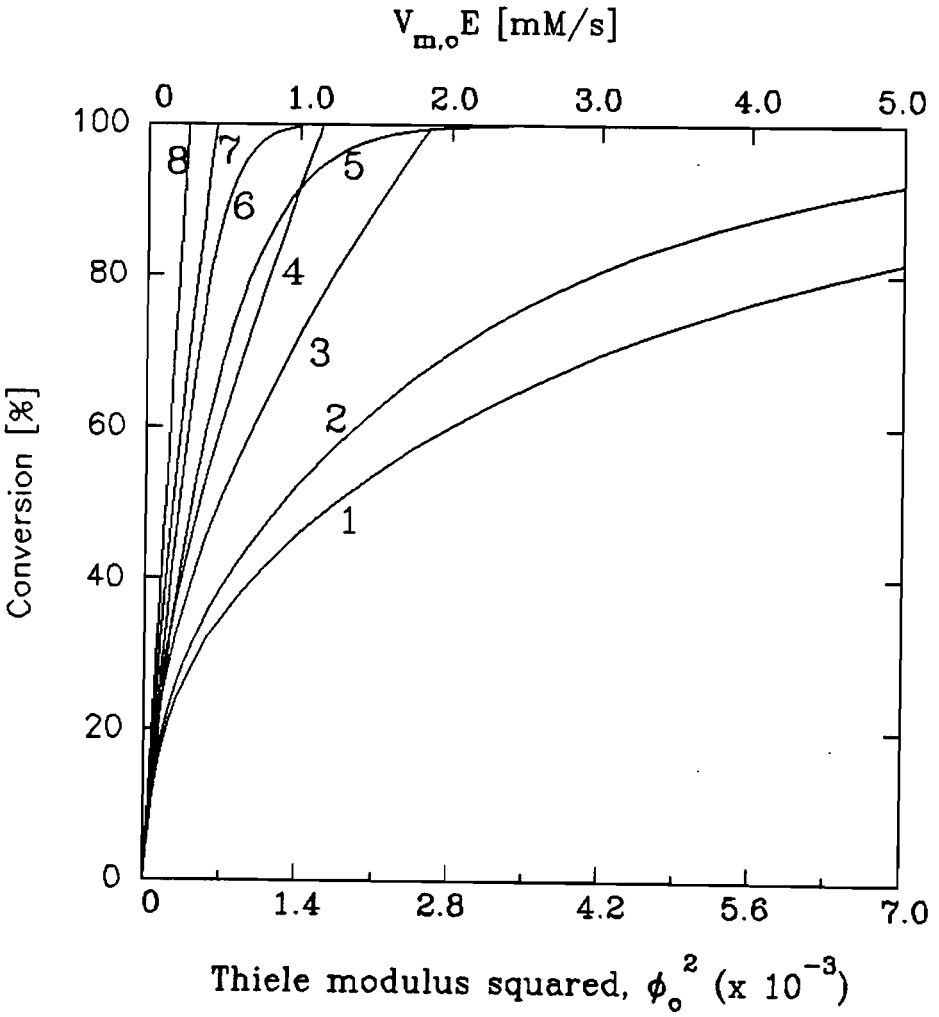

Figure 4–16.

FBR performance under various kinetic conditions using 500 μm diameter microcapsules. Other simulation conditions are the same as Figure 4–15.

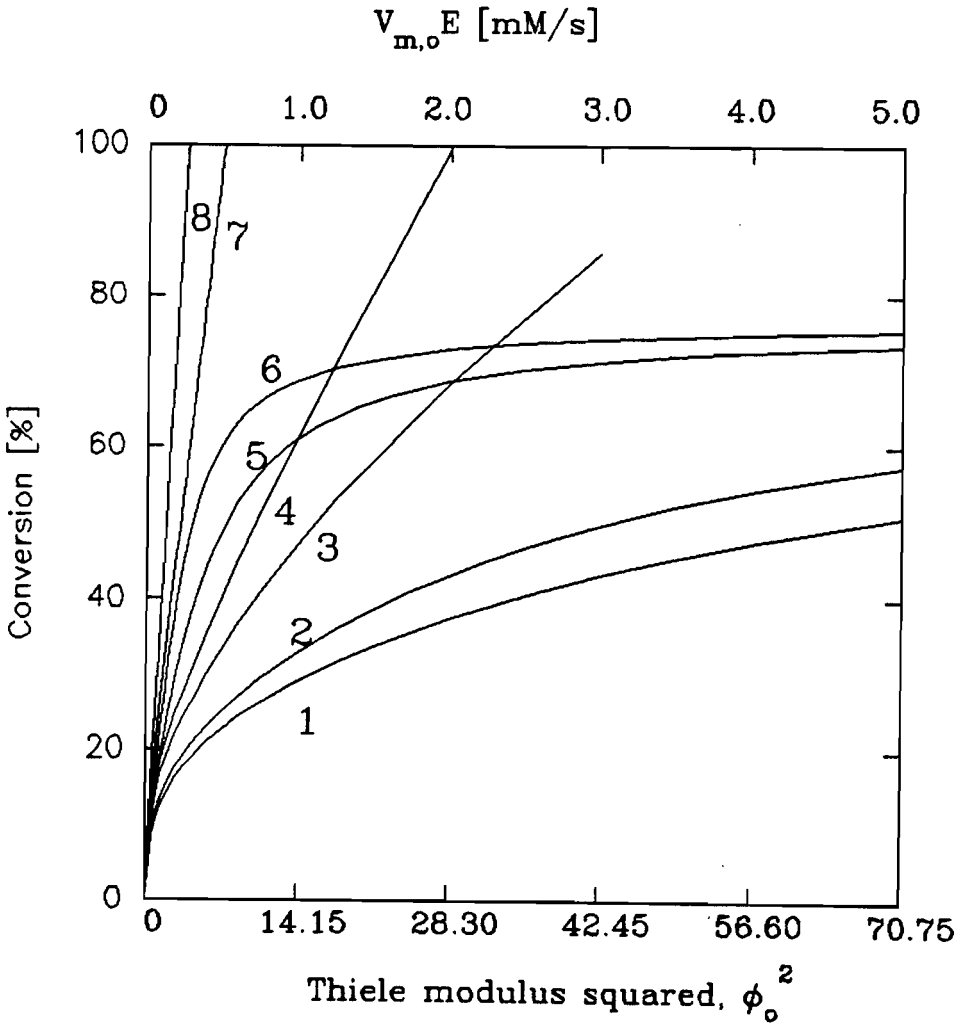

Table 4-7.
Steady state FBR operating conditions for the various case studies examined, with a microcapsule diameter of 5 μm.

($V_{m,o}$ = 0.25 mM/s)

	CASE 1	CASE 2	CASE 3	CASE 4	CASE 5	CASE 6	CASE 7	CASE 8
pH(ex) pH(av)	8.46 7.89	8.52 7.91	8.66 8.01	8.73 8.03	7.40	7.40	7.40 7.40	7.4
NH_4^+(ex) NH_4^+(av)	4.49 2.91	nil nil	5.80 3.81	nil	8.66 4.75	nil	12.85 7.00	nil
S_r(ex) S_r(av)	7.40 8.37	7.15 8.24	6.37 7.74	5.86 7.48	5.61 7.58	4.43 7.06	3.49 6.44	18.80 9.47
K_m(ex) K_m(av)	9.83 7.84	10.10 8.07	n/a	n/a	4.85 4.85	4.85 4.85	n/a	n/a
η(av.)	0.99	0.99	0.99	0.99	0.996	0.998	0.997	1.0
Conv.(%)	26.03	28.49	36.26	41.39	43.90	55.68	65.14	95.33
f_η(%)	0	0	0	0	0.6	0.8	0.7	1.0
f_c(%)	0	9.5	39.3	59.0	68.7	113.9	150.2	266.2

Table 4-8.
Steady state FBR operating conditions for the various case studies examined, with a microcapsule diameter of 5 μm.

($V_{m,o}E$ = 1 mM/s)

	CASE 1	CASE 2	CASE 3	CASE 4	CASE 5	CASE 6	CASE 7	CASE 8
pH(ex) pH(av)	8.73 8.19	8.77 8.22	8.81 8.32	8.84 8.36	7.40	7.40	7.40	7.4
NH_4^+(ex) NH_4^+(av)	6.95 4.93	0 0	9.97 6.82	0 0	18.05 11.52	0 0		0 0
S_r(ex) S_r(av)	5.42 6.92	4.77 6.54	2.81 5.37	0.84 4.35	0.85 4.14	0.04 3.10		
K_m(ex) K_m(av)	11.01 9.59	11.16 9.78	0 0	0 0	4.85 4.85	4.85 4.85	0 0	0 0
η(av.)	0.98	0.98	0.98	0.99	0.99	0.97		
Conv.(%)	45.77	52.34	71.92	91.60	91.54	99.63	100	100
f_η(%)	0	0	0	1.0	1.0	-1.0		
f_c(%)	0	14.3	57.1	100.1	100.0	117.7	118.5	118.5

Table 4-9.
Steady state FBR operating conditions for the various studies examined, with a microcapsule diameter of 500 μm.

($V_{m,o}$ = 0.25 mM/s)

	CASE 1	CASE 2	CASE 3	CASE 4	CASE 5	CASE 6	CASE 7	CASE 8
pH(ex) pH(av)	8.15 8.08	8.22 8.12	8.42 8.24	8.52 8.29	7.40	7.40	7.40	7.4
NH_4^+(ex) NH_4^+(av)	3.29 3.17	0 0	4.28 4.07	0 0	6.79 6.48	0 0	10.65 10.09	0 0
S_r(ex) S_r(av)	8.23 7.94	8.07 7.76	7.56 7.17	7.21 6.80	6.55 6.11	5.51 4.96	4.60 3.93	
K_m(ex) K_m(av)	8.22 8.45	8.61 8.77	0 0	0 0	4.85 4.85	4.85 4.85	0 0	0 0
η(av.)	0.456	0.465	0.463	0.493	0.718	0.774	0.779	
Conv.(%)	17.74	19.28	24.45	27.90	34.45	44.92	53.99	95.35
f_η(%)	0	2.0	1.5	8.1	57.5	69.7	70.8	
f_c(%)	0	8.7	37.8	57.3	94.2	153.2	204.3	437.5

Table 4-10.
Steady state FBR operating conditions for the various case studues examined, with a microcapsule diameter of 500 μm.

($V_{m,o}E$= 1 mM/s)

	CASE 1	CASE 2	CASE 3	CASE 4	CASE 5	CASE 6	CASE 7	CASE 8
pH(ex) pH(av)	8.54 8.32	8.62 8.36	8.79 8.45	8.88 8.49	7.40	7.40	7.40	7.4
NH_4^+(ex) NH_4^+(av)	4.89 4.66	0 0	7.11 6.69	0 0	12.04 11.86	0 0		0 0
S_r(ex) S_r(av)	7.09 6.63	6.71 6.21	5.29 4.62	4.09 3.34	3.89 2.91	3.13 1.97		
K_m(ex) K_m(av)	10.15 10.05	10.46 10.28	0 0	0 0	4.85 4.85	4.85 4.85	0 0	0 0
η(av.)	0.328	0.348	0.424	0.500	0.404	0.330		
Conv.	29.07	32.93	47.14	59.06	61.06	68.69	100	100
f_η(%)	0	6.1	29.3	52.4	23.2	0.6		
f_c(%)	0	13.3	62.2	103.2	110.0	136.3		

Figure 4–17.

Effect of kinetic conditions on the effectiveness factor using 5 μm diameter microcapsules. Effectiveness factor is plotted as a function of enzyme activity or ϕ_o^2. The various simulations are identified by the case study designation as summarized in Table 4–2.

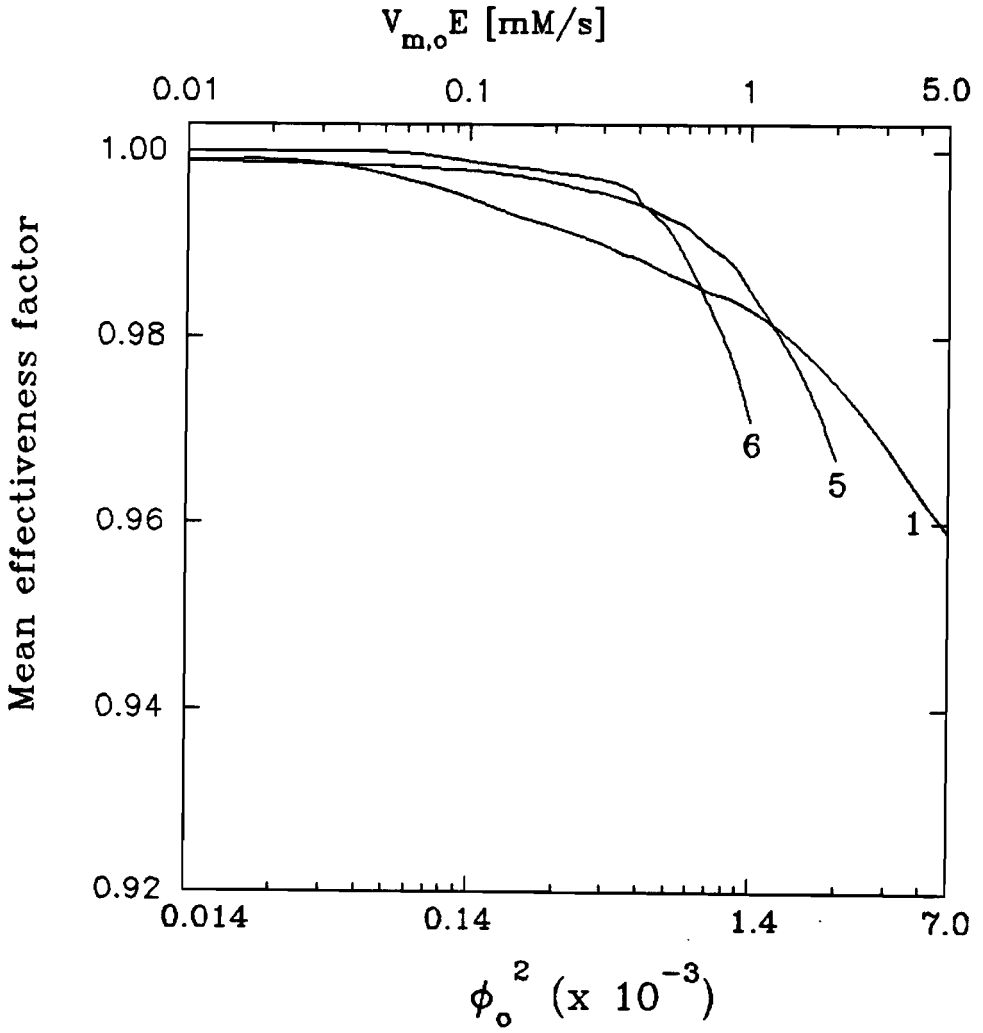

Figure 4–18.

Effect of kinetic conditions on the effectiveness factor using 500 μm diameter microcapsules. Other simulation conditions are the same as Figure 4–17.

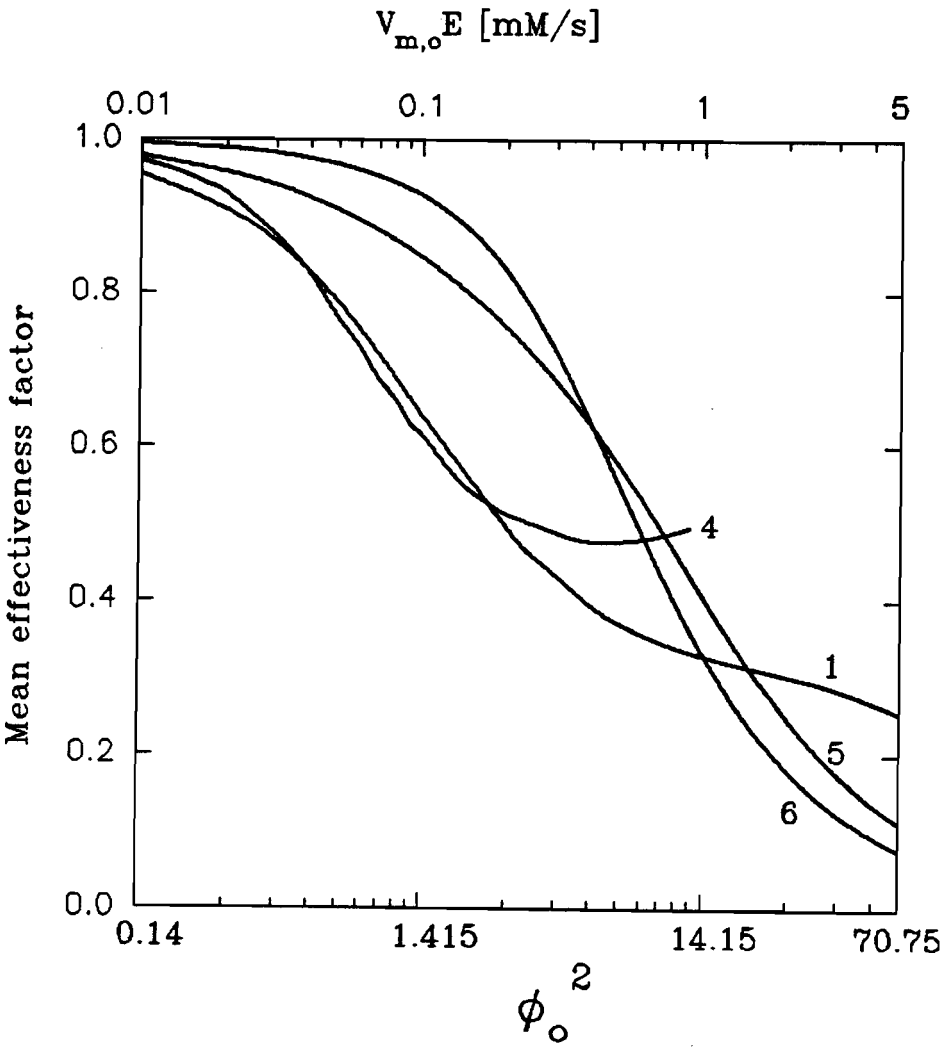

factors (ammonium ion inhibition, pH kinetic effects and substrate depletion) which are inherent in Case 1 limit the rate of reaction within the microcapsule. The degree of limitation is higher than Case 5 (ammonium ion and substrate depletion) and Case 6 (substrate depletion only). Hence, the effectiveness factor tends to increase from Case 1 to Case 6. The urea depletion within the microcapsule is in the order of Case 6 > Case 5> Case 1. At high enzyme activities, the residual urea concentration may decrease dramatically to below $K_{m,o}$ (Michelis constant) leading to a drastic reduction in the reaction rate within the microcapsule. The dramatic decrease in the urea concentration may be prevented of reaction limitation factors. Thus, at high enzyme activities, the mean effectiveness factor would decrease from Case 1 to 6 as shown in Tables 4-7 and 4-8 (5 μm diameter) and 4-9 and 4-10 (500 μm diameter).

4.2.3 External Mass Transfer Resistances

Two dominant resistances, namely liquid film and membrane film, are responsible for external diffusion limitations in a microencapsulated enzyme system. In fact, with microencapsulated enzymes, the study of external diffusion effects alone cannot be readily done, especially if Michaelis-Menten type reaction is involved, because in such cases internal diffusional effects also have to be taken into account. Nevertheless, it is possible to describe the film diffusional effects under certain assumptions. Since membrane and external film resistances produces combined effects, in this study, an attempt is made to isolate the contribution by each of these factors.

4.2.3.1 Liquid film resistance

The calculations for this section were based on the following conditions for both reactor configurations: 1) an initial dialysate concentration of 10 mM urea at pH = 7.4 and a temperature of 25°C; 2) a membrane thickness (δ) of 0.02 μm; 3) a microcapsule loading (reactor void volume, α) of 0.5, and a dialysate residence time (τ_f) of 46s. For simplicity, only the modified Michelis-Menten kinetic model which accounts for product inhibition, substrate depletion and pH effects (Case 1) was considered for this study.

In order to describe mass transfer through the external liquid film, the mass transfer coefficient for urea, $k_{s,L}$, defined by Eq. (3-25) (CSTR) or Eq. (3-32) (FBR) was used in the calculations. This was sometimes transformed to a dimensionless form as the mass transfer Nusselt number which is defined as

$$N_{u_{m,s}} = k_{s,L} \frac{d_p}{D_s} \tag{4-3}$$

The limiting values of the mass transfer Nusselt number are 2 (lowest value) and infinity (maximum). The influence of external liquid film resistance on the urea conversion was calculated by maintaining the particle diameter, d_p, and the diffusion coefficient, D_s, in Eq. (4-3) constant. By using various values of $k_{s,L}$ the results for the 5 and 500 μm microcapsules are as shown in Fig. 4-19 (CSTR) and 4-20 (FBR). These figures show that the conversion profile is independent of $k_{s,L}$, since a single profile (dashed curve) is always obtained. Hence, for a small diameter microcapsule, the external liquid film mass transfer resistance is negligible. However, for a large diameter capsule, 500μm, there is an effect of film resistance as shown by curves A, B, and C in Figs. 4-19 and 4-20. Curve A represents the situation whereby $k_{s,L}$ is infinite whereas curve C denotes the lowest value as predicted by Eq. (4-3). The detailed data is shown in Table 4-11, as the substrate mass transfer Nusselt number is varied from 2 to infinity.

Figure 4–19.

Effect of external liquid film resistance on the urea conversion in a CSTR. Conversion is plotted as a function of enzyme activity.

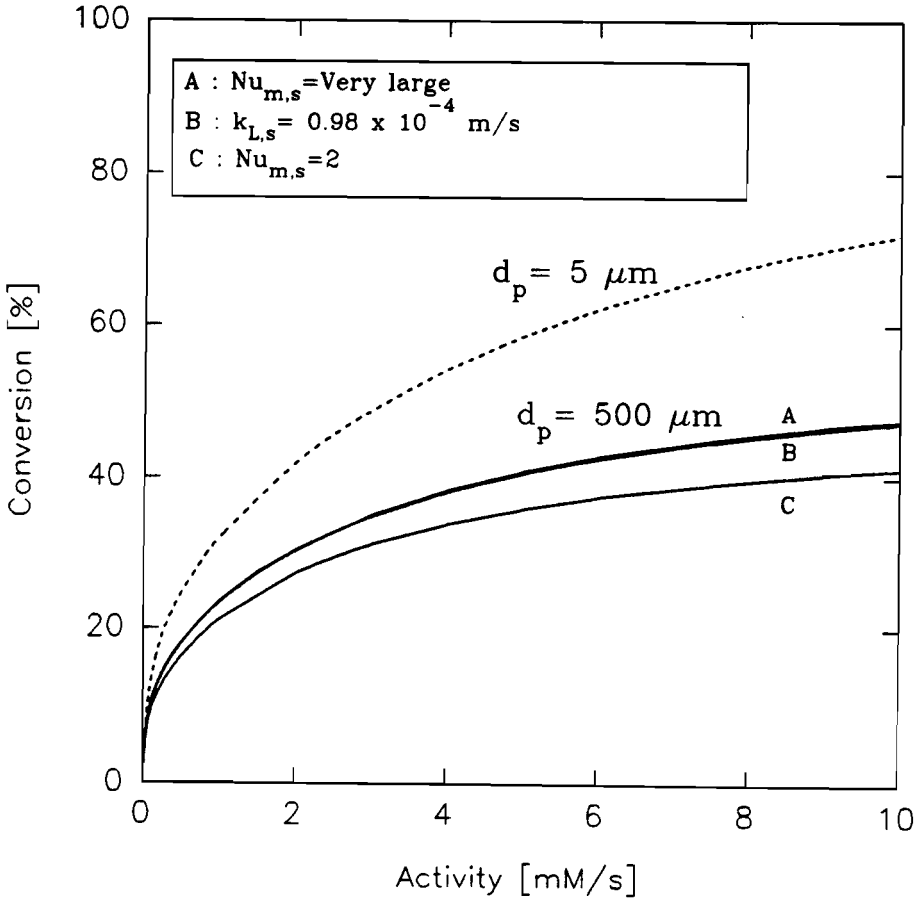

Figure 4–20.

The effect of external liquid film diffusion on the urea conversion in a FBR.

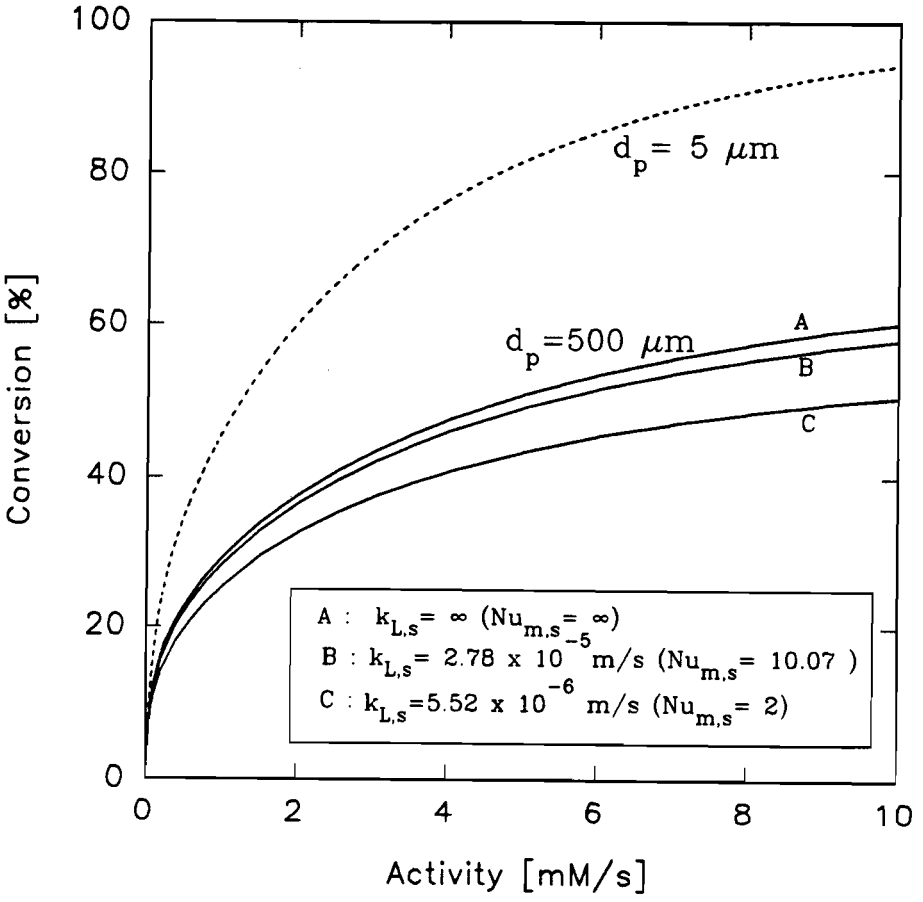

Table 4-11.
Data on the effect of liquid film resistance on reactor performance in a CSTR with a microcapsule diameter of 500 μm.

($V_{m,o}E$ = 10.0 mM/s)

	Case A	Case B	Case C
$Nu_{m,s}$	Large	35.7	2
pH_b $pH(r_2)$ $pH(r_1)$ ΔpH	8.77 8.77 8.93 0	8.766 8.769 8.926 0.003	8.71 8.77 8.93 0.06
$NH_4^+{}_b$ [mM] $NH_4^+(r_2)$ [mM] $NH_4^+(r_1)$ [mM] ΔNH_4^+ [mM]	7.17 7.17 9.62 0	7.13 7.20 9.61 0.07	6.40 7.48 9.60 1.08
$S_{r,b}$ [mM] $S_r(r_2)$ [mM] $S_r(r_1)$ [mM] ΔS_r [mM]	5.23 5.23 2.14 0	5.27 5.19 2.13 0.08	5.88 4.53 1.86 1.35
$k_{M,s}$ [m/s]	0.28E-5	0.28E-5	0.28E-5
$k_{L,s}$ [m/s]	Large	0.98E-4	0.55E-5
$k_{O,s}$ [m/s]	0.28E-5	0.27E-5	0.19E-5
$Bi_{m,s}$ [-]	0.253	0.247	0.168
η	0.276	0.270	0.189
Conv.[%]	47.66	47.29	41.22
f_η[%]	0	-2.37	-31.52
f_c[%]	0	-0.78	-13.51

$Nu_{m,s}$ is varied by changes in the film mass transfer coefficient. With low film resistance, the surface pH, NH_4^+, S_r are close to that of the bulk solution. As film resistance increases, a gradient increases in a thin film external to the microcapsule membrane. Therefore, the lower the film resistance ($1/k_{s,L}=0$), the higher the conversion and vice-versa as expected.

4.2.3.2 Membrane Wall Resistance

The calculations for this section were based on the following conditions for both reactor configurations: 1) an initial dialysate concentration of 10 mM urea at pH = 7.4 and a temperature of 25°C; 2) a microcapsule loading (reactor void volume, α) of 0.5, and a dialysate residence time (τ_r) of 46s; 3) negligible film resistance ($k_{s,L}=\infty$).

The effect of different membrane thicknesses on urea conversion was studied by varying the membrane thickness between 0.02 and 0.2 μm in simulation studies. Fig. 4-21 (a and b) illustrates the effect of membrane thickness on the urea conversion in a CSTR at various urease activities for d_p = 5 μm and d_p = 500 μm respectively. For d_p = 500 μm, there is a general decrease in the conversion with increasing membrane thickness. Although variations in conversion were obtained for the 5 μm microcapsule (Fig. 4-21a), they were only minor. In contrast, the liquid film effect (Fig. 4-19) resulted in a single profile for all film resistances. The variations seen in Fig. 4-21a show that, membrane wall resistances are of greater significance than liquid film resistances for small diameter microcapsules. These effects are magnified for the 500 μm diameter microcapsule (Fig. 4-21b), where the conversion could drop dramatically, especially at thicknesses greater than 0.02μm. Tables 4-12 and 4-13 show the detailed data for Figure 4-21. $Bi_{m,s}$ is varied by changes in the membrane thickness. With thinner membranes, pH, NH_4^+, S_r at the exterior surface of the membrane is close to those at the interior

Figure 4-21.

Effect of membrane thickness on urea conversion in a CSTR for 5 μm (a) and 500 μm (b) microcapsules. Simulations are presented for membrane thickness ranging from 0.02 to 0.2 μm.

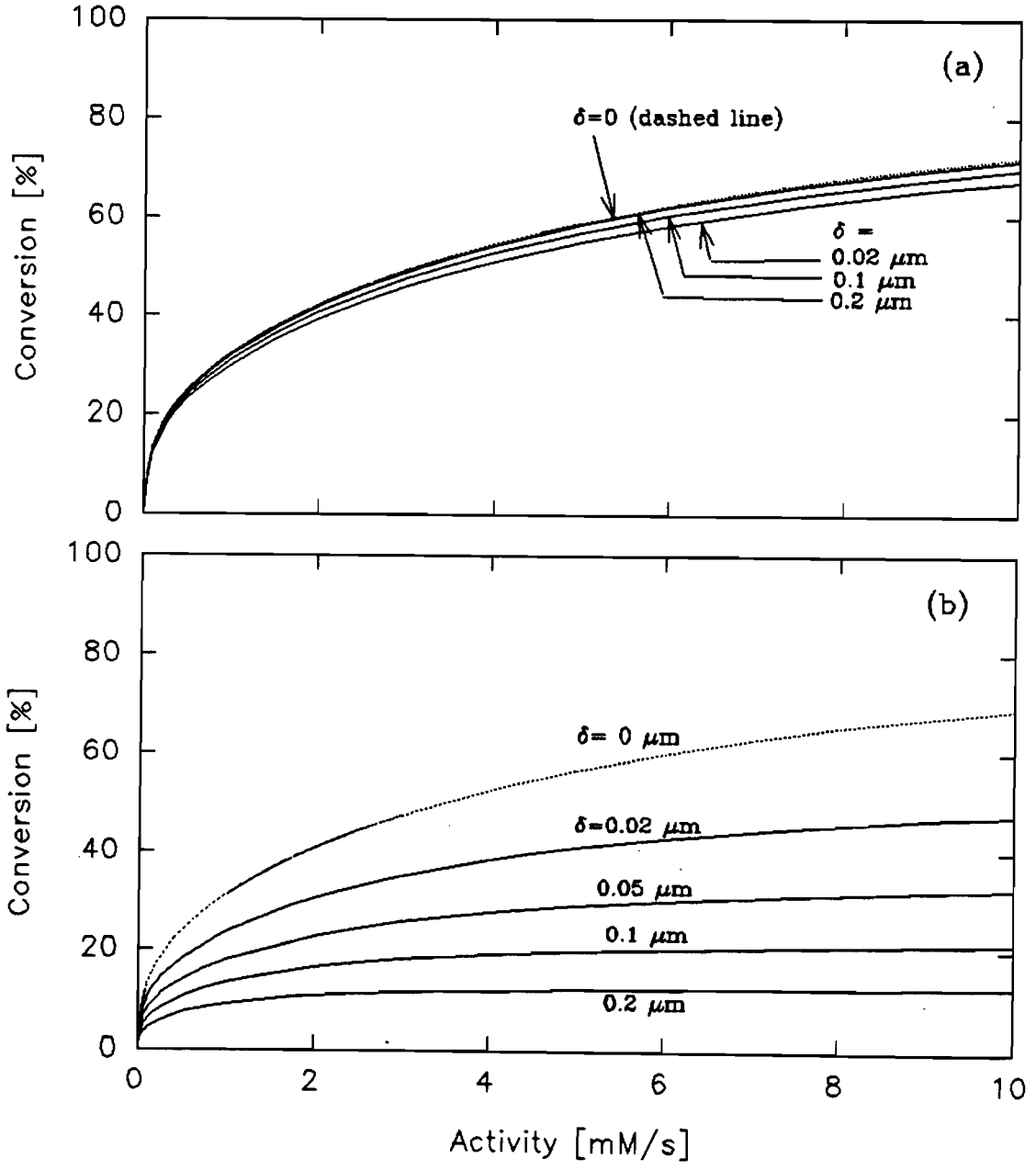

Table 4-12.
Data on the effect of membrane thickness on reactor performance in a CSTR with a microcapsule diameter of 5 μm.

($V_{m,o}E$ = 10.0 mM/s)

	δ [μm]	δ [μm]	δ [μm]	δ [μm]	δ [μm]
	0	0.02	0.05	0.1	0.2
$pH(r_2)$	8.90	8.90	8.89	8.89	8.88
$pH(r_1)$	8.90	8.90	8.90	8.90	8.90
ΔpH	0	0	0.01	0.01	0.02
$NH_4^+(r_2)$ [mM]	10.0	9.95	9.87	9.74	9.46
$NH_4^+(r_1)$ [mM]	10.0	9.99	9.96	9.92	9.83
ΔNH_4^+ [mM]	0	0.04	0.09	0.18	0.37
$S_r(r_2)$ [mM]	2.78	2.83	2.90	3.02	3.26
$S_r(r_1)$ [mM]	2.78	2.78	2.79	2.79	2.79
ΔS_r [mM]	0	0.05	0.11	0.23	0.47
$k_{M,s}$ [m/s]	N/A	0.28E-5	0.11E-5	0.56E-6	0.28E-6
$Bi_{m,s}$ [-]	N/A	0.25E-2	0.10E-2	0.51E-3	0.25E-3
η	1	0.981	0.955	0.913	0.836
Conv.[%]	72.19	71.70	70.98	69.78	67.40
f_η[%]	1.9	0	-2.7	-6.9	-14.8
f_c[%]	0.7	0	-1.0	-2.7	-6.0

Table 4-13.
Data on the effect of membrane thickness on reactor performance in a CSTR with a microcapsule diameter of 500 μm.

($V_{m,o}E$ = 10.0 mM/s)

	δ [μm] 0	δ [μm] 0.02	δ [μm] 0.05	δ [μm] 0.1	δ [μm] 0.2
$pH(r_2)$ $pH(r_1)$ ΔpH	8.89 8.89 0	8.77 8.93 0.16	8.59 8.95 0.36	8.30 8.97 0.67	7.88 8.98 1.10
$NH_4^+(r_2)$ [mM] $NH_4^+(r_1)$ [mM] ΔNH_4^+ [mM]	9.67 9.67 0	7.18 9.62 2.44	5.34 9.56 4.22	3.83 9.51 5.68	2.42 9.49 7.07
$S_t(r_2)$ [mM] $S_t(r_1)$ [mM] ΔS_t [mM]	3.08 3.08 0	5.23 2.15 3.08	6.74 1.47 5.27	7.86 0.97 6.89	8.74 0.57 8.17
$k_{M,s}$ [m/s]	N/A	0.28E-5	0.11E-5	0.56E-6	0.28E-6
$Bi_{m,s}$ [-]	N/A	0.254	0.101	0.051	0.025
η	0.849	0.277	0.103	0.033	0.009
Conv.[%]	69.17	47.70	32.57	21.32	12.62
f_η[%]	206.5	0	-62.8	-88.1	-96.8
f_α[%]	45.0	0	-31.7	-55.3	-73.5

surface of the membrane. As membrane thickness increases, a considerable gradient is present within the membrane. Similar results were obtained for the FBR (Fig. 4-22). Fig. 4-23 shows the calculated results for the effectiveness factor for the two microcapsule diameters in a CSTR. Again, thicker membranes are responsible for sharp drops in the effectiveness factor, especially at high enzyme activities.

Intraparticle profiles for various membrane thicknesses at various positions in a FBR were calculated and presented in Figs. 4-24 and 4-25. Fig. 4-24 shows the profiles for a 5 μm microcapsule at 3% and 96% of the reactor length using δ=0.02 and 0.2 μm. These are flat profiles without any gradient, and small membrane thickness results in reduced diffusional resistance. The results for the 500μm (Fig. 4-25) are different. At the bottom 3% of the bed, the profiles are parabolic and the gradient decreases with the thickness of the membrane wall. The profiles at the top 96% do reveal shallow parabolic profiles. This is due to the fact that the concentration of urea at the bottom of the FBR is higher than at the top and therefore the intraparticle concentration gradients tend to be steeper in particles at the lower than at the upper portions of the reactor.

4.2.4 Model Verification

Attempts were made to verify the theoretical model with the aid of available experimental data in the literature. The CSTR data obtained by Ortmanis and Neufeld (1984) was used for model testing. By using their experimental parameters in the CSTR model, the steady-state conversion of urea at various flow velocities was calculated for Case 1 (Table 4-2) which included substrate depletion, pH kinetics and ammonium ion inhibition effects. Fig. 4-26 shows the comparison of the theory with the experimental points. There is good agreement between the theory and experimental data, particularly, the trend of decreasing conversion with increasing flowrate due to short residence times.

Figure 4–22.

Effect of membrane thickness on urea conversion in a FBR. Simulations are presented for membrane thickness ranging from 0.02 to 0.2 μm.

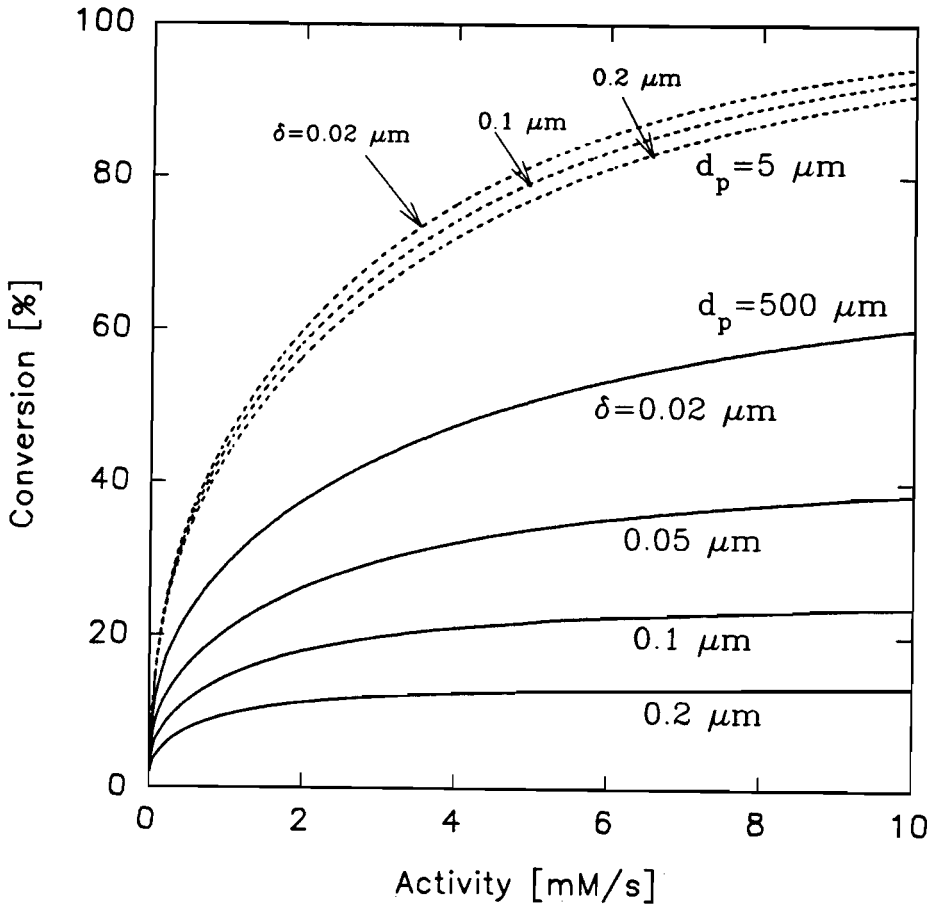

Figure 4-23.

Effect of membrane thickness on effectiveness factor in a CSTR for 5 μm (a) and 500 μm (b) microcapsules. Simulations are presented for membrane thickness ranging from 0.02 to 0.2 μm.

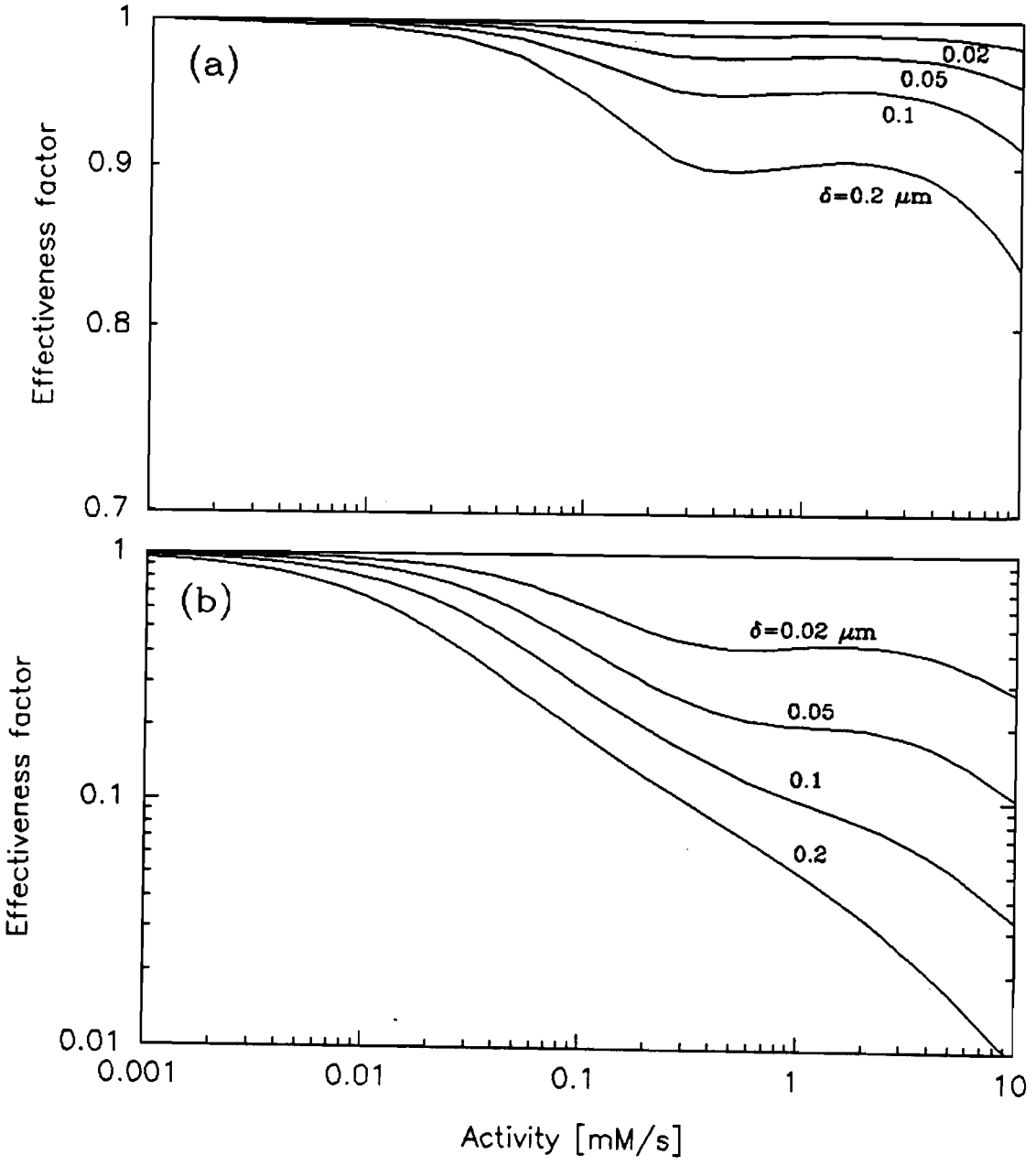

Figure 4-24.

Plot of urea concentration as a function of dimensionless radial position with the microcapsule in a FBR for d_i=5 μm at $V_{m,o}E$= 5 mM/s. z measures the dimensionless height of the column from the bottom.

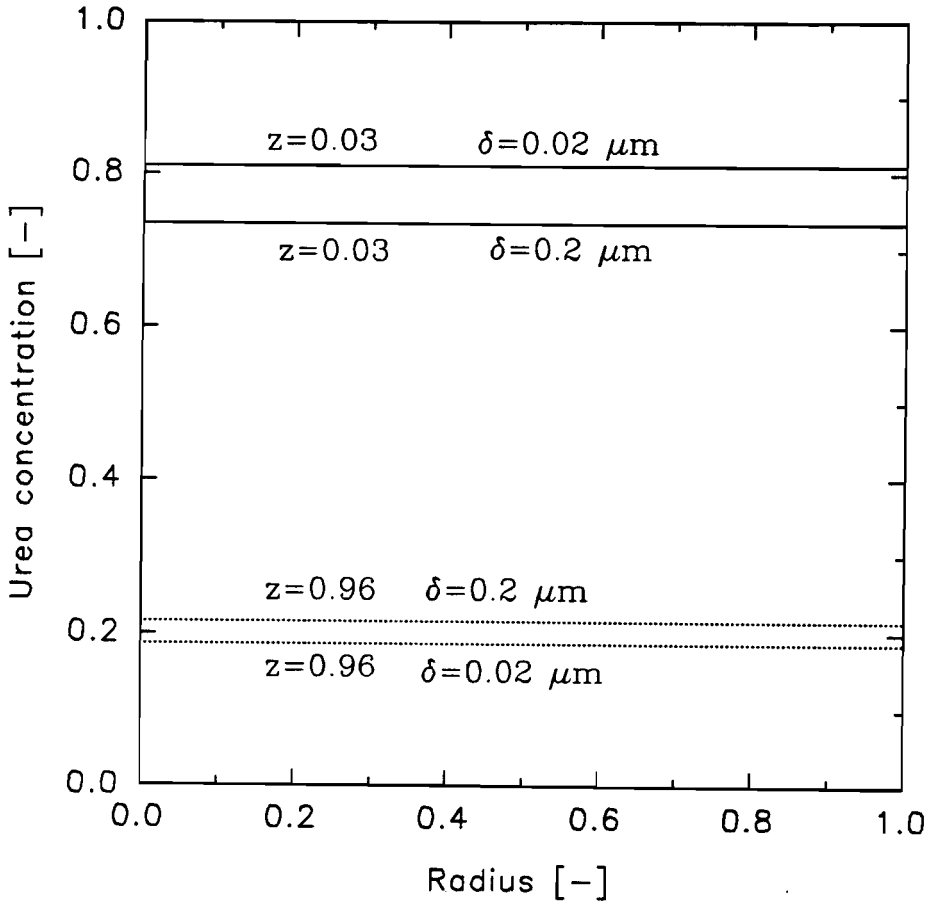

Figure 4–25.

Plot of dimensionless urea concentration as a function of dimensionless radial position with the microcapsule in a FBR for d_i=500 μm at $V_{m,o}E$= 5 mM./s. Other simulation conditions are the same as Figure 4–24.

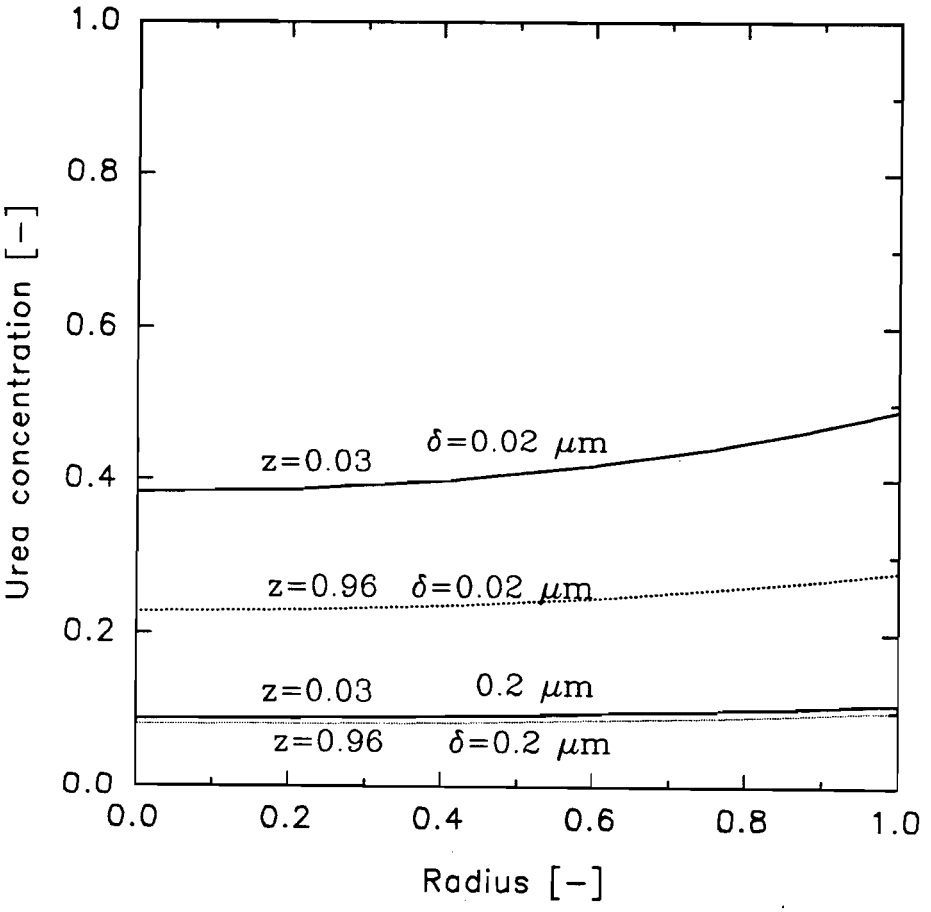

Figure 4–26.

Comparison of model predictions with experimental data from Ortmanis and Neufeld (1984). The solid line denotes the simulation result.

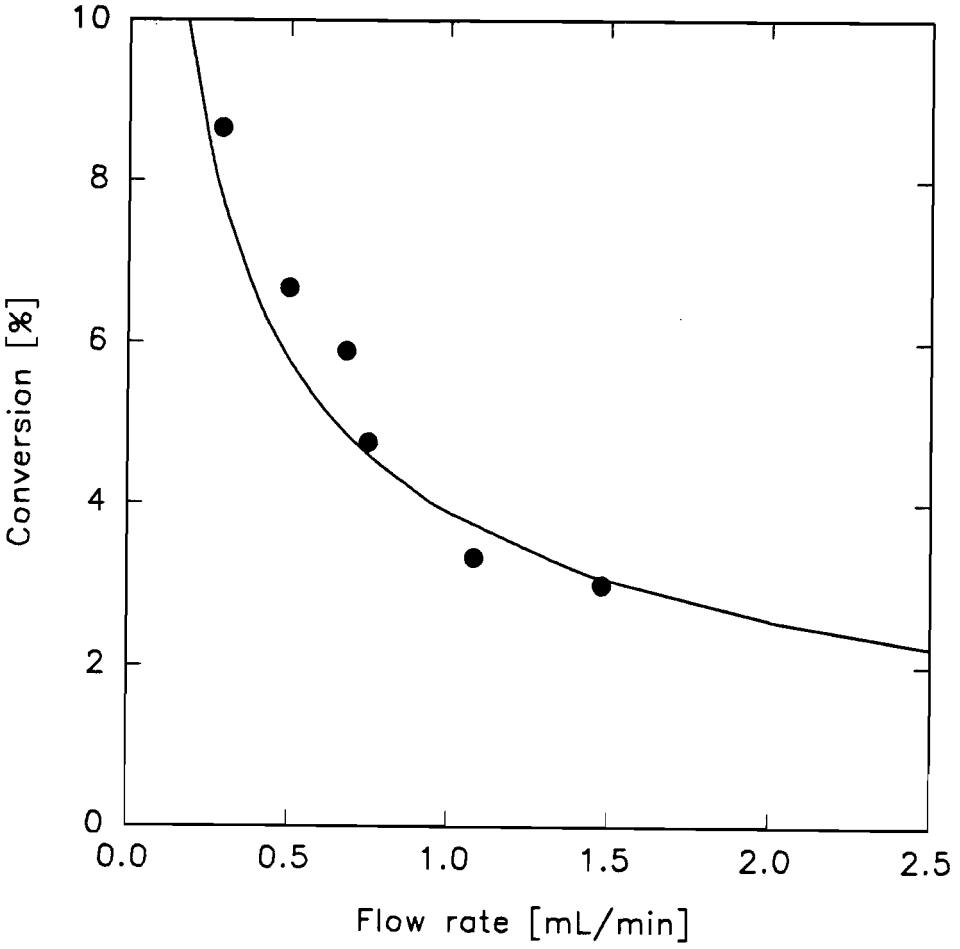

A second testing was to calculate the rate of ammonia formation rate as a function of the residence time in the reactor. Again, the experiment (triangular points) is well predicted by the theory as shown in Fig. 4-27.

Figure 4–27.

Comparison of model predictions with experimental data from Ortmanis and Neufeld (1984). The solid line denotes the simulation data.

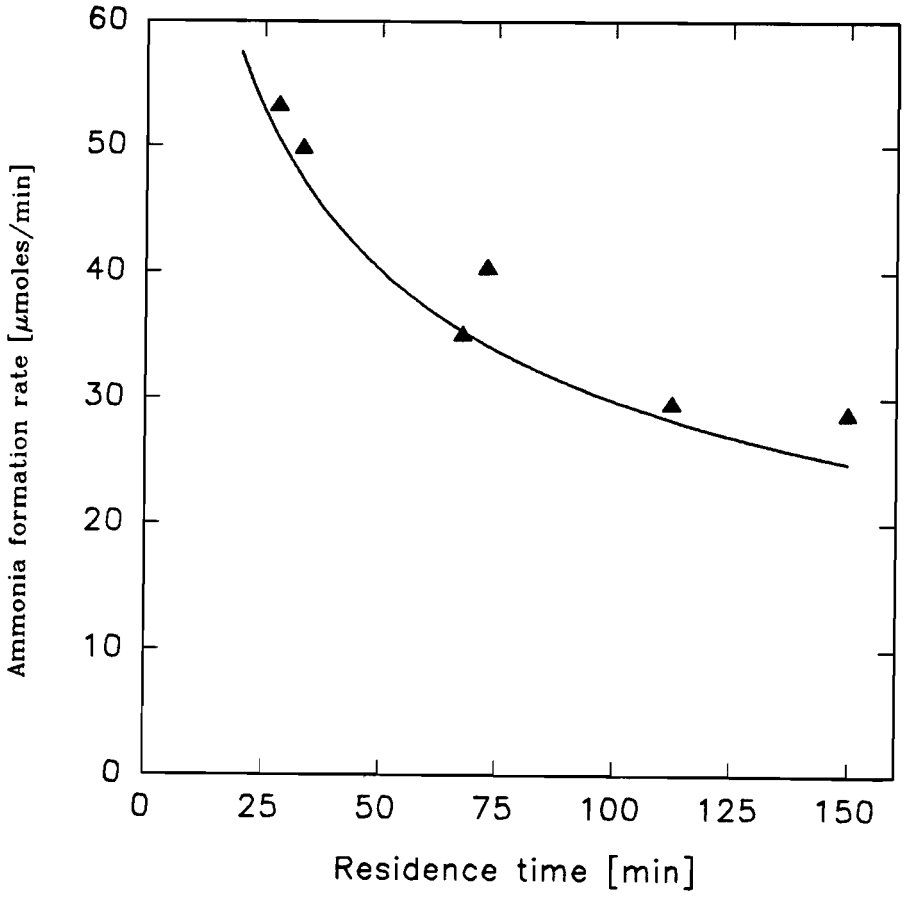

CHAPTER 5

SIMULATION OF BLOOD UREA CLEARANCE WITH MICROENCAPSULATED UREASE

The function of the human kidneys is to clear the blood of body wastes, processing up to 1500 mL of blood each minute (Cooney, 1976). The amount of water and urea excreted varies with body mass, diet, and intake of water. Normal renal function includes the removal of the end products of metabolism such as urea, uric acid, creatine, ammonium, sulfates, and phenol; regulation of the body chemistry; regulation of the amount of water in the body to prevent edema and hypertension; and the removal of the substances that are not utilized or metabolized in the body, such as drugs and toxins, thus preventing renal poisoning. During malfunctioning of the kidneys, the patient becomes progressively ill; metabolic waste products, excess electrolytes and water accumulate and the chemical balance is upset and may lead to death within days. Intermittent treatment with a mechanical device such as the artificial kidney reduces the accumulation of waste products, normalizing the blood conditions.

The conventional artificial kidney system developed by Kolf and Berk (1944) and has been in clinical use ever since 1943 and about about half a million patients worldwide are being supported by hemodialysis (Nosé, 1990). Hemodialysis is a procedure for clearing the body of metabolic wastes and excess species. Blood from a major vessel is fed to a device containing a membrane which separates the blood from a dialysate solution and the partially cleansed blood is recirculated to the body. The porosity of the membrane permits transport of all species except proteins and blood cells. The rate of waste metabolite removal depends on the thickness and area of the membrane available for diffusion.

Although hemodialysis has been effective for the treatment of kidney failure, there are a number of related problems. The conventional artificial kidney is bulky, heavy, complex and expensive, and difficult to handle and therefore limiting the mobility of the patient (Chang, 1978). Furthermore, the time required for treatment is long (6-12 hours three times a week) leading to a prohibitive cost of treatment. The amount of dialysate required by a standard artificial kidney for each hemodialysis is ca 300 liters (Krajewska et al., 1988). Dialysate is expensive and requires a complex preparation procedure. Therefore several attempts have been made to simplify the machine and reduce its size (Walker et al., 1977; Denti and Biangini, 1977; Kolf, 1978; Shettigar and Reul, 1982). Dialysate regeneration involves a physicochemical process for removing uraemic metabolites and leads to a reduction in the amount of dialysate recirculated in the machine.

In this work, a novel artificial kidney system using microencapsulate urease will be modeled. This system consists of blood which leaves a sick patient directly into a fixed bed containing microencapsulated urease. The blood undergoes treatment in the reactor and recycled to the patient. The main objectives is to select an appropriate enzyme activity and design the reactor for optimal operations. Also, the body and reactor transients will be considered and compared to assess the operability of this system.

5.1 Simulation of Blood Urea Clearance

Investigations into the application of the artificial cell as the basis for the construction of an artificial kidney was initiated by Chang (1964). However, the delay in the development of this new concept is partly due to the lack of appropriate theoretical models, for the characterization of the microencapsulation system.

The conceptual model shown in Fig. 3-4 illustrates the patient connected to a

fixed bed reactor. Blood urea diffuses into the microcapsules and undergoes hydrolysis. The products of hydrolysis, ammonia and carbon dioxide, are removed by an ion exchange system and the purified blood is recycled to the patient. It is assumed that the ion exchange resin is coencapsulated with the enzyme urease, which is responsible for the hydrolysis. The main purpose of this study is to model the complete system without considering the details of the ion exchange process. An optimal reactor design and enzyme activity selection will be considered. The body and reactor transients will be modeled for control purposes.

5.1.1 Computational Procedure

The theory underlying this simulation has already been presented in section 3.3 of CHAPTER 3. Generally for this system, Eqs. (3-10)-(3-12), (3-55) and (3-37)-(3-39) have to be solved simultaneously to obtain information on the capsule core, bulk reactor, and the body urea concentration profiles. Generally, the human blood contains a bicarbonate buffer system. Therefore, the intracapsular and bulk charge balances given by Eqs. (3-56) and (3-57) respectively, will be required for a complete solution. Decoupled solutions could only be obtained with the aid of the equilibrium relations given by Eqs. (3-47)-(3-51) and the reaction rate equation Eq. (3-54) which accounts for the deactivation of the enzyme. Due to the complexity of the problem involved, certain assumptions were made to facilitate the computation without loss of details in the trends of the simulation.

It was initially assumed that the enzyme is coencapsulated with ion exchange resins for the removal of ammonia and for pH control. Thus, ammonium ion inhibition and pH kinetic effects were eliminated. This reduces Eq. (3-54) to a newly-modified Michelis-Menten model which accounts for urease deactivation as follows:

$$R_s = \frac{A_e S}{(S + K_{m,o} + S^2/K_s)} \xi \qquad (5\text{-}1)$$

where A_e is the enzyme activity as defined by Eq. (4-1) in CHAPTER 4, and ξ is the enzyme deactivation factor which is empirically determined by Eq. (3-53) in CHAPTER 3. Secondly, the urea production rate by body metabolism, G_s (in Eq. (3-55)), was assumed to be zero. Bell et al. (1965) and Popovich et al. (1975) have reported that the use of a single-pool model provides sufficient clinical accuracy.

Steady-state calculations were initially made across the reactor for better choice of enzyme activity and reactor dimensions. This was followed by transient-state calculations for reactor start-up operations and the body's response to the treatment. For steady-state calculations, pH and enzyme activities are fixed, and a steady-state urea concentration within the reactor and the microcapsule are assumed for iteration using the method of collocation described in section 3.4. The transient-state calculations were made with an initial assumption that the intracapsule and bulk urea concentrations are zero. The body blood pool was chosen to be 50 liters with an initial urea concentration of 10 mM. The microcapsule diameter was chosen as 100 μm.

5.2 RESULTS AND DISCUSSION

The operation of a microencapsulated urease artificial kidney for the treatment of a patient has been simulated. In this section, the details of the simulation model will be discussed.

5.2.1 Reactor Design

An optimal design for a urease microencapsulate fixed bed reactor involves the

proper choice of enzyme activity as a first step. The appropriate enzyme activity was selected by calculating the conversion after one pass through the reactor for a flow of 200mL/min and a reactor volume of about 126mL. In order to study residence time effects for a constant reactor volume, the length to diameter ratio was varied. The steady state conversion for the various length to diameter ratios was computed by assuming various enzyme activities. The results which are shown in Fig. 5-1 show that for a constant fixed bed reactor volume, the overall conversion is independent of the length to diameter ratio (residence time) but rather dependent on the enzyme activity. The conversion increased with an increase in enzyme activity from 0.1 to 10 mM/s. A transient calculation was made to monitor the exit urea concentration with time at various enzyme activities as shown in Fig. 5-2. At activities greater than 5 mM/s, the gain in conversion was only marginal. For the purpose of this study, an activity of 10 mM/s was chosen as optimal on the basis of cost and level of conversion achieved after one pass through the reactor. At lower activities, conversions of less than 90% were achieved whereas at activities greater than 10mM/s, the cost of the enzyme could be very high with a maximum gain of only 6% in the conversion.

The effect of initial blood urea concentration on the conversion (after one pass through the reactor) was calculated using an optimal enzyme activity of 10 mM/s for various reactor height to diameter ratios as presented in Fig. 5-3. The higher the substrate concentration, the lower the conversion. Blood urea concentration of 10mM was used as a practical representation for computing the reactor exit urea concentration with time, for various length to diameter ratios. The results (shown in Fig. 5-4) reveal that there is only a marginal difference in the steady state conversion values for reactor length to diameter ratios between 1 and 10. Beyond a ratio of 10, there is no gain in conversion.

Figure 5-1.

Effect of enzyme activity on urea conversion
for the various column length to diameter ratios.

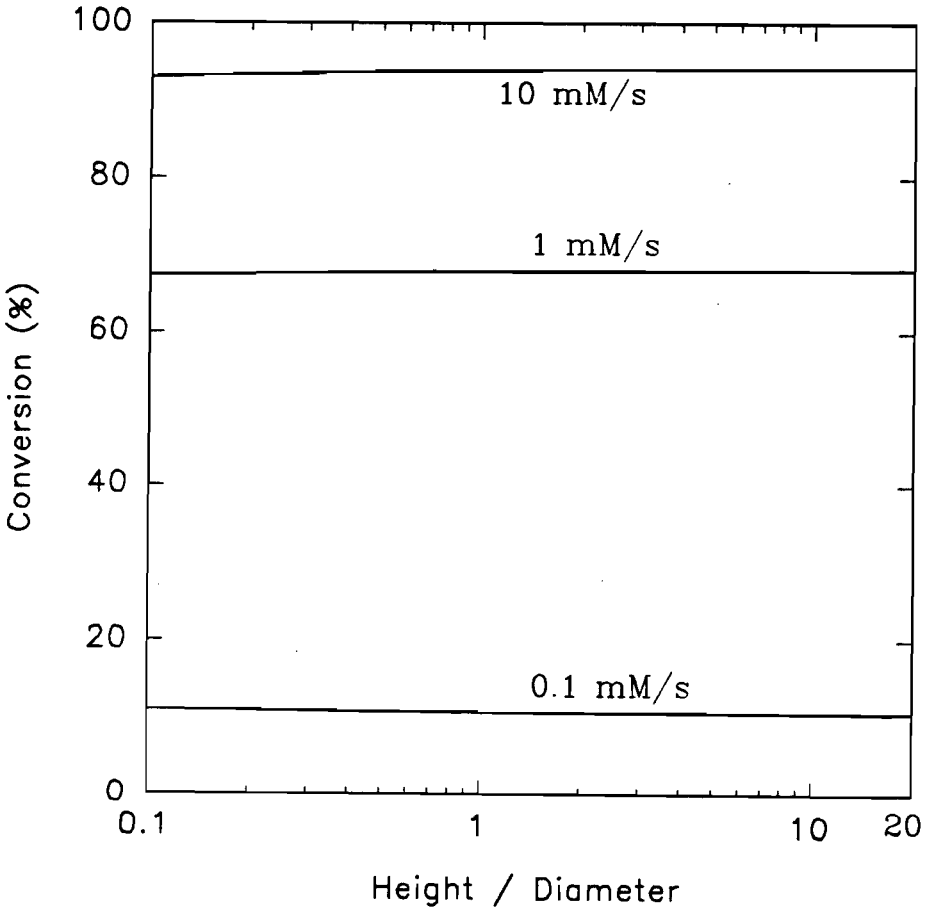

Figure 5-2

A transient profile of the exit urea concentration with time at various enzyme activities.
Column height (H) = 10 cm;
Column diameter (D) = 4 cm

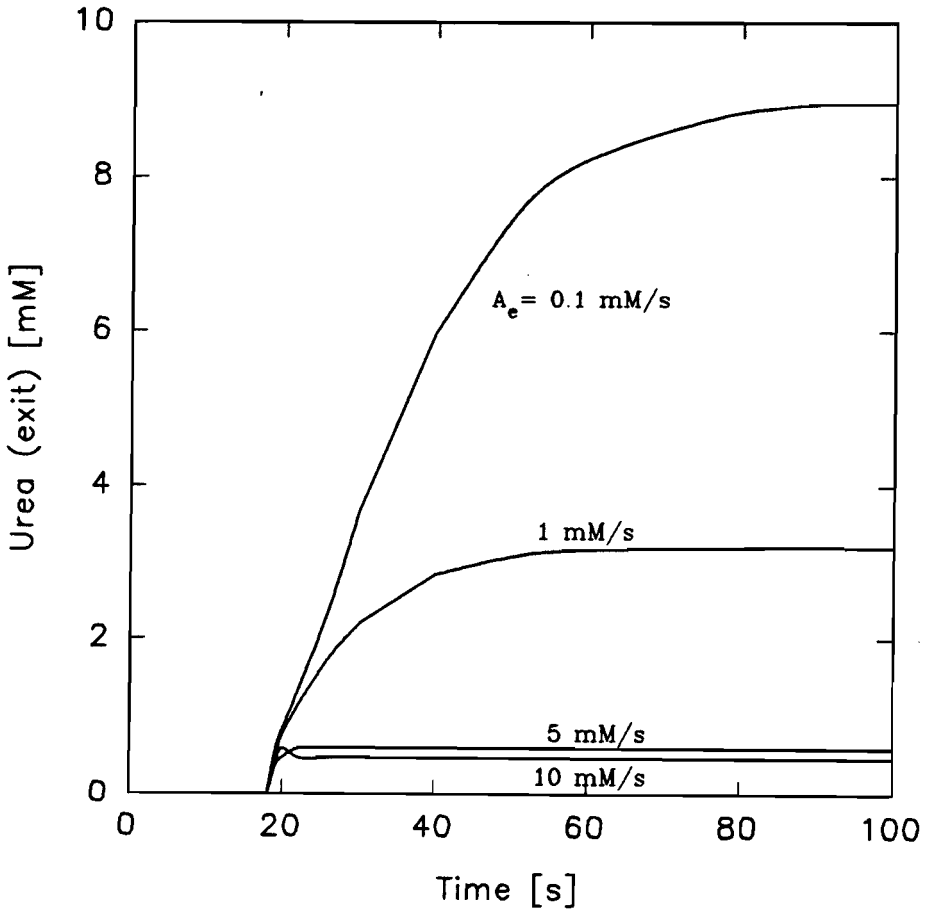

Figure 5-3.

Effect of blood urea concentration on the conversion using an enzyme activity of 10 mM/s for various reactor height to diameter ratios.

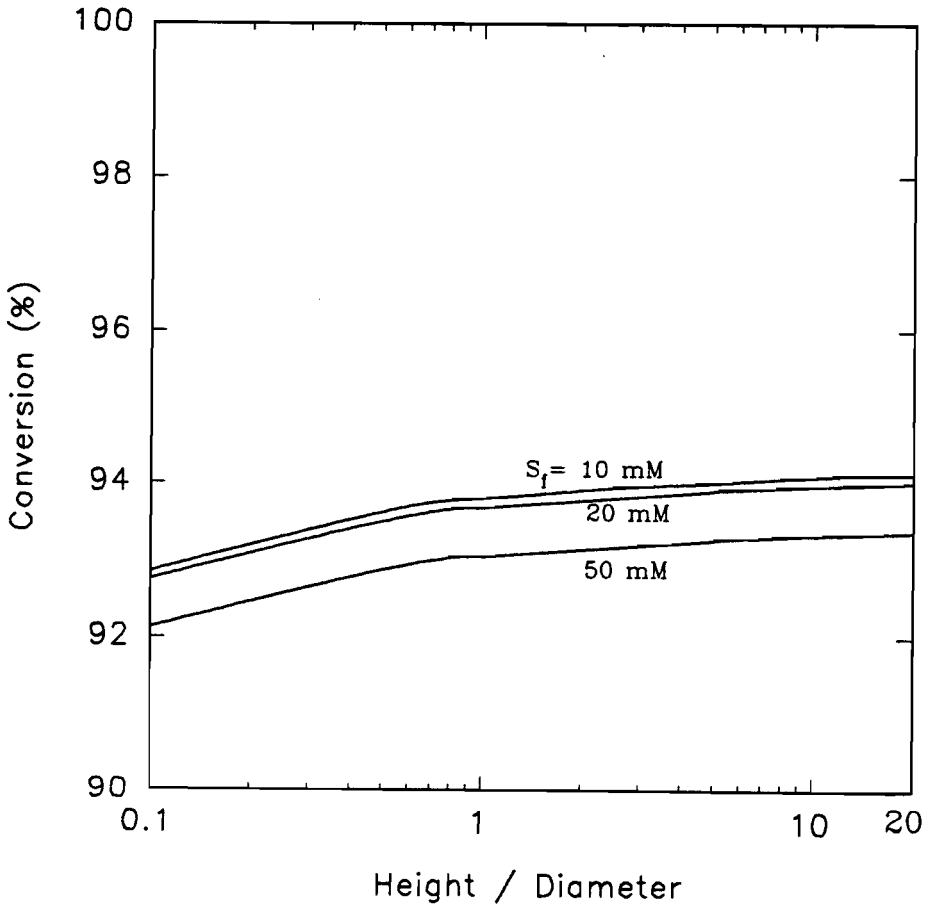

Figure 5–4.

Reactor exit urea concentration profile with time for various reactor length to diameter ratios. (V_T= 125 mL, τ_L= 18.8 s)

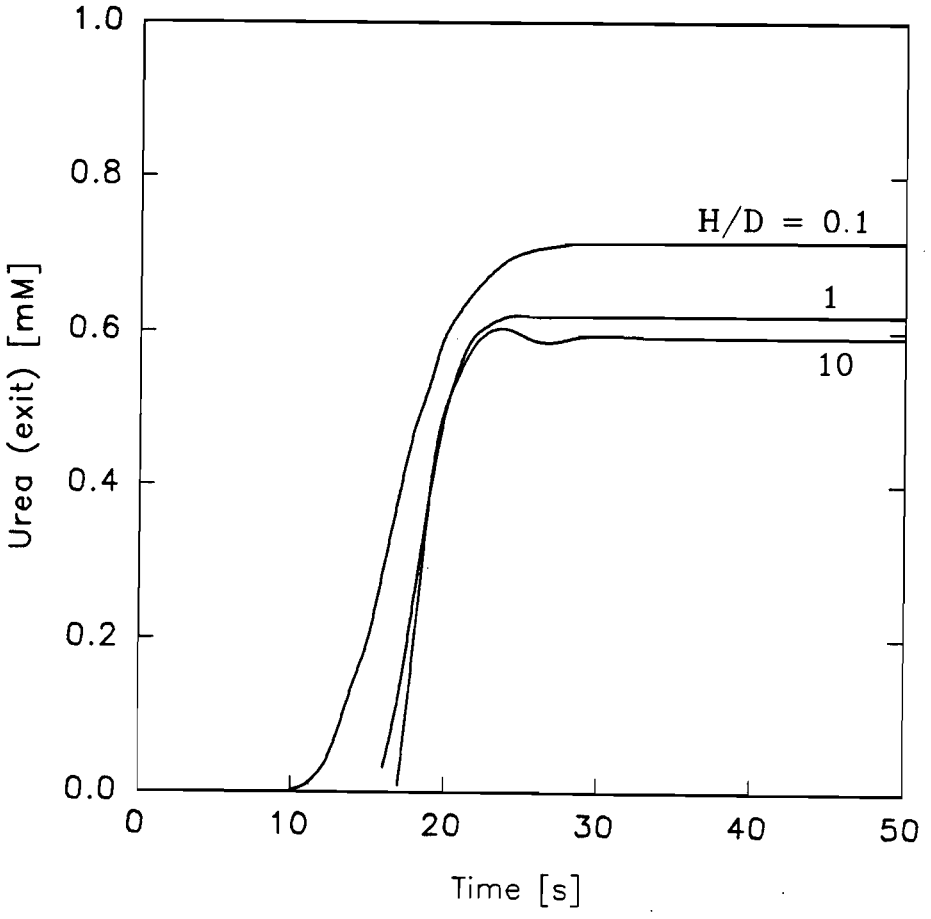

5.2.2 Artificial Kidney with Recycle

The proposed artificial kidney with blood recycle (shown in Fig. 3-4) was studied by modeling the complete process. It was assumed that the treatment process involved 50 liters of body fluid which is completely mixed within the patient. The transients in the artificial kidney (reactor) are coupled with those of the body (patient). The first stage in the modeling was to determine the required volume of reactor to reduce the body urea concentration to reasonable levels. This was achieved by calculating the blood urea level in the body with time for various reactor volumes. In the calculations, a reactor voidage of 0.5 and an optimal enzyme activity of 10mM/s were used. The results which are presented in Fig. 5-5 show the body's response (continuous lines) in comparison to the overall reactor performance (broken). The curves labeled 1-4 represent reactor volumes of 31.4 (2cm x 10cm), 62.8 (2cm x 20cm), 126 (4cm x 10cm) and 252mL (4cm x 20cm), respectively. The results show that large reactor volumes, which are normally associated with large quantities of microencapsulated urease, cause substantial reductions in the body urea level. Nevertheless, the performance is little enhanced for reactor volumes exceeding 126mL (curves 3). Hence, under the conditions used for the calculations, a reactor volume of 126mL (4cm x 10cm) would be enough for an optimal performance for the process. For such a reactor configuration, the body urea level was reduced by about 60% in four hours and 80% in eight hours. Fig. 5-6 shows comparison of the profiles for the reactor's overall and transient urea conversions for the various reactor volumes considered. The overall conversion in the reactor is defined as the percentage of the initial blood urea level which is hydrolyzed, whereas the transient conversion is the percentage of the blood urea entering the reactor which is hydrolyzed after one pass. The profiles in Fig. 5-6 show that the overall urea conversion increases with time; an indication that the body blood urea level is reducing. However, the transient urea conversion is a constant which is dependent on the volume of reactor

Figure 5–5.

The body's response (continuous line) in comparison to the overall reactor performance (broken).
The curves labeled 1–4 represent reactor volumes of 31.4 (2cm x 10cm), 62.8 (2cm x 20cm), 126 (4cm x 10cm) and 252 mL (4cm x 20cm), respectively.

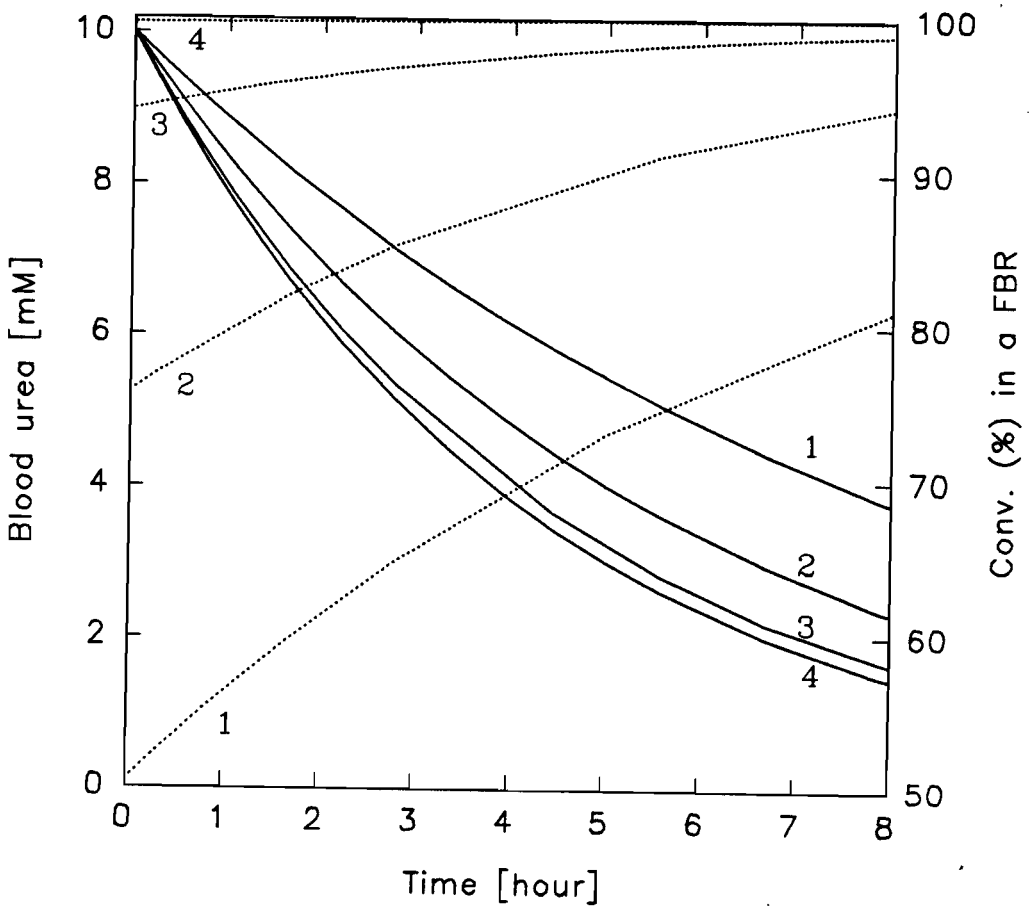

Figure 5–6.

Comparison of the profiles for the reactor's overall (dashed line) and transient (solid line) urea conversions for the various reactor volumes considered. The definitions of the curves labeled 1–4 are the same as Figure 5–5.

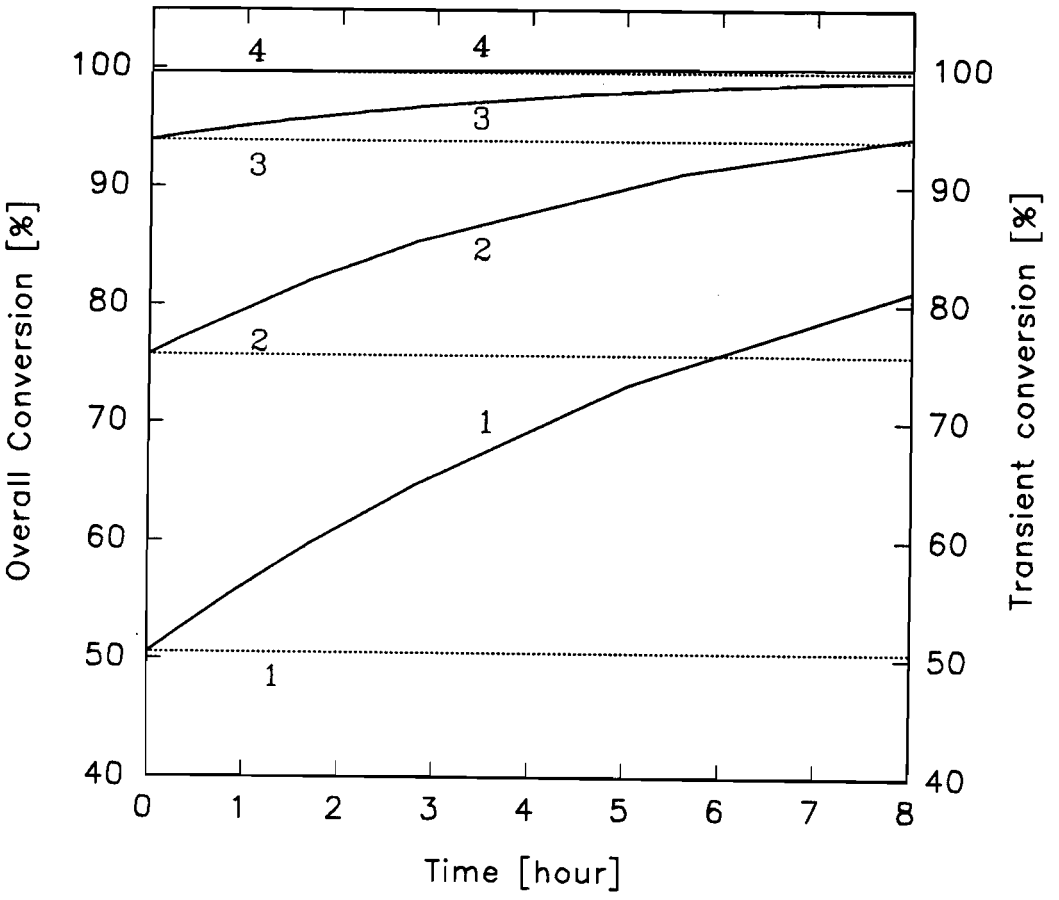

or quantity of microencapsulated urease. From the results shown in Figs. 5-5 and 5-6, a reactor dimension of 4x10cm was chosen as the optimum design and further studies.

Using the optimum dimension of 4x10cm, the effect of flowrate was studied by computing the blood urea level at various volumetric flow velocities. In the calculations, the velocity of blood flow in the recycle system was assumed to be constant. The variation with time of the patient's blood urea level and the overall urea conversion at the various flow velocities are shown in Fig. 5-7. In this figure, curves 1 to 4 represent flow velocities of 100-400mL/min respectively. The slower the flow, the higher the conversion (broken lines) as a consequence of the associated long residence times. It was expected that the high conversions accompanying lower flow velocities would lead to lower blood urea levels. However, higher flow velocities result in lower blood urea levels with time as shown in Fig. 5-7. At high flowrates, the residence time is short and thus the turnover of the reactor volume is large as compared to lower flow velocities. For example, after four hours, the blood urea level was about 5.5 mM at a conversion of 99% for a flow of 100 mL/min in comparison to 2 mM at 94% conversion for a flow of 400 mL/min. During this period, the reactor volume turnover is 190 for a flow of 100 mL/min in comparison to 762 for 400 mL/min flowrate. For a practical flow of 200mL/min, the blood urea level could be reduced from 10 mM/s to 4 mM and 2 mM in four and eight hours respectively. The urea concentration profiles in the fixed bed reactor at various times is shown in Fig. 5-8 for a sample calculation using a flowrate of 200 mL/min, and a reactor capacity of 4x10cm. The profiles show a continuous decrease in the urea concentration along the column. The results have shown the ability of the model to simultaneously predict the reactor performance and patient's blood urea level under various conditions. In principle, the model could be used for control and monitoring of a patient's condition (e.g. Figs. 5-6 to 5-8).

Figure 5–7.

Effect of flow rate on the patient's blood urea level (solid line) and the overall urea conversion (dashed line). Curves 1 to 4 represent volumetric flow rates of 100, 200, 300, 400 mL/min, respectively.

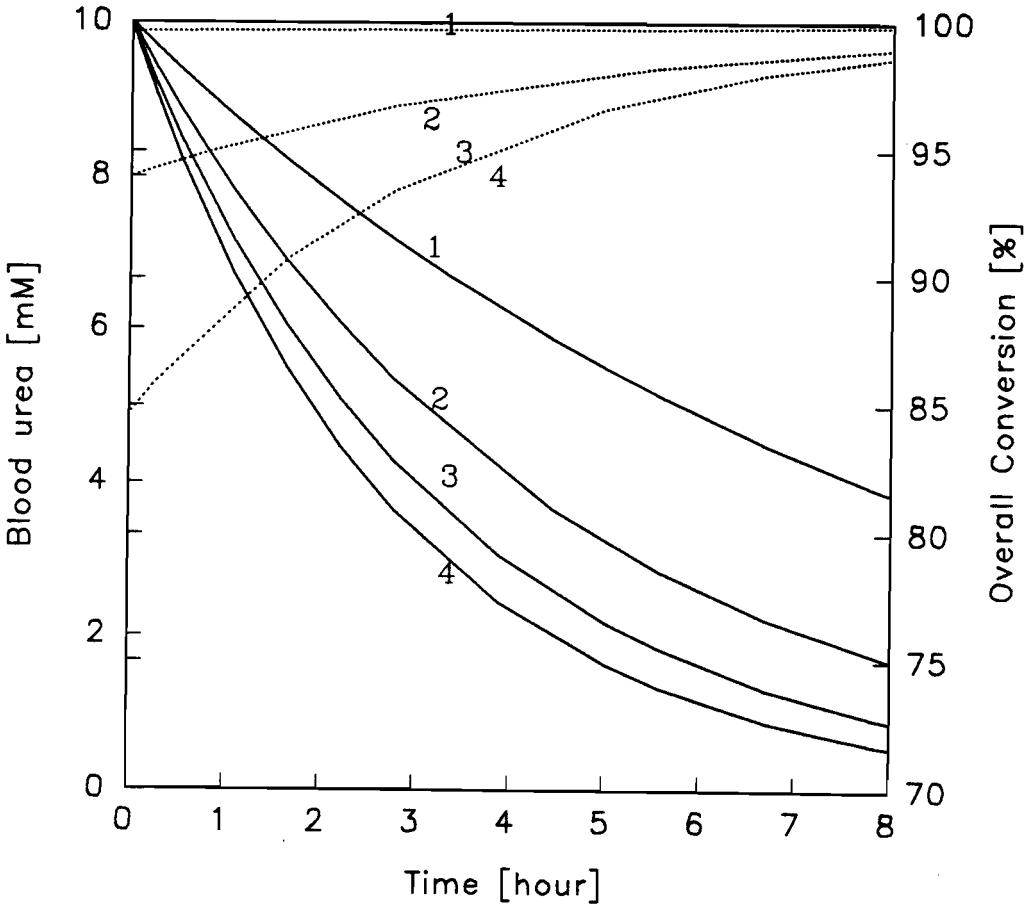

Figure 5-8.

The urea concentration profiles in a FBR at various times using a flowrate of 200 mL/min, and a column dimension of 4x10 cm (H/D=2.5).

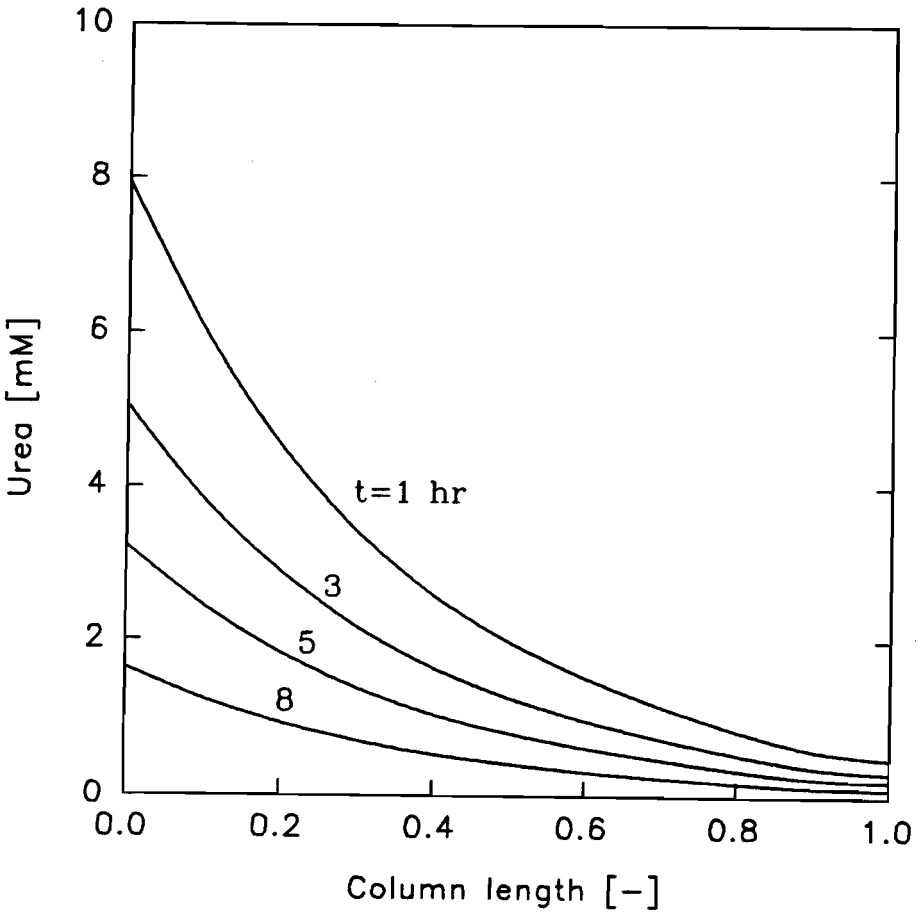

5.2.3 Reactor Start-up and Transients

The reactor start-up and transients are very important for control and operational purposes. The transients in the fixed bed reactor were calculated using a flowrate of 200 mL/min and a reactor configuration of 4x10 cm. It was assumed that the reactor was initially void of urea. The urea concentration profiles along the reactor were calculated for two enzyme activities as shown in Figs. 5-9a (1 mM/s) and 5-9b (10 mM/s). The profiles show the dynamic front of the blood at various times. For example in Fig. 5-9a (1mM/s urease activity), the blood urea concentration is zero at a dimensionless column height of 0.3 after 4s. This is the incipience of blood into the column and therefore the top 70% is void of urea. The column eventually will experience a complete first pass of blood after 20s. Steady-state was reached after 60s which represents 3 replacements of the reactor volume. Similarly, for an enzyme activity of 10 mM/s (Fig. 5-9b), the first pass is after 20s although the urea concentration level within the column is lower than that of a 1 mM/s activity. However, steaty-state was reached only after approximately one pass (in 24s). Similar results (Figs. 5-10a and 5-10b) were obtained for a smaller column of dimensions 2x10 cm (half the optimal size). In these figures, the residence time after one pass is about 4.7s. Meanwhile, steady-state is reached after 4 replacements of the reactor for the 1 mM/s (Fig. 5-10a) as compared to about 1.2 reactor volumes for the 10 mM/s (Fig. 5-10b) enzyme activity.

Using the optimal column dimensions (4x10 cm), a flowrate of 200 mL/min, and enzyme activity of 10 mM/s, the bulk and microcapsule urea concentration at various positions of the reactor were calculated. The results are shown in Figs. 5-11 (bulk) and 5-12 (microcapsule). It could be inferred that steady-state is attained at different times and at different sections of the reactor. The bottom section reaches a higher steady-state

Figure 5–9.

The urea concentration profiles along the column reactor for two enzyme activities: (a) A_e = 1 mM/s; (b) 10 mM/s. See text for the details on the simulation conditions.

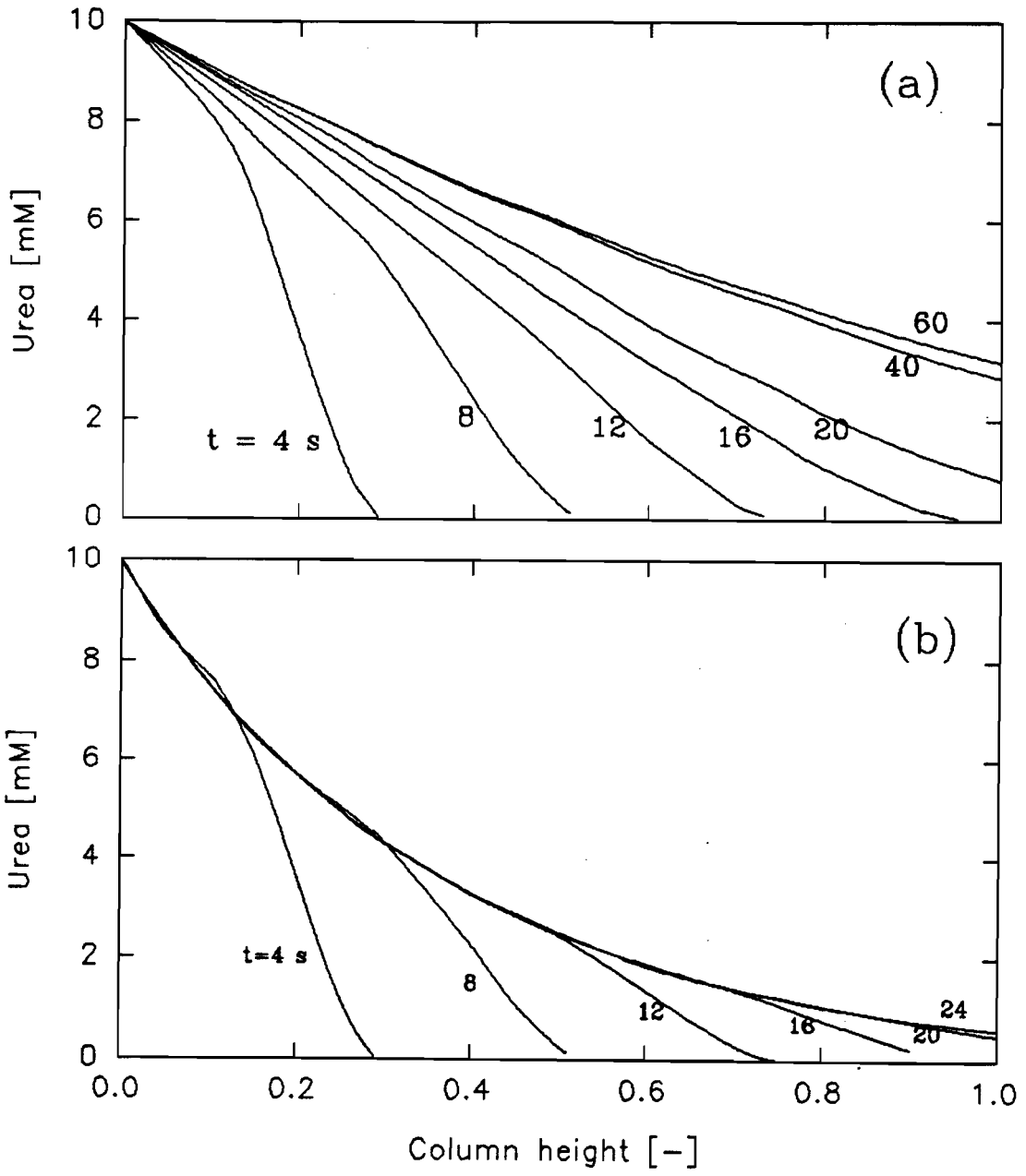

Figure 5-10.

The urea concentration profiles along the column reactor for two enzyme activities: (a) A_e= 1 mM/s; (b) 10 mM/s. Column dimension: 2x10 cm (H/D=5).

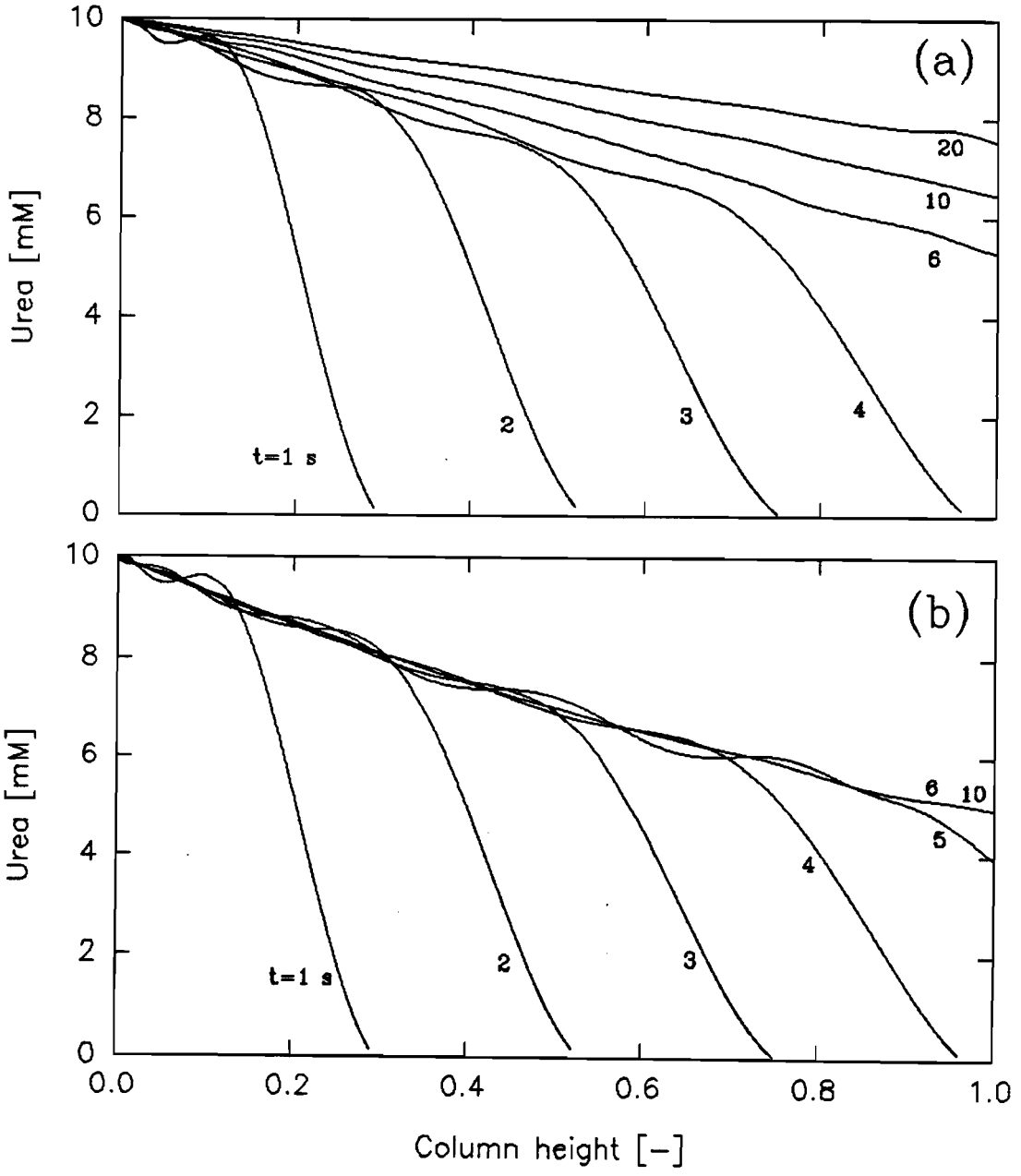

Figure 5-11.

The bulk urea concentration at various positions within the reactor. z denotes the dimensionless height of the column reactor. See text for the details on the simulation conditions.

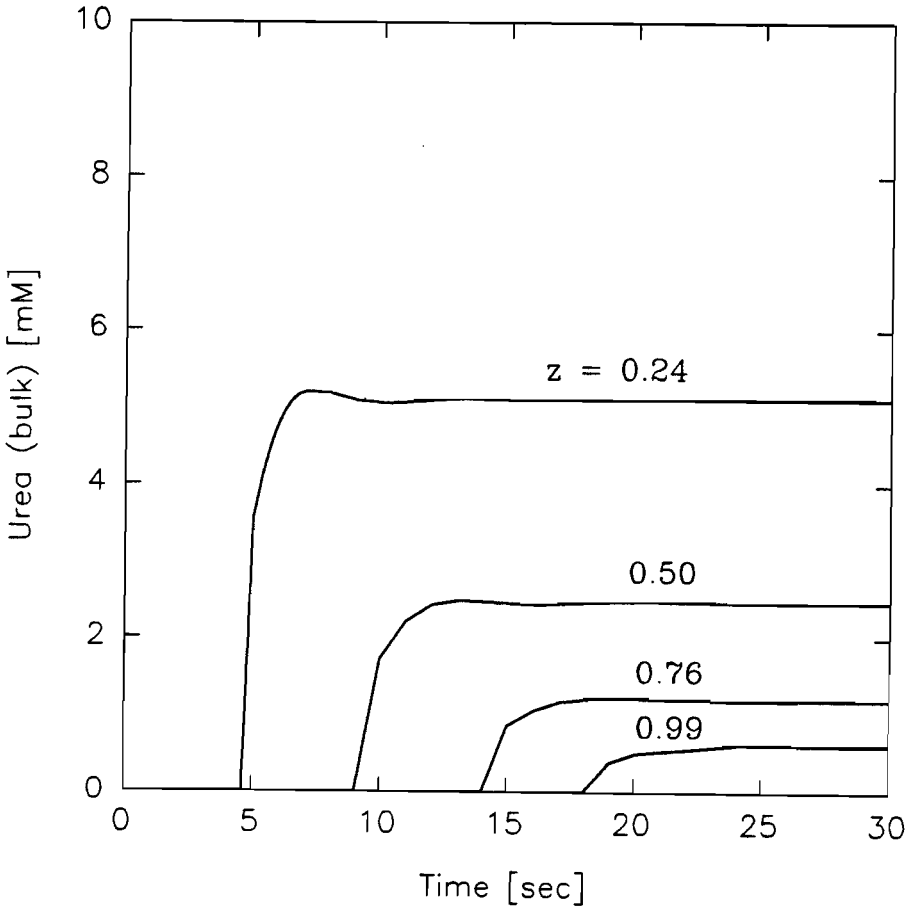

Figure 5-12.

The urea concentration inside the microcapsule at various positions within the reactor. Other conditions are the same as those in Figure 5-11.

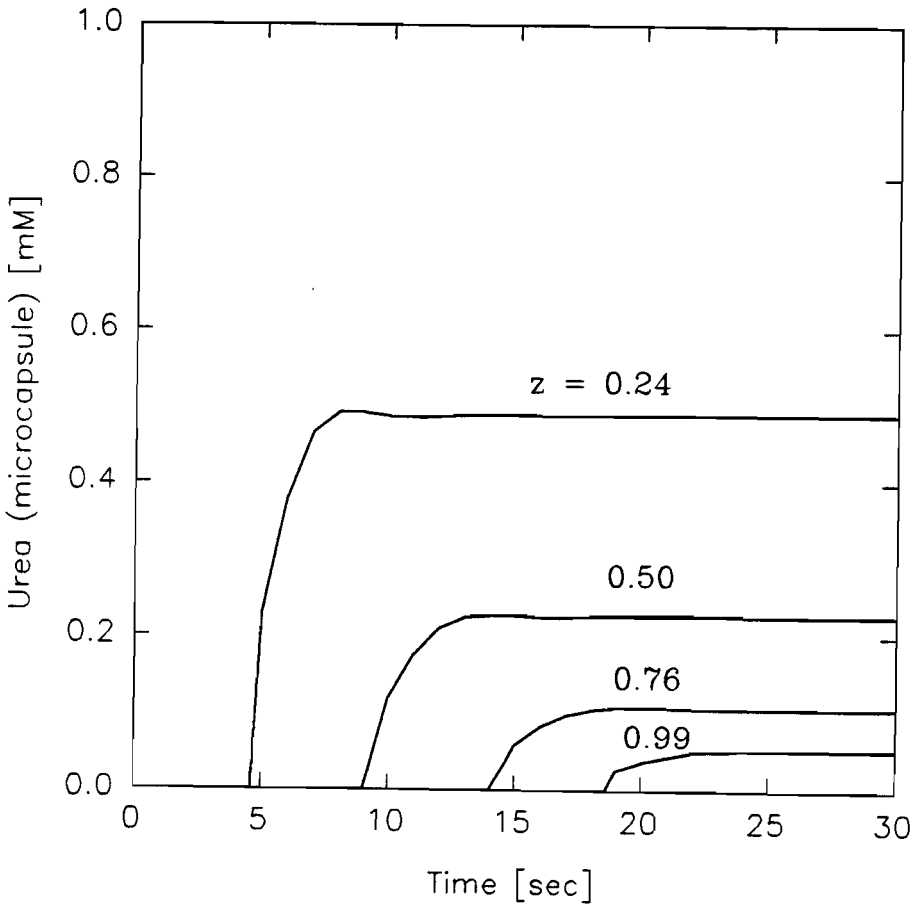

Figure 5–13.

Reaction rate profiles at various positions within the reactor. Other simulation conditions are the same as those in Figure 5–11.

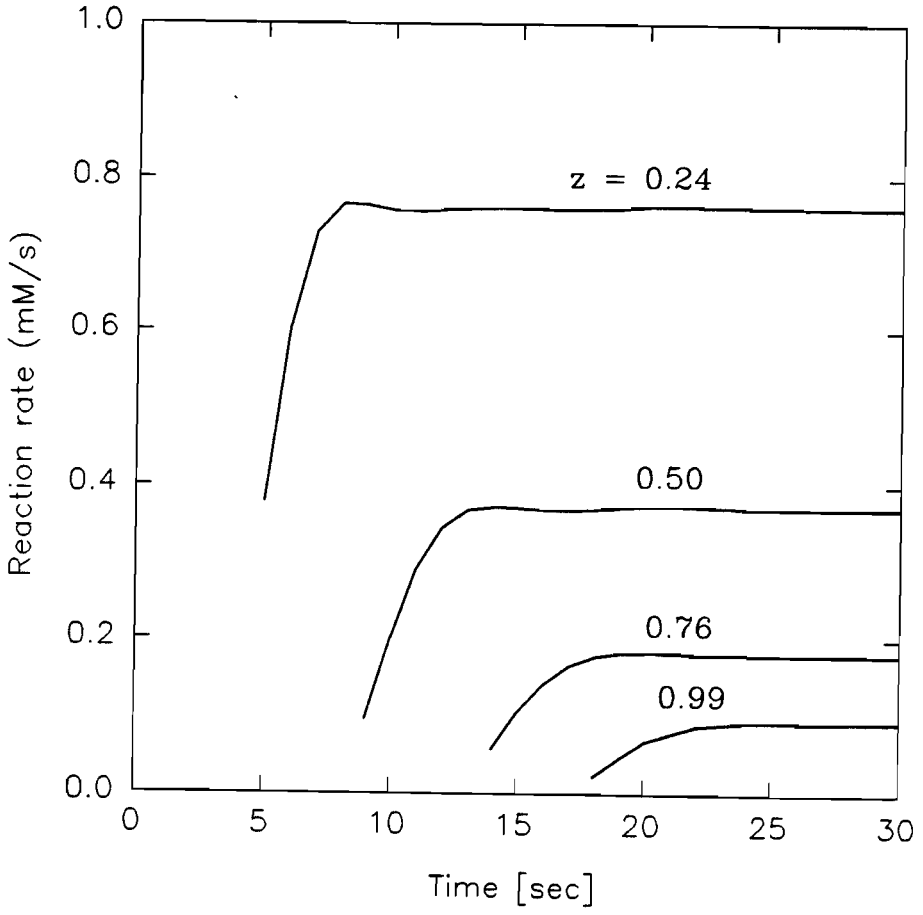

Figure 5–14.

Effectiveness factor profile at various positions within the reactor. Other conditions are the same as those in Figure 5–11.

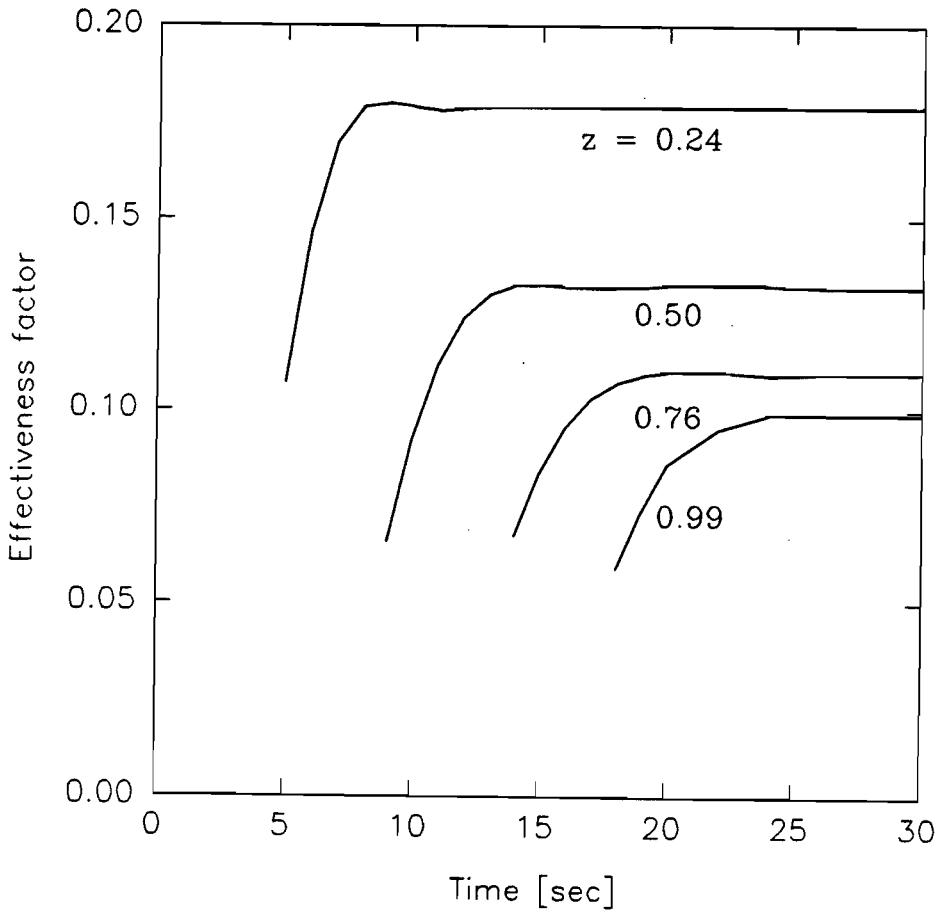

urea concentration in a faster time than the top. This result is also true for the reaction rate (Fig. 5-13) and the effectiveness factor (Fig. 5-14) which are higher at the lower portions of the reactor.

CHAPTER 6

CONCLUSION AND RECOMMENDATIONS

6.1 CONCLUSION

The factors which influence the steady state performance of a continuous stirred tank reactor (CSTR) and a fixed bed reactor (FBR) operation with microencapasulated urease for the regeneration of a dialysated solution have been studied at various enzyme activities. The theoretical model considered microcapsule size effects, pH kinetic effect, product inhibition and substrate depletion effects, in relation to urea conversion and the microcapsule effectiveness factor. The results predicted that small microcapsule diameters yielded higher conversions than large microcapsules. Also, small diameter capsules are more effective over a wide range of enzyme activity than large diameters. This was explained by the low diffusional resistance associated with the small diameter, in comparison to large diameters. The limiting effects of pH kinetics, product inhibition and substrate depletion were also studied individually and in combination under eight case studies. The base case (Case 1) which included these three limiting factors in the reaction process, predicted the lowest urea conversion values at the enzyme activities considered. However, the effectiveness factor for each case at a fixed capsule diameter depended on the enzyme activity. This behaviour was studied for two different microcapsule diameters, 5μm and 500μm. It was revealed that at enzyme activities lower than 1mM/s, Case 6 (Michelis-Menten), which consisted of only substrate depletion, predicted the highest effectiveness factors. On the other hand, beyond 1mM/s enzyme activity, it predicted

the lowest effectiveness factors, although higher conversions than Case 1 were achieved. This might be due to the fast depletion of the substrate at high activities for Case 6, which led to residual substrate concentrations (S_r) lower than the Michaelis-Menten constant $K_{m,o}$; a condition for a dramatic drop in the intraparticle reaction rate. The limiting factors in Case 1 keeps S_r at a relatively higher value than $K_{m,o}$.

External mass transfer resistances were studied using a Michelis-Menten model by isolating the contributions by the external liquid film and the membrane wall resistances. The results revealed that for very small particle sizes, external liquid film resistance was of no consequence to the overall conversion although membrane wall resistance could be important. For large microcapsule diameters, liquid film and membrane resistances could cause an appreciable reduction in the overall urea conversion.

A simulation for the prediction of a patient's response to treatment using a microencapsulated urease artificial kidney system was made, taking into account the deactivation of the urease. The model has the ability to predict the performance of the artificial kidney and the patient's blood urea level simultaneously, at various operating conditions. The major conclusions to be drawn from the simulations are:
a) For a reactor void volume of 0.5, an optimal microencapsulated urease activity of 10mM/s is recommended.

b) Design considerations showed that for an enzyme activity of 10mM/s, reactor height to diameter ratio (H_D) in the range of 1 to 10 is enough for good results. An optimal reactor configuration of 4cm by 10cm (H_D=2.5) was achieved in the simulations.

c) High flowrates led to better responses by the patient in terms of blood urea reduction although the performance of the reactor was better at lower flowrates. This is due to the high turnover of of the reactor volume at high flow.

6.2 RECOMMENDATIONS

The application of the developed model may be varied. However, the most important parameter is the enzyme activity, which influences the reactor design and the efficiency of the microcapsules. The following are recommended:

a) The enzyme urease (irrespective of the source) must be properly characterized experimentally to determine its activity.

b) Experimental studies on the deactivation of microencapsulated urease should be pursued for the optimization of the microencapsulation process. The contributing effects of temperature, the nature of the encapsulation material and process on deactivation require serious considerations.

c) The microcapsule size distribution, membrane wall thickness, strength and permeability are parmeters which directly affect the efficiency of the microcapsule directly. Physicochemical factors which often control these parameters require fundamental studies for improvement in reproducibility. This may accelerate large scale testing of the developed model and its potential application for design of the microencapsulated urease artificial kidney system.

d) More experimental studies on microencapsulated urease for urea hydrolysis, particularly, for the fixed bed system are required for model testing.

NOMENCLATURE

A_{jk}	approximation coefficients for gradient operator
B_{jk}	approximation coefficients for Laplacian operator
A_e	enzyme activity (mM/s)
$\mathbf{Bi}_{m,s}$	Biot number for urea ($\mathbf{k}_{s,0}\mathbf{r}/\mathbf{D}_s$)
Bo	Bodenstein number ($\mathbf{U}_s\mathbf{L}/\mathbf{D}_z$)
C_i	the concentration of species i (M)
$C_{i,1}$	the concentration of species i in the enzyme solution (M)
$C_{i,2}$	the concentration of species i in the membrane (M)
$C_{i,f}$	the concentration of species i in the feed solution (M)
$C_{i,b}$	the concentration of species i in the bulk solution (M)
$C_{i,s}$	the concentration of species i at microcapsule surface (M)
d_i	distance from the center of a capsule to the inner surface of the membrane wall (m)
d_p	distance from the center of a capsule to the outer surface of the membrane wall (m)
$D_{i,1}$	diffusion coefficient of species i in the enzyme solution (m^2/s)

$D_{s,l}$	diffusion coefficient of the substrate urea in the enzyme solution (m^2/s)
D_z	axial dispersion coefficient (m^2/s)
E	enzyme urease concentration inside the microcapsule (M)
F	Faraday constant (coul./equiv.)
f_c	the percentage change in the conversion (%)
f_η	the percentage change in the effectiveness factor (%)
g	acceleration due to gravity (cm/s^2)
G	mass velocity of the fluid through total bed cross section ($g/s.cm^2$)
i	electric current density ($amperes/cm^2$)
K_{e1}	the first ionization equilibrium constant of enzyme urease (M)
K_{e2}	the second ionization equilibrium constant of enzyme urease (M)
K_{es1}	the first ionization equilibrium constant of urea-urease complex (M)
K_{es2}	the second ionization equilibrium constant of urea-urease complex (M)
K_m	pH dependent Michaelis constant (M)
$K_{m,o}$	pH independent Michaelis constant (M)
K_s	substrate inhibition constant (M)
K_i	product inhibition constant (M)
$k_{i,L}$	solid-liquid mass transfer coefficient for species i (m/s)
$k_{i,M}$	mass transfer coefficient for species i through the membrane (m/s)

$k_{i,o}$	combined transfer coefficient of species i for the solid-liquid mass transfer and diffusion through the membrane (m/s)
L	length of the reactor in axial direction (m)
M	molar concentration
$N_{i,l}$	molar flux of species i in the enzyme phase of encapsulated enzyme particle ($M/m^2.s$)
$N_{Pe,i}$	Peclet Number for species i ($U_s d_p/D_i$)
N_{Re}	particle Reynolds number ($d_p G/\mu$)
N_{Sc}	Schmidt Number ($\mu/\rho_f D_i$)
$N_{Sh,i}$	Sherwood Number for species i ($k_{i,L} d_p/D_i$)
$NH_4^+{}_b$	ammonium ion concentration in the bulk liquid.
$NH_4^+(r_1)$	ammonium ion concentration at the inner surface of the membrane.
$NH_4^+(r_2)$	ammonium ion concentration at the outer surface of the membrane.
ΔNH_4^+	difference in ammonium concentration between $NH_4^+{}_b$ and $NH_4^+(r_2)$.
P	the concentration of NH_4^+ (M)
P_b	the concentration of NH_4^+ in the bulk solution (M)
pH_b	pH in the bulk liquid.
$pH(r_1)$	pH at the inner surface of the membrane.
$pH(r_2)$	pH at the outer surface of the membrane.

ΔpH	pH difference between pH_b and $pH(r_2)$.
$P_k(R^2)$	orthogonal polynomial of degree k in R^2
Q_D	volumetric flow rate of dialysate solution (m^3/s)
Q_B	volumetric flow rate of blood (m^3/s)
r	radial distance (m)
R	dimensionless radial distance (-)
r_1	radial distance from the center of a capsule to the inner surface of the membrane wall (m)
r_2	radial distance from the center of a capsule to the outer surface of the membrane wall (m)
R_s	the rate of urea removal (M/s)
R_g	gas constant
S	urea concentration (M)
S_r	residual urea concentration (M)
S_b	urea concentration in the bulk solution (M)
$S_{r,b}$	residual urea concentration in the bulk liquid.
$S_r(r_1)$	residual urea concentration at the inner surface of the membrane.
$S_r(r_2)$	residual urea concentration at the outer surface of the membrane.
ΔS_b	difference in residual urea concentration between $S_{r,b}$ and $S_r(r_2)$.

T	absolute temperature (K).
U_s	superficial velocity (m/s)
U_t	terminal velocity (cm/s)
V_T	volume of a CSTR (m^3)
V_B	volume of body fluid (m^3)
V_c	volume occupied by the microcapsules (m^3)
V_m	pH dependent maximum specific reaction velocity (s^{-1})
$V_{m,o}$	pH independent maximum specific reaction velocity (s^{-1})
W_k	coefficients
Z_i	charge on species i (equiv/mol)
Z	dimensionless length of the reactor in axial direction (-)

Greek Letters

α	the fraction of reactor volume occupied by the microcapsules (-).
η	effectiveness factor (-).
ε	the fraction of the volume occupied by the bulk void space (-).
ψ	electric potential (Volt).

ϕ_o^2 pH-independent Thiele modulus squared (-).

μ_f fluid viscosity (g/cm.s)

ρ_f fluid density (g/cm^3)

δ membrane thickness (m)

δ_l effective boundary layer thickness (m)

τ_r residence time based on liquid reactor liquid volume (s)

ξ activity coefficient (-)

Subscripts

i species

\+ cation

\- anion

1 enzyme phase

2 membrane phase

b bulk solution

f feed solution

aq aqueous phase

s urea

References

Alfrey, A.C., "Dialysis Encephalopathy Syndrome", Ann. Rev. Med., **29**, 93-98 (1978).

Alsugair, K. and T.M.S. Chang, "Kinetic Analysis of a Packed-bed Column Bioreactor for Conversion of Ammonia into Essential Amino Acid Using Micro-encapsulated Multienzyme System", VIII World Congress of the International Society for Artificial Organs", Montreal, August 1991, Paper no. 1, Artificial Organs, **15**, no.4, 271 (1991).

Arbeloa, M., R.J. Neufeld and T.M.S. Chang, "Analysis of a Microencapsulated Urease Fluidized-Bed Reactor under Steady and Transient State Operating Conditions", J. Memb. Sci., **29**, 321-331 (1986).

Atkinson, B., J. Rott, and I. Rousseau, "Characteristics of Unbuffered Gel-Immobilized Urease Particles. I. Internal pH", Biotech. Bioeng., **14**, 1037-1063 (1977).

Atkinson, B. and I. Rousseau, "Characteristics of Unbuffered Gel-Immobilized Urease Particles. II. Overall Rate of Reaction", Biotech. Bioeng., **14**, 1065-1086 (1977).

Bakan, J.A. and J.A. Anderson, "Microencapsulation", in Theory and Practice of Industrial Pharmacy, 2nd ed., L. Lachman, H.A. Lieberman, and J.L. Kanig, Eds., Lea and Febiger, Philadelphia (1976) p. 420.

Bard, A.J. and L.R. Faulkner, "Electrochemical Methods: Fundamentals and Applications", New York, Wiley (1980).

Barker, S.A., P.J. Somers, R.Epton, and J.V. McLaren, "Crosslinked Polyacrylamide Derivatives (Enacryls) as Water-insoluble Carriers of Amylolytic Enzymes", Carbohydrate Research, **14**, 287 (1970).

Bell, R.L., F.K. Curtis, and A.L. Babb, "Analog Simulation of the Patient Artificial Kidney System", Trans. ASAIO 11, 183-189 (1965).

Bernfeld, P. and J. Wan, "Antigens and Enzymes Made Insoluble by Entrapping Them into Lattices of Synthetic Polymers", Science, **142**, 678-679 (1963).

Berzelius, J.J., in "Biochemistry", A.L. Lehninger, Ed., Worth Publishing, 2nd ed., (1975), pp. 183-185.

Blakeley, R.L. and B. Zerner, "Jack Bean Urease: The First Nickel Enzyme", J. Mol. Catal., **23**, 263-292 (1984).

Bollmeier, J.P. and S. Middleman, "Development of Gelatin/Urease Films", Biotechnol. Bioeng., **16**, 859-862 (1974).

Bollmeier, J.P. and S. Middleman, "Hydrolysis of Urea by Gelatin-Immobilized Urease: Separation of Kinetic and Diffusion Phenomena in a Model Immobilized Enzyme Reactor System", Biotech. Bioeng., **21**, 2303-2321 (1979).

Brian, P.L.T. and H.B. Hales, AIChE J., **15**, 419 (1969).

Buchner, in "Biochemistry", A.L. Lehninger, Ed., Worth Publishing, 2nd ed. (1975).

Chang, T.M.S., "Hemoglobin corpuscles", Report of Research Project for B.Sc. Honours, McGill University, Montreal (1957).

Chang, T.M.S., "Semipermeable Microcapsules", Science, 146, 524-525 (1964).

Chang, T.M.S., "Semipermeable Aqueous Microcapsules", PhD. Thesis (Physiology), McGill University (1965).

Chang, T.M.S., "Semipermeable Aqueous Microcapsules "Artificial Cells"): With Emphasis on Experiments in an Extracorporeal Shunt System", Trans. Amer. Soc. Art. Internal Organs, **12**, 13-19 (1966).

Chang, T.M.S., F.C. McIntosh, and S.G.Mason, "Semipermeable Aqueous Microcapsules: I. Preparation and Properties", Can. J. Physiol. Pharmacol., **44**, 115-128 (1966).

Chang, T.M.S., Science J., **3**, 62 (1967).

Chang, T.M.S., L.J. Johnson, and O.J. Ransome, "Semipermeable Aqueous Microcapsules: IV. Nonthrombogenic Microcapsules with Heparin-complexed Membranes", Can. J. Physiol. Pharmacol., **45**, 705-715 (1967)

Chang, T.M.S., "Artificial Cells", C.C. Thomas, Ed., Springfield, Illinois (1972).

Chang, T.M.S., "A Comparison of Semipermeable Microcapsules and Standard Dialysers for Use in Separation", Separation and Purification Methods, **3**, No.2,

245-262 (1974a).

Chang, T.M.S., "Enzymes Immobolized by Microencapsulation: Preparation and Biomedical Applications" in "Insolubilized Enzymes", J.E. Vandagaer, Ed., Plenum Publishing Corp., New York, N.Y. (1974b).

Chang, T.M.S., "Semipermeable Microcapsules as Artificial Cells" in "Microencapsulation", J. Nixon, Ed., Marcel Dekker Inc., New York, N.Y. (1976).

Chang, T.M.S., "Encapsulation of Enzymes, Cell Contents, Cells, Vacciaes, Antigens, Antiserum, Cofactors, Hormones and Proteins" in Biomedical Applications of Immobilized Enzymes and Proteins. T.M.S. Chang, Ed., Plenum Press, N.Y. (1977), pp. 69-90.

Chang, T.M.S., "Introduction", in "Artificial Kidney, Artificial Liver, and Artificial Cells, T.M.S. Chang, Ed., Plenum Press, New York (1978), pp. 3-8.

Chang, T.M.S. and C. Malouf, "Artificial Cells Microencapsulated Multienzyme System for Converting Urea and Ammonia to Amino Acid using α-ketoglutarate and Glucose as Substrate," Trans. Am. Soc. Artif. Intern. Org., **24**, 18-20 (1978).

Chang, T.M.S. and C. Malouf, "Effects of Glucose Dehydrogenase Converting Urea and Ammonia into Amino Acid using Artificial Cells", Artif. Org., **3**, 1, 38-41 (1979).

Chang, T.M.S., "New Approaches using Immobilized Enzymes for the Removal of Urea and Ammonia", in "Enzyme Engineering", H.H. Weetal and G.P. Royer, Eds., Vol.5, Plenum Press, New York (1980), pp.225-229.

Chibata, I., "Immobilized Enzymes: Research and Development", I. Chibata, Ed., John Wiley & Sons, New York (1978).

Christensson, F., H.C.S. Koefoed, A.C. Petersen, and K. Rasmussen, "Equilibrium Constants in the Ammonium Carbonate-Carbamate System. The Acid Dissociation Constant of Carbamic Acid", Acta. Chemica. Scandinavica. A, **32**, 15-17 (1978).

Chung, S.F. and C.Y. Wen, "Longitudinal Dispersion of Liquid Flowing Through Fixed and Fluidized Beds", AIChE J., **14**, 857-866 (1968).

Cousineau, J. and T.M.S. Chang, "Formation of Amino-acid from Urea and Ammonia by Sequential Enzyme Reaction using a Microencapsulated Multi-enzyme System", Biochem. biophys. Res. Commun., **79**, 1, 24-31 (1977).

Cooney, D.O., "Biomedical Engineering Principles - An Introduction to Fluid, Heat, and Mass Transport Processes", G.A. Bekey, D.D. Reneau, Eds., Marcel Dekker, Inc., New York (1976), p. 301

Cussler, E.L., "Diffusion - Mass Transfer in Fluid Systems", Cambridge University Press, Cambridge (1984).

Davies, T.A., "Activated Carbon Fibers in Hemoperfusion Devices", Kidney Int., **7**, S406-S408 (1975).

Denti, E and M. Biagini, "Dialysate Regeneration", in "Artificial Organs", R.M. Kenedi, J.M. Courtney, J.D.S. Gaylor, T. Gilchrist, Eds., Macmillan Press, London (1977), pp. 139-147

Dixon, M. and E.C. Webb, "Enzymes", Academic Press, New York (1964).

Dixon, N.E., J.A. Hinds, A.K. Fihelly, C. Gazzola, D.J. Winzor, R.L. Blakeley, and B. Zerner, "Jack Bean Urease (EC 3.5.1.5. IV. The Molecular Size and the Mechanism of Inhibition by Hydroxamic Acids. Spectrophotometric Titration of Enzymes with Reversible Inhibitors", Can. J. Biochem., **58**, 1323-1334 (1980).

Drukker, W., F.M. Parsons, and J.F. Maher, "Replacement of Renal Function by Dialysis", Martinus Nijhoff Publishers, Boston (1983).

Dueck, C.L., R.J. Neufeld, and T.M.S. Chang, "Hydrodynamics and Urea Hydrolysis in a Microencapsulated Urease, Fluidized Bed Reactor", Can. J. Chemical Eng., **64**, 540-546 (1986).

Engasser, J.M. and C. Horvath, "Diffusion and Kinetics with Immobilized Enzymes", in "Applied Biochemistry and Bioengineering. Vol.1: Immobilized Enzyme Principles", L.B. Wingard, E. Katchalski-Katzir, and L. Goldstein, Eds., Academic Press, New York (1976), pp. 127-220.

Finlayson, B.A., "Nonlinear Analysis in Chemical Engineering", McGraw-Hill Book Co. Inc., New York (1980).

Fishbean, W.N., "The Structural Basis for the Catalytic Complexity of Urease: Interacting and Interconvertible Molecular Species", Annals N.Y. Acad. Sci., **147**, 857 (1969).

Friedman, E.A., M.J. Saltsman, M.M. Beyer, and A.S. Josephson, "Combined Oxystarch-charcoal Trial in Uraemia: Sorbentinduced Reduction in Serum Cholestrol", Kid. Int., **10**, S273-S276 (1976).

Giordano, C., "Sorbents and Their Clinical Applications", Academic Press, New York (1980).

Gordon, A., M.A. Greenbaum, L.B. Marantz, M.J. McArthur, and M.H. Maxwell, "A Sorbent based Low Volume Recirculating Dialysate System", Trans. ASAIO, **15**, 347-352 (1969).

Gordon, A., A.J. Lewin, M.H. Maxwell, and M. Roberts, "Current Stauts of Dialysate Regeneration for the Treatment of Chronic Uremia" in "Artificial Kidney, Artificial Liver, and Artificial Cells, T.M.S. Chang, Ed., Plenum Press, New York (1978), pp. 23-32.

Gu, K.F. and T.M.S. Chang, "Conversion of α-ketoglutarate into L-glutamic Acid with Urea as Ammonium Source using Multienzyme Systems and Dextran NAD^+

immobilized by Microencapsulation within Artificial Cells in a Bioreactor", Bitechnol. Bioeng., **32**, 363-368 (1988a).

Gu, K.F. and T.M.S. Chang, " Conversion of Ammonia or Urea into L-leucine, L-valine, and L-isoleucine using Artificial Cells Containing an Immobilized Multienzyme System and Dextran-NAD^+: I. Glucose Dehydrogenase for Cofactor Recycling", Trans. Am. Soc. Artif. Intern. Org., **34**, 24-28 (1988b).

Gu, K.F. and T.M.S. Chang, "Conversion of Ammonia or Urea into Essential Amino Acids, L-leucine, L-valine, and L-isoleucine using Artificial Cells Containing an Immobilized Multienzyme System and Dextran-NAD^+: II. Yeast Alcohol Dehydrogenase for Coenzyme Recycling", Biotechnol., Appl. Biochem., in Press. (1990a).

Gu, K.F. and T.M.S. Chang, "Conversion of Ammonia or Urea into Essential Amino Acids, L-leucine, L-valine, and L-isoleucine using Artificial Cells Containing an Immobilized Multienzyme System and Dextran-NAD^+: III. L-Lactic Dehydrogenase for Coenzyme Recycling", Biotechnol., Appl. Biochem., in Press. (1990b).

Gu, K.F., "Artificial Cells to Convert Ammonia and Urea into Essential Amino Acids", PhD. Thesis (Chemical Eng.), McGill University (1991).

Guilbault, G.G. and J.Das, "Immobilization of Cholinesterase and Urease", Analytical Biochemistry, **33**, 341-355 (1970).

Hoare, J.P. and K.J. Laidler, "The Molecular Kinetics of the Urea-Urease System. II. The Inhibition by Products", Am. Chem. Soc. J., **72**, 2487-2494 (1950).

Hofstee, B.H.J., "Immobilization of Enzymes Through Non-covalent Binding to Substituted Agaroses", Biochem. Biophys. Res. Commun., **53**, 1137-1144 (1973).

Iyengar, L. and A.V.S. Prabhakara Rao, " Urease Bound to Chitin with Glutaraldehyde", Biotech. Bioeng., **21**, 1333 (1979).

Iyengar, L., P. Bajpai, and A.V.S. Prabhakara Rao, "Behavior of Molecular Sieve Bound Urease", Indian J. Biochem. Biophys., **19**, 130 (1982).

Jalšenjak, I. and T. Kondo, "Effect of Capsule Size on Permeability of Gelatin-Acadia Microcapsules toward Sodium Chloride", J. Pharm. Sci., **70**, 456-457 (1981).

Kissel,T.R., "Study of a Reactor-Separator Membrane Combining an Immobilized Urease Gel and an Anion Exchange Membrane", PhD. Thesis (Analytical Chemistry), The University of Wisconsin, Michigan (1974).

Klein, E. and F.F. Holland, "Hemoperfusion Sorbent System for the Treatment of End Stage Renal Disease", in "Hemoperfusion: Artificial Kidney and Liver Support and Detoxification. Part I", S. Sideman, T.M.S. Chang, Eds., Hemisphere Publishing Corp., New York (1980) pp. 63-79.

Klibanov, A.M., "Immobilized Enzymes and Cells as Practical Catalysts", Science, 219, 722-727 (1983).

Kolff, W.J. and H.T.J. Berk, "The Artificial Kidney - A Dialyzer with a Great Area", Acta. Med. Scand., **117**, 121-134 (1944).

Kolff, W.J., "The Present Status and Perspectives of Hemodialysis", in "Artificial Kidney, Artificial Liver, and Artificial Cells", T.M.S. Chang, Ed., Plenum Press, New York (1978), pp. 11-21.

Kolff, W.J., "Artificial Kidney and Artificial Heart: Further Considerations", Int. J. Artif. Organs, **13**, 7 404-406 (1990).

Kondo, A., "Microcapsule Processing and Technology", J.W. Van Valkenburg, Ed., Marcel Dekker, New York (1979).

Krajewska, B., M. Leszko, and W. Zaborska, "Immobilization of Urease for Dialysate Regeneration System of Artificial Kidney", Post. Fiz. Med., **23**, No.2, 115-130 (1988).

Kydonieus, A.F., "Controlled Release Technologies: Methods, Theory, and Applications", Vol. II, CRC Press, Inc., Boca Raton, Fla. (1980).

Laidler, K.J. and J.P. Hoare, "The Molecular Kinetics of the Urea-Urease System. I. The Kinetic Laws," J. Amer. Chem. Soc. **71**, 2699 (1949)

Lee, K.B., D.K. Boadi and R.J. Neufeld, "Computer Program for Microencapsulated Urease Systems," Dept. of Chemical Engineering, McGill University, Montreal, Canada (1993).

Lehninger, A.L., "Biochemistry", Worth Publishing, 2nd ed., (1975), pp. 183-185.

Lencki, R.W.J., "The Effects of Protein Structural Configuration on the Free Enzyme Kinetic Behavior of Urease", PhD. Thesis (Chemical Eng.), McGill Univ., Montreal (1987).

Levich, V.G., "Physicochemical Hydrodynamics", Prentice-Hall, Englewood Cliffs, New Jersey (1962), pp. 39-136.

Levine, S.N. and W.C. LaCourse, "Materials and Design Consideration for a Compact Artificial Kidney," J. Biomed. Mat. Res., **1**, 275-284 (1967).

Lin, S.H., "A Modified Model for Predicting the Performance of a Compact Artificial Kidney", J. Theo. Biol., **77**, 441-451 (1979)

Martinek, K., V.V. Mozhaev, and I.V. Berezin, in "Enzyme Engineering: Future Directions", L.B. Wingard, I.V. Berezin, and A.A. Klyosov, Eds., Plenum, New York (1980), p. 3.

Maxwell, M.H., A. Lewin, and A. Gordon, "Sorbents in the Treatment ofChronic Renal Disease", Kidney Int., **7**, S383-S386 (1975).

Messing, R.A., "Simultaneously Immobilized Glucose Oxidase and Catalase in Controlled-Pore Titania", Biotech. Bioeng., **16**, 879 (1974a)

Messing, R.A., "A Stannous Bridge for Coupling Urease to Controlled Pore Titanium", Biotech. Bioeng. **16**, 1419 (1974b).

Messing, R.A., "Adsorption and Inorganic Bridge Formation", in "Methods in Enzymology", K. Mosbach, Ed., Vol. 44, Academic Press, New York (1976), pp. 148-169.

Miyawaki, O., K. Nakamura, and T. Yano, "Microencapsulatfon of Urease by Interfacial Polymerization with Liquid-Air Nozzle Method", Agric. Biol. Chem., **43**, no.5, 1133-1138 (1979).

Mogensen, A.O. and W.R. Vieth, "Mass Transfer and Biochemical Reaction with Semipermeable Microcapsules", Biotech. Bioeng., **15**, 467-481 (1973).

Monshipouri, M. and R.J. Neufeld, "Activity and Distribution of Urease following Microencapsulation within Polyamide Membranes", Enz. Microb. Technol., **13**, 309-313 (1991).

Monshipouri, M. and R.J. Neufeld, "Kinetics and Activity Distribution of Urease Co-encapsulated with Hemoglobin within Polyamide Membranes", Appl. Biochem. Biotechnol., **32**, 111-126 (1992).

Mosbach, K. and P.O. Larsson, "Preparation and Application of Polymer-entrapped Enzymes and Microorganisms in Microbial Transformation Processes with Special References to Steroid 11-s-Hydroxylation and Δ^1-Dehydrogenation", Biotechnol. Bioeng., **12**, 19-27 (1970).

Mosbach, K., "Methods in Enzymology", Vol. 44, K. Mosbach, Ed., Academic Press, New York (1976).

Mosbach, K., "Methods in Enzymology: Immobilized Enzymes and Cells, Part B", Vol. 135, K. Mosbach, Ed., Academic Press, Inc., New York (1987).

Moynihan, H.J., C.K. Lee, W. Clark and N.-H.L. Wang, " Urea Hydrolysis by Immobilized Urease in a Fixed-Bed Reactor: Analysis and Kinetic Parameter Estimation", Biotech. Bioeng., **34**, 951-963 (1989).

Mozhaev, V.V. and K. Martinek, Enzyme Microb. Technol., **4**, 299 (1982).

Nakamoto, Y., I. Karube, and S. Suzuki, "Urease-Collagen Membrane: Behavior of Ammonia", J. Ferment. Technol., **53**, 8, 595-598 (1975).

Neufeld, R.J., M. Arbeloa, and T.M.S. Chang, "Design of a Fluidized Bed Reactor for Microencapsulated Urease", Appl. Biochem. Biotechnol., **10**, 109-119 (1984)

Neufeld, R.J., R.W.J. Lencki, and T. Spinney, "Polysaccharide Microspheres and Method of Producing Same", US Pat. 4,822,534, 1989; Can. Pat. Appl. 531,272.

Nielsen, B., "Introduction" in "The Redy System: Experiments and Experiences", Scand. J. Urol. Nephrol. suppl., **30**, 5-7 (1976).

Nosé, Y., "Manual on Artificial Organs: Vol. I. The Artificial Kidney: A Guide to Understanding for the Physician and for the Patient", The C.V. Mosby Co., Saint Louis (1969).

Nosé, Y., "Artificial Kidney Research, Is It Really Not Necessary ?", Artificial Organs, **14**, no.4, 245 (1990).

Ogata, K., M. Ottesen and I. Svendsen, "Preparation of Water-insoluble Enzymatically Active Derivatives of Subtilisin Type Novo by Crosslinking with Glutaraldehyde", Biochem. Biophys. Acta, **159**, 403 (1968).

Ohta, Y., M. Arakawa, and T. Kondo", Membrane, **3**, 283-284 (1978).

Ortmanis, A. and R.J. Neufeld, "Study of Microcapsulated Urease in a Continuous Feed, Stirred Tank Reactor", Enzyme Microb. Technol., **6**, 135-139 (1984).

Pasteur, L. (1869), in "Biochemistry", Lehninger Ed., Worth Publishing, 2nd ed. (1975), pp. 183-185.

Pennington, S.N., H.T. Brown, A.B. Patel, and C.O. Knowels, "Properties of Matrix Supported Acetyloholinesterase", Biochem. Biophys. Acta, **167**, 479 (1968).

Poncelet, D. and R.J. Neufeld, "Shear Breakage of Nylon Membrane Microcapsules in a Turbine Reactor", Biotechnol. Bioeng., **33**, 95-103 (1989).

Poncelet, D., T. Alexakis, B. Poncelet De Met and R.J. Neufeld, "Microencapsulation within Cross-linked Polyethyleneimine Membranes", J. Microencap., in press (1992).

Popovich, R.P., D.J. Hlavinka, J.B. Bomar, J.W. Moncrief, and J.F. Dechard, "The Consequences of Physiological Resistances on Metabolic Removal from the Patient-artificial Kidney System", Trans ASAIO **21**, 108-115 (1975).

Reisel, E. and E. Katchalski, "Preparation and Properties of Water-insoluble Derivatives of Urease", J. Biol. Chem., **239**, 1521 (1964).

Reithel, F.J., in "The Enzymes", P.D. Boyer, Ed., Vol. 4, Academic Press, New York (1971), pp. 1-21.

Satterfield, C.N., "Mass Transfer in Heterogeneous Catalysis", M.I.T. Press, Massachusetts (1978).

Scouten, W.H., "A Survey of Enzyme Coupling Techniques", in "Methods in Enzymology: Vol. 135, Immobilized Enzymes and Cells, Part B", K. Mosbach, Ed., Academic Press, Inc., New York (1987) pp. 30-65.

Senjkovic, R. and I. Jalsenjak, "Apparent Diffusion Coefficient of Sodium Phenobarbitone in Ethylcellulose Microcapsules: Effects of Capsule Size", J. Pharm. Pharmacol., **33**, 279-282 (1981).

Shaldon, S., M.C. Beau, G. Claret, G. Deschodt, R. Oules, P. Ramperez, H. Mion, and C. Mion, "Haemofiltration with Sorbent Regeneration of Ultrafiltrate: First

Clinical Experience in End Stage Renal Disease", Proc. Eur. Dialysis Transplant. Ass., **XV**, 220-227 (1978).

Shapiro, W.B., P.F. Faubert, P.A. Fein, T. Tzeng, K. Salsnan, and J.G. Porush, "Hemofiltration with Sorbent Recycling of Ultrafiltrate in Uremic Dogs", Trans. ASAIO, **24**, 185-192 (1978).

Shemer, L. R. Granot, A. Freeman, M. Sokolovsky, and L. Goldstein, "Multilayer Immobilized-Enzyme Filter Reactors: Urease Bound to Nylon Fabric Filters", Biotech. Bioeng., **21**, 1607 (1979).

Shettigar, U.R., C. Kablitz, R. Stephen, and W.J. Kolff, "A Portable Hemodialysis/Hemofiltration System Independent of Dialysate and Infusion System", Artificial Organs, **7**, 254-256 (1983).

Snoeyink, V. and D. Jenkins, "Water chemistry", John Wiley & Sons, New York (1980).

Sparks, R.E., R.M. Salemme, P.M. Meier, M.H. Litt, and O. Lindan, "Removal of Waste Metabolites in Uremia by Microencapsulated Reactants", Trans. Amer. Soc. Artif. Int. Organs, **15**, 353-359 (1969).

Sparks, R.E., N.S. Mason, P.M. Meier, M.H. Litt, and O. Lindan, "Removal of Uremic Waste Metabolites from the Intestinal Tract by Encapsulated Carbon and Oxidized Starch", Trans. Am. Soc. Artif. Intern. Org., **17**, 229-235 (1971).

Sumner, J.B., "The Isolation and Crystallization of the Enzyme Urease", J. Biol. Chem., **69**, 435-441 (1926).

Sumner, J.B., D.B. Hand, and R.G. Holloway, "Studies of the Intermediate Products Formed during the Hydrolysis of Urea by Urease", J. Biol. Chem., **91**, 333-341 (1931).

Sumner, J.B. and G.F. Somers, "Chemistry and Methods of Enzymes, "Academic Press Inc., N.Y. (1947), p. 155.

Sundaram, P.V., "The Kinetic Properties of Microencapsulated Urease", Biochim. Biophys. Acta, **321**, 319-328 (1973).

Sundaram, P.V. and E.M. Crook, "Preparation and Properties of Solid-Supported Urease", Can. J. Biochem., **49**, 1388-1394 (1971).

Thies, C., "Physicochemical Aspects of Microencapsulation," Polymer Plast. Technol. Eng., **5**, 1 (1975).

Thies, C., "Microencapsulation", in "McGraw-Hill Yearbook of Science and Technology", McGraw-Hill, New York (1979), p. 12.

Vasudevan, P.T., L. Ruggiano, and R.H. Weiland, "Studies on the Deactivation of Immobilized Urease", Biotech. Bioeng., **35**, 1145-1149 (1990).

Vieth, W.R. and K. Venkatasubramanian, "Enzyme Engineering: Parts I-IV", Chemtech., (1973).

Villadsen, J.V., and W.E. Stewart, "Solution of Boundary-Value Problems by Orthogonal Collocation", Chem. Eng. Sci., **22**, 1483 (1967).

Walker, J.M., S.C. Jacobsen, R.L. Stephen, W.J. Kolff, and D. Rose, "The Role of Adsorbents in the Wearable Artificial Kidney", in "Artificial Organs", R.M. Kenedi, J.M. Courtney, J.D.S. Gaylor, T. Gilchrist, Eds., Macmillan Press, London (1977), pp. 139-147.

Ward, M.K., H.A. Ellis, T.G. Feest, I.S. Parkinson, D.N.S. Kerr, J. Herrington, and G.L. Goode, "Osteomalacic Dialysis Osteodystrophy: Evidence for a Waterborne Aetiological Agent, Probably Aluminum", Lancet, **1**, 841-845 (1978).

Watanabe, A. and Hayashi, T., "Microencapsulation Techniques for Fuji Photo Film Co. Ltd., and their Applications", in "Microencapsulation", J.R. Nixon, Ed., Marcel Dekker, New York (1976), chap. 2.

Weetall, H.H. and L.S. Hersh, " Urease Covalently Coupled to Porous Glass", Biochim. Biophys. Acta, **185**, 464 (1969).

Weetall, H.H., "Enzymes Immobilized on Inorganic Carriers", Research & Develop., **22**, 18 (1971).

Winchester, J.F., "Clinical Application of Haemoperfusion in Uraemia", in "Artificial Organs", R.M. Kenedi, J.M. Courtney, J.D.S. Gaylor, T. Gilchrist, Eds., Macmillan Press, London (1977), pp. 188-195.

Zaborsky, O.R., "Immobilized Enzymes", R.C. Weast, Ed., CRC Press, Cleveland, Ohio (1973).

Zaborsky, O.R., "Immobilized of Enzymes by Adsorption", in "Biomedical Applications of Immobilized Enzymes and Proteins", Vol. I, T.M.S. Chang, Ed., Plenum Publishing Corp., New York (1977).

Appendix A.

The derivation of Eq. 3-18

$$-N_{i,1} = D_{i,1}\left(\nabla C_{i,1} + C_{i,1} Z_i \frac{F \nabla \Psi}{R_g T} \right)$$

$$= D_{i,1}\left(\nabla C_{i,1} + C_{i,1} Z_i \nabla \psi \right)$$

$$\because \nabla \psi = \frac{F \nabla \Psi}{R_g T}$$

The current density i[Amperes/cm^2] in an electrolytic solution is due to the motion of charged particles.

$$i = F \sum_i Z_i N_i$$

$$= F \sum_i Z_i \left[-D_i \{ \nabla C_i + Z_i C_i \nabla \psi \} \right]$$

$$\therefore \nabla \psi = \frac{-1}{F \sum_i Z_i^2 D_i C_i} i - \frac{\sum_i Z_i D_i \nabla C_i}{\sum_i Z_i^2 D_i C_i}$$

If electro-neutrality is assumed, the divergence of the current is zero.

$$\therefore \nabla \boldsymbol{i} = 0$$

$$\therefore \boldsymbol{i} = 0$$

Arranging in terms of N_i,

$$- N_i = D_i \left(\nabla C_i - C_i Z_i \frac{\sum_i Z_i D_i \nabla C_i}{\sum_i Z_i^2 D_i C_i} \right)$$

$$- \nabla \cdot N_i = D_i \nabla^2 C_i - \nabla \cdot \left[\frac{Z_i D_i C_i}{\sum_i Z_i^2 D_i C_i} \sum_i Z_i D_i \nabla C_i \right]$$

Since $\nabla \cdot (abc) = bc \cdot (\nabla a) + ac \cdot (\nabla b) + ab (\nabla \cdot c)$,

$$\therefore \nabla \cdot \left[\frac{1}{\sum_i Z_i^2 D_i C_i} Z_i D_i C_i \sum_i Z_i D_i \nabla C_i \right] =$$

$$\nabla \cdot [(\sum_i Z_i^2 D_i C_i)^{-1} Z_i D_i C_i \sum_i Z_i D_i \nabla C_i]$$

$$- (Z_i D_i C_i \sum_i Z_i D_i \nabla C_i) \cdot \nabla (\sum_i Z_i^2 D_i C_i)^{-1}$$

$$+ \{ (\sum_i Z_i^2 D_i C_i)^{-1} \sum_i Z_i D_i \nabla C_i \} \cdot \nabla (Z_i D_i C_i)$$

$$(\sum_i Z_i^2 D_i C_i)^{-1} Z_i D_i C_i (\nabla \cdot \sum_i Z_i D_i \nabla C_i)$$

$$- (Z_i D_i C_i \sum_i Z_i D_i \nabla C_i) \cdot \} \frac{-1}{(\sum_i Z_i^2 D_i C_i)^2} \nabla (\sum_i Z_i^2 D_i C_i) \}$$

$$\frac{\sum_i Z_i D_i \nabla C_i}{\sum_i Z_i^2 D_i C_i} \cdot \nabla (Z_i D_i C_i) + \frac{Z_i D_i C_i}{\sum_i Z_i^2 D_i C_i} (\nabla \cdot \sum_i Z_i D_i \nabla C_i)$$

$$- (Z_i D_i C_i \sum_i Z_i D_i \nabla C_i) \{ \frac{-1}{(\sum_i Z_i^2 D_i C_i)^2} \nabla (\sum_i Z_i^2 D_i C_i) \}$$

$$+ \frac{(\sum_i Z_i D_i \nabla C_i) \{\nabla (Z_i D_i C_i)\}}{\sum_i Z_i^2 D_i C_i} + \frac{Z_i D_i C_i \sum_i Z_i D_i \nabla^2 C_i}{\sum_i Z_i^2 D_i C_i}$$

$$- \frac{-Z_i D_i C_i (\sum_i Z_i D_i \nabla C_i) \nabla (\sum_i Z_i^2 D_i C_i)}{(\sum_i Z_i^2 D_i C_i)^2}$$

$$+ \frac{(\sum_i Z_i D_i \nabla C_i) \{\nabla (Z_i D_i C_i)\}}{\sum_i Z_i^2 D_i C_i} + \frac{Z_i D_i C_i \sum_i Z_i D_i \nabla^2 C_i}{\sum_i Z_i^2 D_i C_i}$$

$$\therefore \quad - \nabla \cdot N_i = D_i \nabla^2 C_i -$$

$$\left[\frac{-Z_i D_i C_i (\sum_i Z_i D_i \nabla C_i) \sum_i Z_i^2 D_i \nabla C_i}{(\sum_i Z_i^2 D_i C_i)^2} + \frac{(\sum_i Z_i D_i \nabla C_i) (Z_i D_i \nabla C_i)}{\sum_i Z_i^2 D_i C_i} \right.$$

$$\left. + \frac{Z_i D_i C_i (\sum_i Z_i D_i \nabla^2 C_i)}{\sum_i Z_i^2 D_i C_i} \right]$$